Titre: Title:	Development of microporous polypropylene by stretching
Auteur: Author:	Farhad Sadeghi
Date:	2006
Type:	Mémoire ou thèse / Dissertation or Thesis
Référence: Citation:	Sadeghi, F. (2006). Development of microporous polypropylene by stretching [Thèse de doctorat, École Polytechnique de Montréal]. PolyPublie. https://publications.polymtl.ca/7787/

UNIVERSITÉ DE MONTRÉAL

DEVELOPMENT OF MICROPOROUS POLYPROPYLENE BY STRETCHING

FARHAD SADEGHI
DÉPARTMENT DE GÉNIE CHIMIQUE
ÉCOLE POLYTECHNIQUE DE MONTRÉAL

THÈSE PRÉSENTÉE EN VUE DE L'OBTENTION
DE DIPLÔME DE PHILOSOPHIAE DOCTOR
(GÉNIE CHIMIQUE)
Décembre 2006

Your file Votre référence
ISBN: 978-0-494-24549-1
Our file Notre référence
ISBN: 978-0-494-24549-1

UNIVERSITÉ DE MONTRÉAL

ÉCOLE POLYTECHNIQUE DE MONTRÉAL

Cette thèse intitulée :

DEVELOPMENT OF MICROPOROUS POLYPROPYLENE BY STRETCHING

présentée par: SADEGHI Farhad

en vue de l'obtention de diplôme de : Philosophiae Doctor

a été dûment acceptée par le jury d'examen constitué de :

M. DUBOIS Charles, Ph. D., président

M. CARREAU Pierre J., Ph. D., membre et directeur de recherche

M. AJJI Abdellah, Ph. D., membre et codirecteur de recherche

Mme HEUZEY Marie-Claude, Ph.D., membre

M. KAMAL Musa, Ph. D., membre

ACKNOWLEDGEMENTS

I wish to thank all those who helped me in the completion of this study.

First of all, I am indebted to my supervisors, *Professor Pierre Carreau* and *Dr. Abdellah Ajji* for their helpful guidance, corrections and suggestions and encouragements.

I would like also to express my thanks to the technicians of IMI (Industrial Material Institute) that without their helps this project could not go through. Special thanks to *Jacques Dufour, Francois Vachon , Karine Théberge, Eric Cloutier* and *Robert Lemieux* for their helps.

I finally like to extent my thanks to the entire technical staff of the Chemical Engineering Department in Ecole Polytechnique de Montreal.

RÉSUMÉ

Les processus pour la production de membranes à partir du polypropylène par étirage ont été conçus il y a environ 30 ans. La première et la plus importante étape pour la fabrication d'une telle membrane est la génération d'une structure lamellaire. Tandis que beaucoup de progrès a été accompli dans ce domaine, une étude approfondie et détaillée de ce processus est absente dans la littérature scientifique. La principale raison est un manque de connaissances au sujet de la formation de ce genre de structure. Le contrôle de la cristallisation induite sous contrainte, ce qui est habituellement réalisé industriellement, est très difficile.

Dans ce travail, on présentera d'abord un sommaire des procédés de production avec une attention particulière sur le processus d'étirage. Par après, des résultats expérimentaux concernant le polypropylène seront présentés. Il est important de noter que des études concernant certains aspects de la production de telles membranes à partir d'autres polymères, tels POM (polyoxyméthylène), PMP (poly 4-méthyle-1-pentène) et PE (polyéthylène) ont été présentées ailleurs (Johnson., 2000).

Les étapes de la production de membranes par étirage sont catégorisées en deux parties principales:

1-La préparation des films précurseurs avec une morphologie cristalline appropriée (structure lamellaire).

2- Étirage des films précurseurs pour former des pores et l'établissement d'une structure poreuse.

Pour la première partie, cinq homo-polypropylènes avec différentes distributions de

poids moléculaires ont été sélectionnés et l'effet de la structure moléculaire et du processus d'extrusion a été étudié. Les facteurs ayant une influence importante dans la génération de structure lamellaire sont divisés en deux catégories : ceux du matériau, qui seront appelés facteurs du matériau, et ceux du procédé de fabrication.

Outre les facteurs du processus, le temps de relaxation des chaînes polymères était le facteur le plus important du matériau, ce qui est une fonction de la structure moléculaire. Le taux de refroidissement et le taux d'étirage du film fondu de polymère à la sortie de la filière sont également des facteurs primordiaux pour obtenir un film précurseur uniforme et stable. Lors du processus d'extrusion, le contrôle du refroidissement du polymère fondu à la sortie de la filière est le paramètre-clé, puisqu'un refroidissement efficace empêche la relaxation rapide des chaînes. Un taux de refroidissement élevé permet de préserver l'alignement des chaînes allongées lors de l'extrusion.

Les caractéristiques de la résine et le processus d'extrusion influencent l'orientation des films précurseurs. Nous avons constaté qu'une orientation minimale des lamelles cristallines dans la direction de la machine (l'orientation d'Herman) de 0.3 pour le film précurseur, est nécessaire pour obtenir une membrane microporeuse. Une orientation élevée de lamelles empilées résultera en de meilleures interconnectivités entre les pores de la membrane. Ceci sera exploité dans le processus d'étirage ultérieur de la membrane. Après l'extrusion, il faut placer les films précurseurs dans un four pour enlever les défauts et pour épaissir les cristaux lamellaires. Il semble que la température de recuit est plus importante que le temps de recuit. Le recuit améliore l'orientation et affecte la réponse de l'échantillon aux essais de tension et forme deux types de distribution

lamellaire. L'étirage à température ambiante entraîne une séparation des lamelles et il y a création des pores. La quantité de pores et leur taille dépendent de l'épaisseur des lamelles et de la force des chaînes de liaison (tie-chains), raccordées aux lamelles. Les paramètres les plus importantes pour cette étape sont la température et le taux d'étirage.

Les membranes fabriquées à partir de la résine de la plus faible masse moléculaire contiennent une plus petite quantité de pores, mais ils sont légèrement plus grands lorsque comparés aux pores des membranes de polypropylène qui possède une masse moléculaire moyenne. La quantité inférieure de pores est due à une orientation faible des lamelles, à une plus grande taille et à une densité plus faible des chaînes de liaison. La situation pour le polypropylène de grande masse moléculaire est différente; ce polymère génère un grand nombre de fibrilles qui lient les lamelles fortement ensemble et limitent ainsi leur séparation. Une certaine quantité de chaînes de grande masse moléculaire est nécessaire, puisqu'elles améliorent le processus avec une augmentation de la capacité d'étirage du polymère fondu. Elles forment également de longues fibrilles, qui permettent d'établir un fort réseau pour le processus d'étirage subséquent. Cependant, un grand nombre de fibrilles crée beaucoup de liens entre les lamelles, ce qui rend la séparation difficile.

Lors de l'étirage à température élevée, une partie des couches à la surface des lamelles est localement détachée et réorientée pour former des ponts reliant des lamelles. En fait, nous croyons qu'il existe deux sources dans la formation des ponts. Les ponts sont créés par : (1) des chaînes de liaison (tie-chains) qui seront étirées et cristallisées dans l'étape subséquente; et (2) des parties détachées des couches minces des lamelles qui se

réorientent et se cristallisent durant l'étirement. La perméabilité de la membrane, qui représente une mesure de sa performance, est contrôlée par l'orientation et la structure des films précurseurs. On observe différents comportements pour la perméabilité avec et sans application de la pression. Lorsqu'une faible pression est appliquée, la diffusion de Knudsen régit le processus.

Lorsque la membrane est sous haute pression, elle est principalement régie par le flux de Poiseuille. La résistance à la perforation, une des propriétés mécaniques les plus importantes pour les membranes, a été évaluée. La résine qui a un poids moléculaire modéré et qui possède la plus grande perméabilité a montré la résistance la plus élevée à la perforation.

Abstract

The process for the production of membranes from polypropylene by stretching has been developed since 30 years ago. The first and most important step for making such membranes is the generation of a row nucleated lamellar structure. While many progresses have been made in this field an extensive and detailed academic study for this process is absent in the scientific papers and the main reason for this is the lack of knowledge about the formation of the lamellar structure during melt crystallization.

In this work a brief summery of the membrane production processes with a particular focus on the stretching process is described in the literature review section. Then our experimental results concerning the development of the microporous membranes from polypropylene by stretching in form of three papers are presented. In the process of the membrane production by stretching two main steps are studied:

1-Preparation of the precursor films with appropriate lamellar morphology (row nucleated lamellar structure).

2-Stretching of the prepared precursor films with such lamellar structure to create pores and establishing a porous structure.

For the first part five homo polypropylenes different in molecular weight and molecular weight distribution were selected and the effect of molecular structure and extrusion process were studied.

From an engineering standpoint the process parameters (extrusion and cooling) need to be controlled to obtain uniform and stable precursor films, while from a research point

of view the molecular structure of the resins are crucial in morphology formation and determination of an appropriate lamellar structure.

Among the resin factors, the relaxation time of polymer chains was the most important factor which is a function of polymer chain structure. For the process, a smooth extrusion aids to obtain the uniform and stable precursor films. The cooling of the extrudate right after the die prevents the quick relaxation of the elongated chains. Draw ratio controls the number and degree of the chain extension at the die. As it will be mentioned later, the long elongated chains act as the nuclei for later lateral lamellae crystallization, which is called row-nucleated lamellar structure.

Resin characteristics and extrusion process influence the orientation of the lamellae crystals in the precursor films. The orientation of the crystalline structure was revealed to be a key parameter in obtaining an appropriate lamellar structure. It was found that a minimum orientation of 0.3 for crystal lamellae along machine direction (Herman's orientation) for the precursor film is necessary for obtaining a microporous membrane. High orientation of stacked lamellae facilitates the lamellae separation in the subsequent stretching process and also improves the interconnection between the pores through the membrane. After extrusion, annealing is performed on the precursor films to remove the defects and thicken the crystal lamellae. It was revealed that controlling the annealing temperature is more effective than controlling the annealing time. However, a period time of 10 minutes for annealing was necessary to achieve a stable annealed structure. Annealing improves the orientation for both crystalline and amorphous phases and significantly changes the response of the sample to tensile tests with the formation of

two lamellae distributions. In cold stretching (room temperature) lamellae get separated and pores are created. The amount of the pores and their size depend on the orientation, thickness and connection of the lamellae. Temperature and stretching ratio of cold stretching are the process parameters controlling the extension and structure of the pores. Membranes made of a low molecular weight resin contains a smaller amount of pores, but slightly bigger when compared with membranes obtained from medium molecular weight polypropylene. However, a caution should be considered while comparing the pore size from the SEM micrographs obtained from the surface. In fact, interconnection between the pores determines the effective pore diameter (passing through the thickness of the membrane). Further mercury porosimetery tests showed that the effective pore diameter and porosity were smaller for the membranes based on the low molecular weight resin. For the resin with low molecular weight, the lower amount of pores is attributed to poor orientation of the lamellae, where most of the stress in the stretching process will be spent on the motion and rotation of crystal blocks rather than separating them.

The situation for high molecular weight polypropylene is different since it renders a large number of fibrils where they bond the lamellae strongly together and limits lamellae separation. Generally, high molecular weight chains have advantages as:

1- They improve the process ability with an in increase in melt draw ability, 2-They also generate long fibrils for nuclei in melt stretching at the die to improve the lamellar crystallization. However, a large number of the fibrils create strong connections between the lamellae, which make the lamella separation difficult.

In hot stretching some parts of the lamellae (thin surface layers) are locally broken and reoriented to form some more connected bridges. We believe that the sources for the formation of the interconnected bridges are: 1-Stretched tie chains, which will be crystallized afterward and 2-The separated crystal parts of the lamellae, which will be reoriented with stretching and join the very thin bridges to reinforce them.

The permeability of the membrane, which represents the performance of the membrane, is controlled by the orientation and structure of the precursor films. It was observed that the largest permeability is achievable for the sample with the initial largest orientation that possesses the moderate molecular weight.

Different behaviors were observed for the gas permeation in the presence of pressure. In low pressure range, Knudsen diffusion controls the process while in high pressure the Poiseuille flow dominates.

Puncture resistance is one of the most important mechanical properties for the membranes. It was evaluated and the resin with the largest permeability showed the highest resistance.

CONDENSÉ EN FRANÇAIS

Il y a une grande demande dans le marché pour le développement et les modifications de membranes à un coût inférieur et un rendement plus élevé. Il existe plusieurs méthodes pour la production de membranes où la technique principale est basée sur la séparation de phases.

La méthode de la séparation de phases est un processus coûteux et il est souvent nécessaire d'éliminer le solvant ou le non-solvant dans le produit final.

Le processus d'étirage peut être appliqué pour développer la membrane à partir d'un film précurseur avec une microstructure appropriée. Des membranes microporeuses sont obtenues par la séparation des lamelles cristallines dans un film possédant une structure lamellaire initiale. Cette technique, réservée aux polymères semi-cristallins,

a été employée commercialement pendant les trois dernières décennies, mais une étude académique approfondie et détaillée pour le polypropylène est absente de la littérature scientifique.

Dans la technique d'étirage, une structure lamellaire est d'abord produite pour le polypropylène et l'étirage subséquent aura comme conséquence la séparation des lamelles et la création de pores. Les étapes de la production des membranes par étirage sont catégorisées en deux parties principales:

1-La préparation des films précurseurs avec une morphologie appropriée (la structure lamellaire (avec une certaine orientation des cristaux).

2- Étirage des films de précurseurs préparés pour la formation des pores et l'établissement d'une structure poreuse.

La première et la plus importante étape pour créer une telle membrane est la génération d'une structure lamellaire.

Pour la première étude, cinq homo-polypropylènes avec différentes distributions de masses moléculaires ont été sélectionnés et l'effet de la structure moléculaire et du processus d'extrusion a été étudié.

Les facteurs ayant une influence importante dans la génération d'une structure lamellaire sont divisés en deux catégories : ceux du matériau, qui seront appelés facteurs du matériau, et ceux du procédé de fabrication.

Parmi les facteurs du matériau, le temps de relaxation des chaînes polymères était le plus important, ce qui est une fonction de la structure moléculaire. Pour les facteurs du procédé, le taux de refroidissement et le taux d'étirage, qui nous permettent d'étirer de façon importante le film polymère fondu à la sortie de la filière, sont également primordiaux pour obtenir un film précurseur uniforme et stable. Lors du processus d'extrusion, le contrôle du refroidissement du polymère fondu à la filière empêche la relaxation rapide des chaînes. Le taux de refroidissement est un facteur dominant pour conserver l'alignement des chaînes étirées à la sortie de la filière.

Les caractéristiques de la résine et le processus d'extrusion influencent l'orientation des films précurseurs. Nous avons constaté qu'une orientation minimale des lamelles cristallines, dans le sens de la direction de machine (l'orientation d'Herman) de 0.3 pour le film précurseur, est nécessaire pour obtenir une membrane microporeuse. Une orientation élevée des lamelles empilées résultera en une meilleure interconnectivité entre les pores de la membrane. Ceci sera exploité dans le processus d'étirage ultérieur

de la membrane. Le changement d'une cristallisation de type sphérulite à une structure lamellaire entraîne un changement important de la réponse en tension en fonction de la déformation du film solide. Ceci se traduit par la disparition de la transition entre le domaine élastique et le domaine plastique et, en second lieu, par une apparition précoce de l'écoulement du matériau. Ce comportement est dû à la formation de deux distributions de lamelles. Le polypropylène peut former de différentes structures lamellaires (épaisseur de lamelles) dépendant de sa masse moléculaire. La masse moléculaire influence l'orientation plutôt que l'épaisseur des lamelles.

Après la production des films précurseurs, un recuit a été effectué. Habituellement, le recuit est effectué pour éliminer les défauts dans la structure cristalline et pour épaissir les cristaux lamellaires. Le recuit améliore fortement l'orientation des phases cristallines et amorphes des films précurseurs. En se basant sur les résultats de la DSC (calorimétrie différentielle à balayage), nous avons constaté que le processus de recuit pour les films de polypropylène, avec un taux élevé de refroidissement initial, n'a pas affecté de manière significative l'épaisseur du cristal. Le recuit a une tendance à orienter les lamelles dans une morphologie planaire. Nous avons trouvé que la température de recuit est très efficace aussi longtemps qu'elle ne met pas en danger la structure initiale des lamelles. Le temps efficace de recuit était de dix minutes et, au delà de ce temps, la structure n'a pas changé avec le temps. Le recuit a également un impact important sur la réponse de l'échantillon aux essais de tension puisqu'il change l'allure de la courbe avec une pente plus raide et une recouverence beaucoup plus prononcé. En outre, le prolongement au repos a également diminué, ce qui pourrait être dû à l'orientation de la

phase amorphe.

Après, les échantillons subissent l'étape d'étirage à température ambiante. Cet étirage résulte en la création des pores initiaux en raison de la décohésion entre chaînes et lamelles. Les pores sont plus larges pour la résine à faible masse moléculaire en raison d'une densité plus faible des chaînes de liaison, mais ils sont moins nombreux et moins interconnectés en raison d'une orientation plus faible. Dans le cas d'une résine à forte masse moléculaire, les pores sont plus petits puisqu'un réseau plus fort de lamelles existe. Cependant, il y a une plus grande quantité de pores à cause de l'orientation plus élevée des lamelles.

La perméabilité des échantillons à la vapeur d'eau, à la fin de l'étirage à une température ambiante, a été évaluée. On a observé une perméabilité très basse pour les membranes produites à partir de la résine de la plus grande masse moléculaire. En revanche, les PP avec un poids moléculaire de distribution modérée et bimodale ont résulté en des membranes de plus grande perméabilité.

Après le processus d'étirage à température ambiante, les échantillons ont été étirés davantage à une température de 140°C. Une température élevée facilite la mobilité des blocs cristallins. Cet étirage agrandirait les vides qui sont déjà formés pendant le processus d'étirage à température ambiante. Les températures élevées stabilisent également la structure cristalline des échantillons. Les lamelles sont séparées tandis qu'elles sont encore reliées par les chaînes de liaison. Nous avons observé que le nombre de ponts (reliant les lamelles) a augmenté lors de l'étape d'étirage à une température élevée. Ceci a pu être causé par:

1-La cristallisation des chaînes de liaison étirées

2-Le détachement de quelques couches extérieures des lamelles et de leur réorientation pour former de nouveaux ponts.

La perméabilité à la vapeur d'eau des films des membranes finales a suivi l'ordre de l'orientation des films précurseurs, avec l'exception de la résine de la plus haute masse moléculaire.

La résine de la plus haute masse moléculaire produira un grand nombre de longues fibrilles qui se colleront fortement aux lamelles et rendront la séparation bien plus difficile. Lorsque les échantillons sont examinés pour la perméabilité à l'azote sous la pression, deux comportements ont été trouvés pour la courbe d'écoulement en fonction de la pression. Pour les membranes obtenues à partir de films produits, la diffusion de Knudsen domine à une basse pression. D'autre part, on a observé l'écoulement de Poiseuille alors que la pression était augmentée. Pour les membranes obtenues pour des films fortement étirés, on a observé une grande perméabilité à la vapeur d'eau, avec un comportement de Poiseuille sans la transition.

Le comportement de la courbe l'écoulement en fonction de la pression peut refléter la structure de la membrane microporeuse. Les pores reliés ensemble le long de l'épaisseur de la membrane déterminent la longueur effective et le diamètre des pores.

Des essais de porosimétrie ont été également effectués pour déterminer la distribution des pores. Il a été montré que les membranes fabriquées à partir de la résine à faible masse moléculaire possédaient de plus petits pores (dans la gamme de 0.1μm.) Tandis que, les membranes basées sur la résine à masse moléculaire moyenne avaient des pores

de 0.15μm. La même tendance a été observée pour la porosité lorsqu'elle a été augmentée de 41% à 47%, pour une résine à masse moléculaire moyenne à une résine à faible masse moléculaire.

Ces membranes sont le plus largement utilisées dans des séparateurs de batterie où elles sont exposées à des surfaces inégales. Pour évaluer la performance des membranes en contact avec les surfaces inégale, la résistance à la perforation a été examinée. L'échantillon avec la plus grande perméabilité a démontré la résistance maximale à la perforation.

TABLE OF CONTENTS

List of Tables

List of Figures

List of Symbols

G'	Elastic module
G''	Loss module
η^*	Complex viscosity
τ	Relaxation time
$H(\tau)$	Relaxation time spectrum
ω	Frequency
f	Herman orientation function
β	The angle between the stretch direction (machine direction) and the b-axis of the crystal
φ	The angle between crystal axis unit with machine, transverse, or normal direction.
λ	$\lambda = G'/(G''\omega)$, which is also called a characteristic elastic time
η_0	Zero-shear viscosity
M_w	Molecular weight
$\eta_e^+(t)$	Transient elongational viscosity
S	Intensity of the peak in the FTIR spectrum obtained in MD, TD or ND
A	Absorbance in FTIR
f_c	The orientation of crystalline phase
f_a	The orientation of amorphous phase
DR	Draw ratio
θ	The angle between beam and sample in WAXD

Chapter 1

Introduction

Membranes are increasingly employed for separation processes. From energy and process reliability points of view, they progressively compete the conventional separation process such as distillation. Polymers are among the best candidates for the development of membranes covering a broad range of microfiltration to reverse osmosis. The most common technique for production of membranes is based on solution casting followed by phase separation. Costly process and difficulties in dealing with solvent (or non-solvent) contamination are two drawbacks of such method. The process to develop membranes by stretching from neat polymer (without using solvent or extra component) has been introduced since 30 years ago for some semicrystalline polymers. The technique is based on the stretching of a polymer film with the row nucleated lamellar structure. Once the sample is stretched, pores are created as the result of the separation of the crystal blocks. This method is relatively less expensive in comparison to the other methods and there is no solvent contamination. The major disadvantage is low tear resistance of the final membranes in stretching direction.

The formation of the membrane through this method is carried out in three main consecutive stages: 1-Production of the precursor sample with lamellar morphology (row nucleated structure), 2-Annealing of the sample, 3-Stretching of the sample at low temperature to create voids and then at high temperature to enlarge and stabilize them.In fact the main issue in this process is the generation of a proper initial row nucleated

lamellar structure. Type of polymer and applied extrusion conditions are the key factors for the production of the precursor films with such crystalline structure. These factors determine the thickness, orientation, position and connection of the crystals blocks in the precursor film, which in turn control the final membrane structure. Annealing in turn will remove the defects such as disruption of chain folding from crystalline phase and also improve the long period. Stretching at room temperature separate the lamellae and creates voids, which will be enlarged and stabilized in a hot stretching step. Some works have already been published discussing the process for polyethylene (Yu, 1995), poly (4-methyl-1-pentene) (PMP) and polyoxymethylene (POM), (Johnson, 2000). However, no investigation for polypropylene in the open literature has been found. In this work the method for the development of microporous membranes from polypropylene by stretching is studied the following sections:

1- Literature review, mainly methods for membrane production by stretching. We also discuss the conditions for the generation of the crystalline lamellar structure.

2-First paper: The study for the parameters involved in production of the polypropylene precursor films for the generation of a lamellar structure.

3-Second paper: The physical and mechanical properties of the precursor films and examination of the draw ratio effect.

4-Third paper: The process for the formation of the polypropylene microporous membrane by stretching followed by structure and performance evaluation of the membrane.

5-Finally in the section of General discussion, a full review of the process is presented.

Chapter 2

Literature review

Membranes are generally classified into two types:

a) Microporous membrane: In this type of membranes interconnected pores in range of 0.01-10 μm are randomly distributed through the thickness. Separation mostly takes place for the solute, which has components with particles smaller than the pore size. Generally only components, which differ considerably in their particle size, can be separated by this type of membranes.

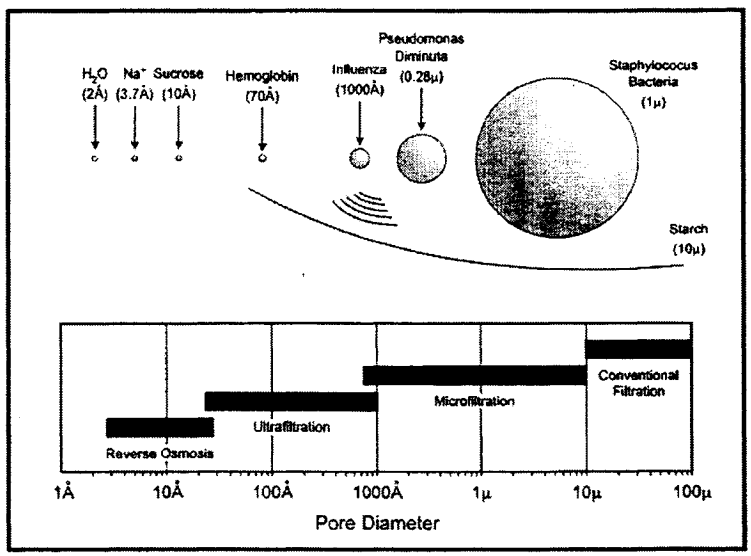

Fig.2.1 Particle size of separated components by membrane (Cheryan, 1998).

b) Nonporous dense membrane: this is a solid film, through which permeates a component by diffusion under the driving force of a pressure, concentration, electrical potential gradient (or a combination of two or three). The main mechanism is adsorption and diffusion of components through the membrane, which is a function of diffusivity

and solubility of the permeate. With this technique material with similar size can be separated due to a difference in their diffusion rate through the membrane (which depends on their solubility in membrane). Gas separations and reverse osmosis that are normally slow processes are favored by this kind of membranes. In practice to increase the permeate flow, the membranes are made very thin and to improve the strength, they are formed on a substrate which acts as a support. The substrate is usually a microporous membrane with larger thickness. The membrane with this structure (composed of two layers) is called asymmetric membranes. It should be noted that the process for the formation of two layers takes place during the phase separation and solvent removing stage. The Loeb-Sourirajan technique was one of the first commercial processes to manufacture reverse osmosis membranes through this method (Cheryan, 1998).

2.2 Membrane preparation methods

The three major production methods for membranes are phase separation, irradiation and stretching.

2.2.1 Phase separation

A polymer with other component phases is separated by adding a non-solvent, cooling or solvent evaporation. The first phase is solid rich in polymer that forms the matrix and the second is poor in polymer that forms the pores. Except of the polymer, the other components will be removed later to stabilize the structure. The most common method is that known as Loeb-Souirajan based on phase separation by immersion in a non-solvent (Cheryan, 1998). Almost all the reverse osmosis, ultrafiltration and many gas separation

membranes are produced in this way. The process is illustrated in Fig. 2.2. A solution usually of 20% dissolved polymer is cast onto a moving drum. As the drum goes into the water the polymer is precipitated and forms a dense layer on the top. The dense skin thickness varies from 0.1 to 1 μm, and this skin will act as a barrier for further water permeation from the depth.

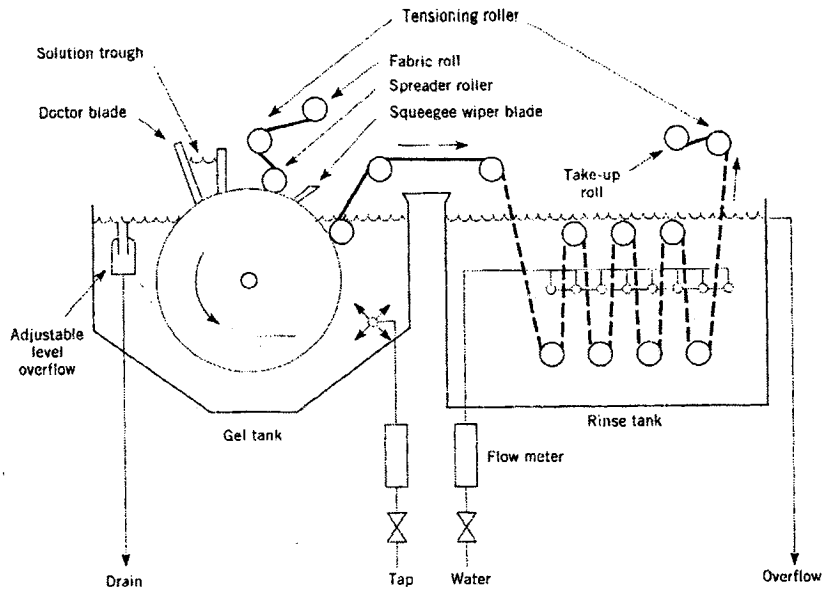

Fig. 2.2 Loeb-Souirajan process (Cheryan, 1998).

This causes a very slow precipitation for the under layers, which gives more time for formation of large pores. The ideal case is to make the skin as thin as possible and defect free. The pores (if are formed) in the skin are very small in the range of nanometer. The thickness of the skin is usually around 50 to 100 nm and the total membrane thickness goes over 50 μm. A ternary phase diagram in Fig. 2.3 shows the phase evolution during the membrane formation.

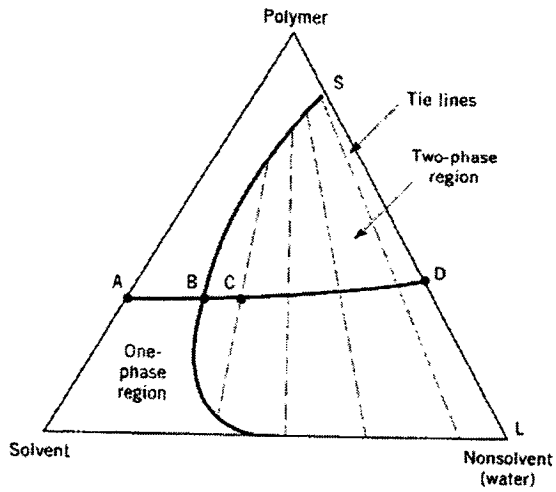

Fig.2.3 Phase diagram showing the composition pathway traveled by a casting solution during the preparation of a porous membrane A: Initial casting solution, B: point of precipitation C: point of solidification (Cheryan., 1998).

The precursor solution is at point A and it moves towards B as the precipitation begins. At point C a solid rich polymer is formed as a solid dense layer is in equilibrium with other phase that is liquid poor in polymer. The composition is fixed at D where the non-solvent is extracted totally. Kinetics of the process determine the time of the pathway of A-D. One example of this type of the membrane is DuPont polyamide membrane.

2.2.2 Irradiation

The polymer film is exposed to a flow of charged particles generated from a irradiation source. This will cause the chain scission and damaged tracks, which with further etching leads to cylindrical pores along the thickness. The time period of exposition and the etching time determine membrane performance such as pore diameter. For this membrane the tortuosity is very close to 1 (Fig.2.4). Usually the porosity of this kind of membrane is very low and therefore the flux is small. However, this membrane is used

when a precise analytical separation is to be carried out. This kind of membrane was initially developed by Nuclepore Corp (Cheryan, 1998).

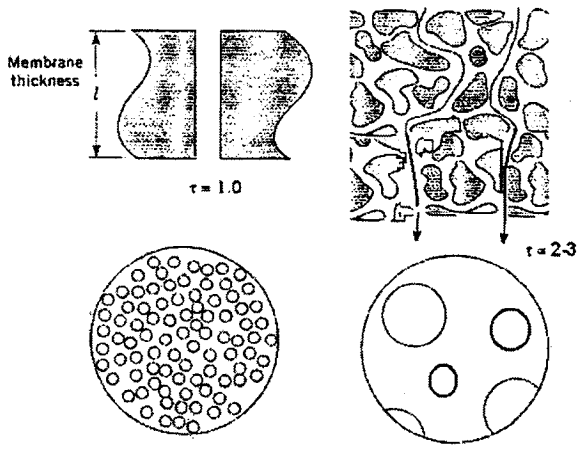

Fig.2.4. The schematic of two different tortuosity paths (Cheryan, 1998).

2.2.3 Stretching

It is based on the stretching of a polymer film containing dispersed elements for which upon stretching pores are created due to stress concentration at the boundary of these sites. The precursor films for these membranes are produced in three ways:

1-Stretching of a filled polypropylene (polypropylene films incorporated with a filler), 2-Stretching of a polypropylene film with a β crystalline structure, 3- Stretching of a polypropylene film with a well arranged stacked lamellar structure. These methods are explained in the following.

2.2.3.1 Membranes by stretching of a filled polypropylene

This kind of membranes generally contains big pores (in the range of 1 μm). A filled polypropylene film with filler such as calcium carbonate is stretched out in a drawing

process and pores are generated due to crack initiation and propagation at the interface of the filler particles with matrix. The filler can be mineral or organic compound. Porosity and also pore distribution depend on the type of the filler and its interaction with the polymer matrix, blending process, percentage of the filler and also film thickness. The most important stage is filler incorporation, which includes dispersion and distribution of the filler through out of the matrix.

Different inorganic fillers can be used; that among them, calcium carbonate and barium sulfate are particularly preferred (Aoyama et al. 1990). The important issues are the shape of the particle, the price, the whiteness, the interaction with the matrix and the availability. The average particle size of inorganic filler according to ASTM C-721-76 should be 0.4 to 4 μm or smaller. Using a filler larger than that might limit the stretchability and create a non-uniform pore distribution and, in some cases, breakdown might occur. The amount of the inorganic filler to be added should be sufficient to attain the desired porosity, but it depends to some extend on the kind and particle size of the inorganic filler. Inorganic fillers such as calcium carbonate are preferably surface treated to be hydrophobic so that the filler can repel water to reduce agglomeration of the filler. For calcium carbonate a preferred coating is calcium stearate or steraric acid (Kundu et al., 2003).

Membranes have been developed by mixing polypropylene with inorganic filler ($CaCO_3$) in the following recipe (Nago et al., 1992): PP powder 39%, $CaCO_3$ (filler) 59%, plasticizer and antioxidant 2%, mixed and then extruded at 230 °C as a sheet, then stretched first in machine direction at a draw ratio of 2.8 and at 90°C and then stretched

in transverse direction at 120 °C with draw ratio of 1.8, Nago et al. found that as the mean particle size of filler became smaller, the effective porosity was increased and also the equivalent pore size became smaller. Table 2.1 and Figure 2.5 show the pore size distribution of the sheets and the optimum value of the filler size for obtaining a narrow pore distribution.

Table 2.1 Properties of the microporous PP sheets (Nago et al., 1992)

Sample No.	Mean Particle Size of $CaCO_3$ μm	Relative number of Particles*	Thickness μm	Porosity ε (%)	Maximum Pore size D_{max} (μm)
1	3.0	1	216	67	3.8
2	1.7	5.5	200	68	2.3
3	0.8	52.8	250	70	1.6
4	0.08	52800	50	72	0.46

*The weight for a particle size D_i is calculated by $4\pi (D_i/2)^3(\rho/3)$ (ρ is the density), so for a constant weight the proportion of particle numbers can be calculated (Nago et al., 1992)

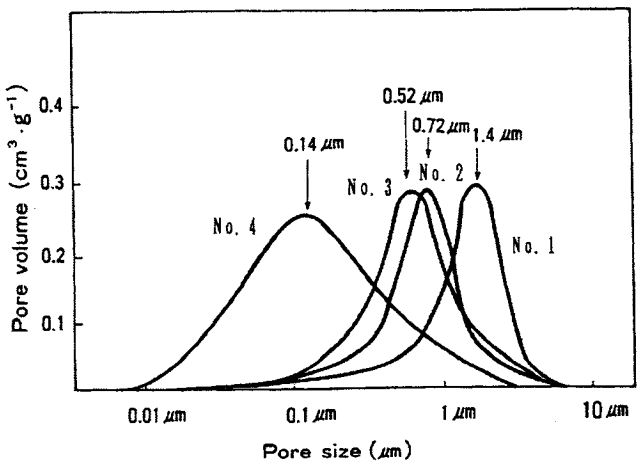

Figure2.5 Pore size distributions of the biaxially stretched samples (Nago. et al., 1992)

2.2.3.2 Membranes based on crystal transformation

This method is utilized for the polymers that have different types of crystal phase, which can be transformed under specific conditions. The most common polymer of this kind is polypropylene.

Formation of the beta crystals

The most common crystal form of polypropylene is the alpha (α), or monoclinic form, which melts at about 160°C for Zeigler-Natta polymerized homopolymers. In an injection molded or extruded parts over 95% of the crystals are typically of this type. A less common form, known as the beta (β) or hexagonal crystal form generally comprises less than 5% of the total crystals. There are some specific nucleating agents that if compounded with PP in the molten state can generate a high amount of β crystals. The red quinacridone dye is an example, although some colorless nucleating agents are also available (William et al., 1997). Fujiyama M. et al. (1988) showed the effect of process parameters and also nucleating agent on the phase transformation of polypropylene. Without using nucleating agent, the amount of β crystal would be low (less than 10% in the maximum case), and also for getting the desired amount of β crystals, the process conditions should be set properly. The authors have discussed the effect of different parameters on the β crystal amount and the most effective parameter was likely cooling conditions.

Transformation of β to α crystal

The β crystalline form is not stable and under stress transforms into other stable forms. The work of Shi et al. (1994) revealed that the β form crystal transforms into a smectic

form at a drawing temperature below 80 °C, but transforms to the more stable α form at higher temperature. Since the density of β crystals is lower than α (0.921 in comparison to 0.936 g/cm^3), this transformation causes volume contraction in the polymer bulk that leads in the creation of voids.

Chu F. et al. (1994) discussed the process of micro void formation in PP during phase transformation. PP films with different crystalline states were prepared by using 0.1% of a novel nucleating agent (NU-100 from NJStar Co.) and changing the crystallization temperature over the range from 10 to 110 °C. Crystalline structure parameters of the β form PP obtained in the process are listed in Table 2.2.

Table 2.2 Effect of the crystallization temperature on the structure parameters of PP films (Chu. et al., (1994)).

			Crystal size (A^0)		Crystallinity (%)	
T_{cr} (°C)	K^a	S^a	$t_{(300)}$	$t_{(301)}$	X_β	X_α
10	0.87	0.13	182	118	45	6.7
50	0.90	0.13	182	120	49	5.2
70	0.90	0.13	185	127	53	6.1
110	0.91	0.14	190	152	56	7.1

a: see the text in the following for the definitions

The planes in Fig. 2.6 are usually represented by their normal vectors (like 001). Sometimes, the result from WAXD is associated with a certain distance that doesn't cover a full side. For example the plan (040) represents the vector of [0, 1/4, 0]. The (300) lattice plane is parallel to the molecular chain direction, corresponding to β crystal units, and the (301) plane intersects the plane of the chains.

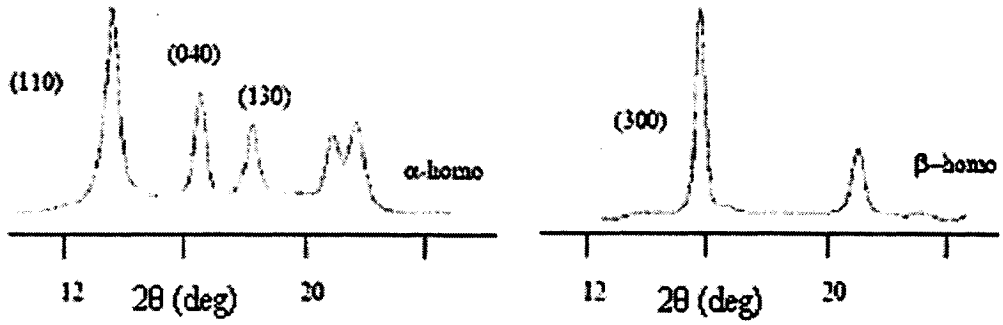

Fig 2.6 The typical WAXD spectrum for (α) and (β) crystals (Chu et al., 1994).

The content of the β crystalline part was quantified using the *K* value:

$$K = \frac{H_{(300)}}{H_{300} + H_{110} + H_{040} + H_{130}} \qquad (2.1)$$

H is diffraction intensity of the (*hkl*) lattice plane of alpha and beta crystals (measured by X-ray diffraction). *K* reaches values as high as 90% regardless of the crystallization temperature due to utilization of a nucleating agent. β crystals formed under lower temperatures had a similar order as those which formed at the higher temperatures in terms of crystal lattice. The degree of the order of the molecular chain packing in the β crystal lattice (packed in the direction perpendicular to the *c*-axis direction) was represented by the *S* value, which was given by $H_{301}/(H_{300} + H_{301})$. The value of t_{301} increased significantly with crystallization temperature. When the film was crystallized at low temperatures, the molecular chains were frozen quickly and chains could only then array parallel within limited dimensions in the direction of the *c*-axis although they are able to fold well to grow lamellae and crystallites. In contrast, in the film crystallized

at high temperature, the crystallites grow, increasing the dimensions of the crystallites along the *c*-axis.

The crystallinities of the α and β forms are introduced as below:

$$X_\alpha = \frac{H_{110} + H_{040} + H_{130}}{H_{300} + H_{110} + H_{040} + H_{130} + H_a} \qquad (2.2)$$

$$X_\beta = \frac{H_{300}}{H_{300} + H_{110} + H_{040} + H_{130} + H_a} \qquad (2.3)$$

$$X_a = 1 - X_\alpha - X_\beta \qquad (2.4)$$

where H_a is the intensity peak of the amorphous phase.

It was noted that the porosity decreased with increasing drawing temperature. At the same drawing temperature, the higher the crystallization temperature, the larger was the porosity. For the uniaxialy stretching, the results indicated that the most of the pores were formed in the early stages of the deformation. It was, therefore, deduced that in the later stages of the deformation, where the porosity reached the highest value, the micro fibrils were packed more densely in order to decrease the pore size. Biaxial drawing of the films crystallized at 10, 50, and 70 °C was difficult because of the occurrence of necking, while that of the films crystallized at 110°C and cooled in air was successfully performed at relatively higher drawing temperature. Table 2.3 shows the effect of the drawing ratio on the porosity of PP films. Chu et al (1994) claimed that the quantity and dimensions of the micro voids increased with the drawing ratio up to an optimum value. A biaxial draw ratio of 2.0×1.9 was reported an optimum value for homogenous pore distribution and porosity value at the same time.

Table 2.3 Draw ratio versus porosity for the β films drawn biaxially at 125°C

(Chu et al., 1994)

Drawing ratio	Porosity (%)
1.1×1.4	16.1
1.3×1.5	23.6
1.7×1.9	39.3
2.0×2.1	38.1
2.8×2.6	39

2.2.3.3 Membranes based on lamellae separation

If a thin precursor film with an initial proper stacked lamellar morphology is stretched pores will be generated as a result of lamellae separation. Generally, the fabrication of this type of membrane is in three main stages: 1-Production of the precursor film with lamellar morphology, 2-Annealing of the film to improve the stacked lamellae orientation and remove the defects, 3-Stretching of the film at low temperature to create voids and then at high temperature to enlarge and stabilize the voids (see Fig.2.7). A proper row-nucleated lamellar structure is necessary for the beginning of the process.

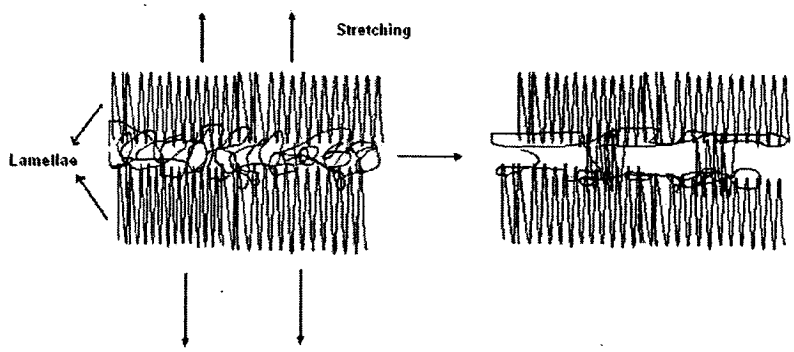

Fig. 2.7 Schematic of the pore creation by stretching

Generally three crystalline morphology types are considered for semi crystalline polymers: spherulitic, row nucleated-lamellar and fibrillar structure. Spherulites are

formed when melt is crystallized in a quiescent state (free of any stress) where the lamellae crystals grow in all directions to make an isotropic configuration

If a large enough stress is applied to the melt during the crystallization there will be a potential for formation of a row nucleated lamellar morphology. Upon applying stress the chains are entangled and stretched to form an elongated substrate that act as a base for later lamellae crystallization. As the temperature goes down the shorter chains are crystallized on the elongated substrate to form a row-nucleated lamellar structure. Figure 2.8 shows a SEM micrograph obtained in our lab depicting a lamellar structure.

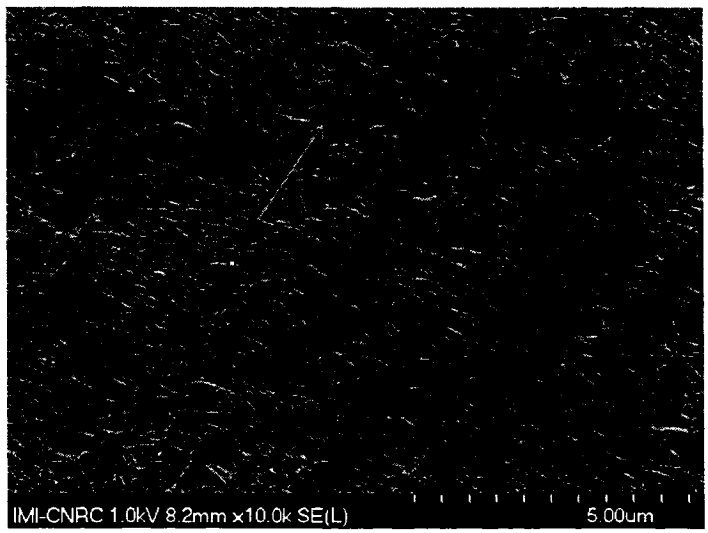

Fig.2.8 A typical row nucleated lamellar structure from HDPE.

For the fibrillar structure the best example is when the spherulitic structure goes under high stress deformation. In this case the initial crystal lamellae are broken apart in small pieces and reorient and recrystallizied in the form of long fibrils in direction of stress as shown in Fig.2.9.

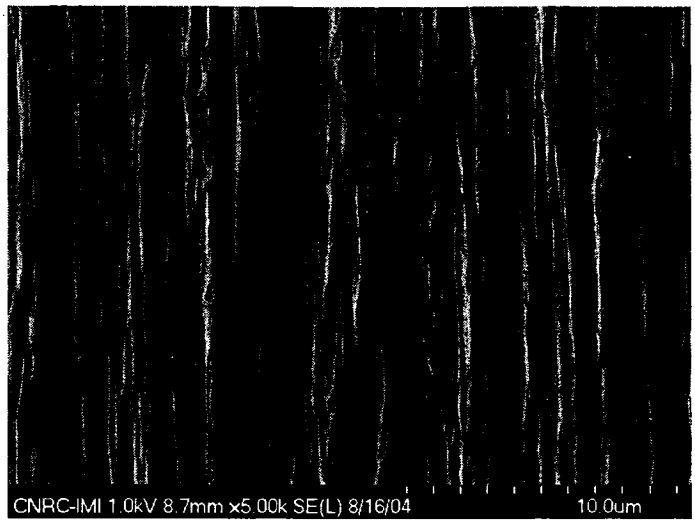

Fig.2.9 Fibrillar structure obtained from a stretched HDPE.

Row nucleated lamellar structure

The important issues for obtaining the proper lamellar structure are: 1-The number of threads (initial elongated nuclei), 2-The length and diameter of the threads, 3- The lamellae thickness and the orientation 4- The amorphous phase orientation and content (which include the density of tie chains per area and their length).

The lamellar morphology can be obtained by controlling the crystallization process. To generate well-oriented and highly planar lamellae, we suggest the utilization of a high extensional stress during extrusion with polymers of relatively long uniform chains that quickly crystallize (Sadeghi et al., 2005). This can be controlled through a rapid cooling process in conjunction with a limited film thickness to achieve a good rate of heat transfer. Rapid cooling will prevent chain relaxation and polypropylene and polyethylene generally show relatively fast crystallization kinetics, which promotes the preservation of extended chains. Self-seeding is the nucleation mechanism by which

row-nucleated lamellae occurs where the nucleating sources are generally the extended-chain (threads). Faster cooling rates will generate more elongated fibrils (nucleating sites) that upon crystals growth, they might interfere with each other. This is important because if lamellae grow very long (without any interruption), there will be a possibility for lamellae twisting as illustrated in Fig. 2.10. Keller et al. (1993) further proposed that the extended chain crystals (thread-like precursors) are essential to the formation of planar stacked lamellae morphology. According to Keller et al. (1993), the level of stress influences the concentration of the extended-chain fibrils, which then influences the degree of the lamella twisting. After thread formation, lamellae are built based on these threads through the process of secondary crystallization. This crystallization takes place after the primary crystallization (Agarwal et al., 2003).

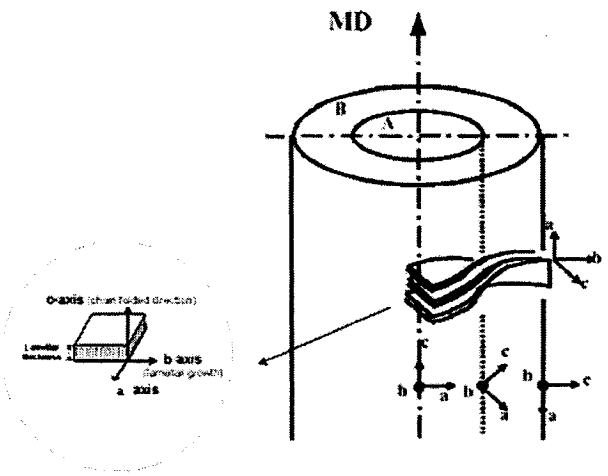

Figure 2.10 Scheme depicting the reasons behind intermediate orientations between predominant *c*-axis and a-axis orientation in terms of increasing diameter between row nucleating crystals as proposed by Nagasawa et al., (1973).

Higher concentrations of extended-chain crystals then lead to a greater number of nucleation sites and thus sooner and more lamella impingements will occur. The theory

of impingements was first proposed by Nagasawa. et al. (1973). The cylinder diameter representing the growth of the lamellae as shown in Fig 2.10 is a function of the concentration of nucleating fibers in a given sample. Kumaraswamy et al. (1999) investigated shear induced crystallization in polypropylene. They related the online measured birefringence to the arrangement of the polymer chains in the melt state and also crystal state.

Kumaraswamy et al. (1999) declared that upon applying a certain amount of shear stress on the polypropylene melt, the birefringence during crystallization jumps suddenly, which suggests the generation of the long oriented chains during shear. They also suggested that temperature should also be kept low for the following step to preserve the oriented states for the chains; otherwise, chains will relax after stretching due to their tendency to return to their initial coil state. However, the effect of temperature in extrusion process is surprising: although a lower crystallization temperature preserves the initial extended state of the polymer chains, but in the other hand reduces the processability of the melt to be stretched at the die. The low temperature also adversely affects the chain mobility for the secondary crystallization (lamellae growth). Therefore, an optimization of the temperature seems necessary.

Somani et al. (2003) investigated the shear induced crystallization of PP by SAXS (Small Angle X-Ray Scattering). In crystallization at 140° C and after step shear (shear rate 102 s^{-1}, strain = 14.28), no equatorial reflections, which the most probably corresponded to threads were seen in the SAXS patterns. One explanation is there might be very few thread crystals and far apart that they could not be detected in SAXS.

In planar morphology (mostly seen in fiber spinning) some tiny primary nuclei, difficult to be identified by SAXS or TEM (transmission electron microscopy), can be responsible for the growth of the oriented crystals (see Fig.2.11). Yu et al. (1995) mentioned the same phenomenon (well stacked lamellar morphology without any detectable fibrils) for polyethylene. It can be concluded that initial threads can be formed either by some singular extended chains (which are not visible through SEM or SAXS) or a linear assembly of oriented chains, which form primary crystals visible by SEM and SAXS.

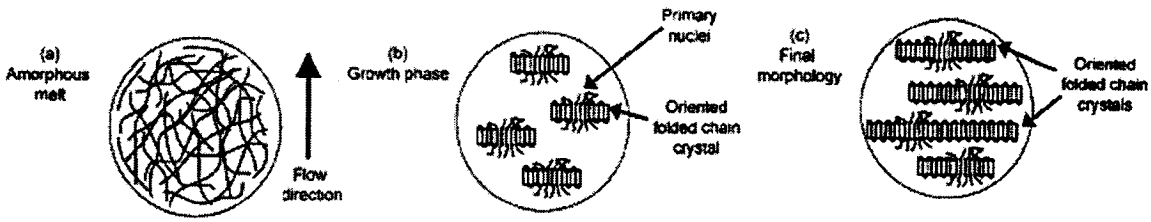

Figure 2.11 Schematics of the formation of shear-induced primary nuclei and subsequent growth of oriented crystals at the surface undergoing maximum orientation in step-shear experiments (Somani et al., 2003).

Somani et al. (2003) also showed that the deformation rate must be high enough to orient and align the polymer chains in the melt to form stable nuclei in the flow direction. After a certain value of deformation rate, the fraction of oriented material reaches a plateau. There is dependency between the critical rate (rate above which oriented chains are detected) and molecular weight, Keller et al. (1993) proposed the following relationship in the case of elongation flow:

$$\dot{\gamma} \propto M^{-\beta} \qquad (2.5)$$

where γ is the critical elongation rate, M is the critical molecular weight, β is a factor found to be equal to 1.5 for polyethylene solutions. In addition to deformation rate, strain is also important; at low strains (even at high deformation rate) the orientation and alignment of polymer chains are not sufficient to form nuclei. Compared to the elongation flow, shear flow is usually considered a weaker flow to provide extension of polymer chains. At a given shear rate, only those molecules having a chain length (molecular weight) above a critical value can form stable oriented row nuclei, while the rest of the molecules will remain unstretched. Then the result would be a bimodal distribution of chain molecules represented by a dual population of oriented and non-oriented chains. Increasing shear rate does not promote the chain extension any more substantially, but increases the amount of elongated chains by increasingly "cutting into" the distribution from the high molecular tail downward, see Figure 2.12 (Somani et al., 2003).

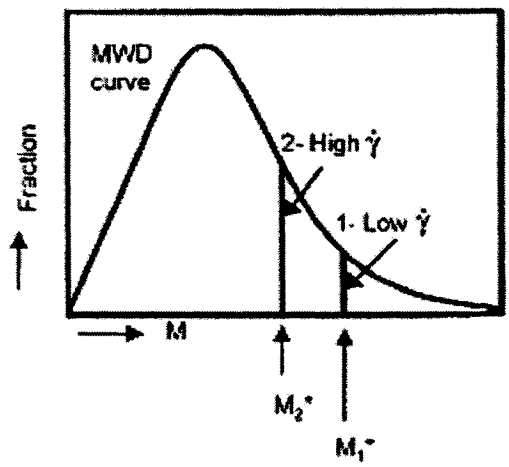

Figure 2.12 Critical molecular weight (M^*) on MWD curve based on the imposed shear conditions (Somani et al., 2003).

The "critical molecular weight" (M^*) on the curve shifts to a higher value at low deformation rates as showed by lines (1- low shear rate) and (2- high shear rate). The area under the MWD curve represents the fraction of material above or below the critical molecular weight. It was claimed that the value of M^* is more sensitive at low shear rates than at high shear rates, reaching a plateau at high shear rates. The most important issue in the stretching of the chains is the chain relaxation process, it has been shown that temperature dependency of the relaxation time is much stronger than that of the zero shear viscosity (Somani et al., 2003). Nogales et al. (2001) have studied shear-induced crystallization of isotactic polypropylene with different molecular weight distribution. They suggested that the development of the oriented morphology in the resin with higher molecular weight is much faster than that for the lower molecular weight resin.

The motion of polymer chains due to an applied deformation field is governed by several factors, such as entanglement density, friction coefficient (due to local interactions between chain segments), chain stiffness, relaxation time, etc. Under isothermal conditions, the molecular weight and chain architecture are expected to play major roles in governing the extent of elongation and stability of the oriented structures after cessation of shear. Longer chains and branched molecules both take a longer time to relax after deformation than shorter ones, and thus, have a better chance of being oriented. The longer chains from the high molecular weight tail would give rise to orientation-induced nuclei due to higher orientation compared to the shorter chains. The short chain molecules relax in a very short time after deformation and hence cannot form nuclei under flow.

Nogales et al. (2001) proposed a method for calculating the critical molecular weight for orientation. They considered the oriented structure based on the change in the radius of gyration and the degree of chain extension is represented as the ratio of the radius of gyration of the extended chain to that of non-oriented chain. The comparison between the radius of gyration in direction parallel to the deformation field ($R_g \parallel$) and the radius of gyration in the perpendicular direction to the deformation field ($R_g \perp$) can represent finally the orientation. For their chosen experimental conditions (T = 150 °C and shear rate of $57\,s^{-1}$) they reported a value of 250 (kg/mol) for the critical molecular weight of polypropylene.

Later on, Seki et al. (2002) prepared a very high molecular weight polypropylene with M_w = 923.2 (kg/mol), through the fractionation of a regular PP, and blended it with a moderate molecular weight PP, Using this approach they showed that the addition of less than one percent of this polypropylene to a typical iPP with moderate molecular weight (186 kg/mol) significantly influenced the crystallization kinetics and results in a lamellar morphology.

Agarwal et al. (2003) studied the shear induced crystallization in chain branched polypropylene. They investigated several polypropylenes with different branching index while their number-average molecular weights were relatively constant and the higher molecular weights (M_w, M_z and M_{z+1}) increased with the branching level. They used four PPs: PP01, PP05, PP07 and PP13 coded based on branching. It was found that the branching level does not change the melting and crystallization temperatures. They studied the SAXS pattern for shear induced crystallization of a branched polypropylene.

The showed that equatorial and meridian maxima appeared when shear was applied to the melt. They attributed the equatorial peaks to fibrils and meridians to lamellae and also revealed that the intensity of the patterns was enhanced with increasing branching (see Fig.2.13 and Fig.2.14).

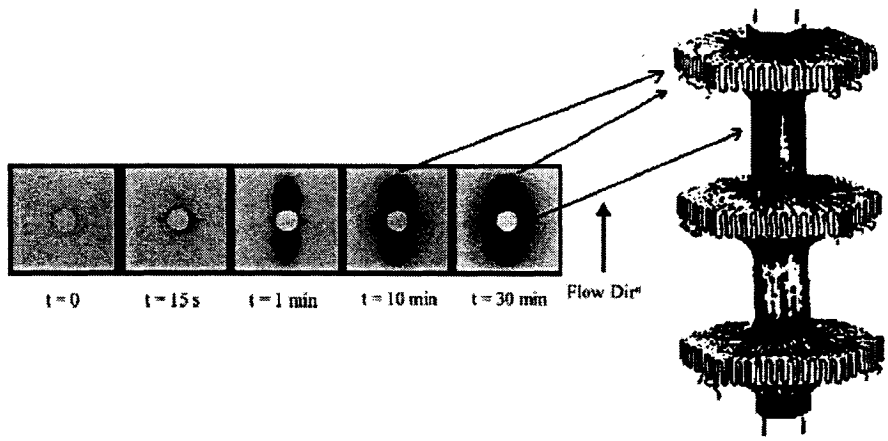

Fig.2.13. 2D SAXS patterns of the LCB 013 polymer melt before and at selected times after shear: shear rate) $60s^{-1}$, t_s(shearing time) 0.25 s, *T)* 140 °C (Agarwal et al., (2003)).

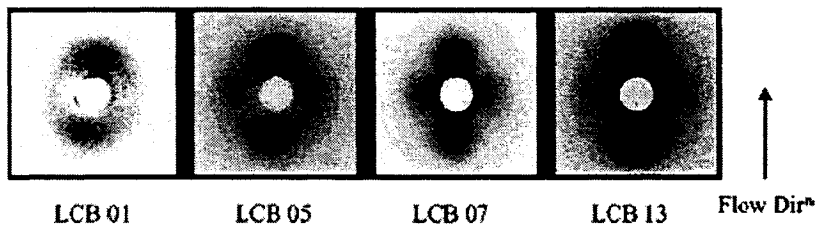

Fig.2.14 Comparison of 2D SAXS patterns of the four LCB-iPPs,: shear rate) $60s^{-1}$, t_s(shearing time) 0.25 s, *T)* 140 °C (Agarwal et al., (2003)).

The emergence time of the meridian maximum was estimated as 30 and 60s for LCB13 and LCB07, respectively. It is important to note that equatorial streak emerged before the meridian maximum. The long spacing was reported to be in the range of 23-28 nm. The crystal orientation was stronger for the branched polypropylene in comparison to linear PPs. A larger crystallization rate for the branched PP was also reported in

comparison to linear PPs. The higher crystallization rate in branched PPs is likely due to greater nucleation rate as a result of chain orientation. Agarwal et al., (2003) calculated the Avrami crystallization constant for the samples, as shown in Fig.2.15.

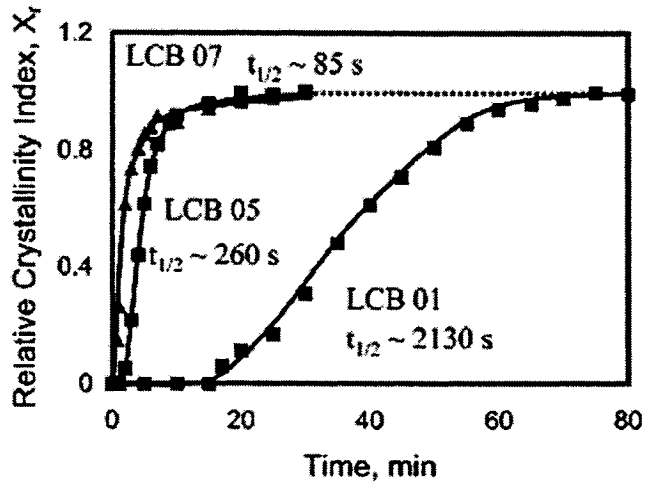

(a)

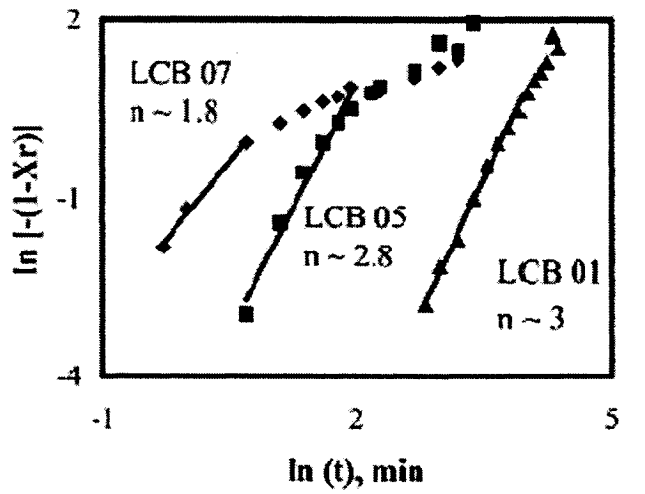

(b)

Fig.2.15 (a) Half-time of crystallization for LCB 01, 05, and 07 polymers after: shear rate = 60 s^{-1}, t_s =0.25 s, T= 140°C, (b) Avrami plot of the crystallization data for LCB 01, 05, and 07 polymers at 140 °C after shear rate = 60 s^{-1}, t_s (shearing time)= 0.25 s, (Agarwal et al., 2003).

In the Avrami model ($1-X=e^{-kt^n}$) k is dependent on the shape of the growing crystals and the type and amount of nuclei (thermal or isothermal). The exponent n depends on

the nucleation type and growth geometry but not on the amount of nuclei. In isothermal type of nucleation for n equal to one, a linear or rod like crystal growth geometry is observed. For n equal to 2 a disk-like geometry is expected and for $n = 3$ it would be a spherical form. For a linear polypropylene, n was found to be equal to 3, which indicates non-oriented spherulitic crystal growth. The branched grades n values less than 3 was reported that indicates rod/disk like crystal growth. The most probably rod structure for LCB07, where n was near one, is due to the larger percentage of extended chains, while for LCB05 it is more disk like.

2.4 Membranes from HDPE by stretching

In a specific study by Yu (1995) two high density polyethylene (HDPE) resins differing in M_w but with similar M_n, were melt-extruded under approximately the same conditions. These two melt extruded HDPE films possessed similar values of crystalline orientations, yet their morphologies were different. Specifically, the film produced from the higher M_w resin had evident crystal threads whereas the lower M_w film did not show pronounced threads as studied by TEM (transmission electron microscopy) and WAXS. However, both films possessed planar lamellar morphologies. Melting temperature and crystallinity were not affected significantly by the process conditions. Measuring the orientation for the films, they claimed that the share of amorphous orientation in total orientation function was very small. Yu found that using a larger die gap could increase the concentration of fibril nuclei where a larger draw ratio (higher melt speed and strain rate) and melt strain should be used to obtain the desired thickness.

The presence of fibril nuclei improved the mechanical properties such as the tensile modulus. It also enhanced the orientation function. They performed annealing under a slight strain (3%) for the samples and observed that it was more effective in comparison to a free annealing stage. The annealing temperature was in the range of 105°C to 120°C and it was noted that the annealing time after a certain period had no effect on the structure. The samples were cold stretched at room temperature in the range of 40-80 %, and hot stretched around 120 % at temperature of 115 °C. Cold stretched samples at higher percentage (more than 40%) showed a lower permeability at constant hot stretching. The smaller the amount of micro voids created by the cold stretching, the larger the micro pore size was, as expected for the hot stretch process. Microporous structure was more uniform with the resin of broader molecular weight distribution. The micro voids were possibly initiated in the region with less density of the tie chains. Yu concluded that a certain level of orientation (f=0.45 measured by WAXD) in the precursor film is necessary in order to produce higher permeable membranes. There was a thermal shrinkage in the membrane after stretching and the shrinkage was calculated by measuring the length between two marks labeled on the sample along the stretching direction. Annealing at 120 °C in comparison to 105°C could significantly increase the dimension and uniformity of long spacing (overall crystal and amorphous phases thickness) in the HDPE films.

2.5 Membranes from PMP and POM by stretching

Johnson (2000) developed membranes from poly (4-methyl-1-pentene) (PMP) and polyoxymethylene (POM) by stretching. Following the extrusion stage, the effect of annealing (second stage) on film properties was investigated. The annealing variables such as the temperature, time, and level of deformation in extension applied during annealing were studied. The annealed films were then subjected to uniaxially stretching (third stage) consisting of a cold and hot step, respectively, with deformation along the extrusion direction. It was found that the starting precursor film morphology and orientation, annealing conditions, and stretching variables had impacts on the final porosity and permeability of the membrane. Johnson (2000) used a blown film unit for film production with different drawing rates (line speed). They could obtain a lamellar morphology by controlling the process conditions, i.e. large drawing rate (draw ratio) and quenching rate. Upon formation of the lamellar morphology, annealing was applied for improving the structure of the lamellae. Pores as the result of lamellae separation could be made through out the film by stretching. Lamellae separation took place at temperatures above the T_g of the specific semi crystalline polymer. This is in contrast to amorphous polymers, which reportedly form voids (crazes) upon deformation at temperatures below their respective T_g. Cold stretching is to nucleate the micro pores via a ductile drawing of the amorphous phase from crystalline part (the chain pullout mechanism). The hot stretching step further increases the pore size by a partial ductile drawing of the crystal phase. To prevent major chain rupture in the hot stretching process, the chains must be pulled out of the crystals with energies below those needed

for rupture. Figure 2.16, shows lamellar separation when stretching is applied.

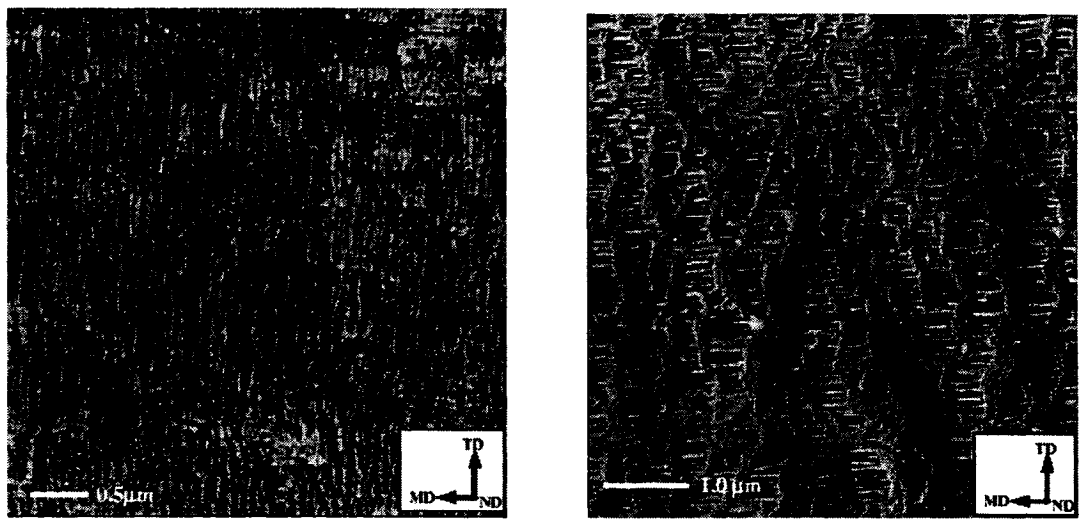

(a) (b)

Fig. 2.16. AFM images of PMP (a) Annealed at T_a= 205°C and t_a = 20 min. (b) cold stretching at 70 °C to 50 %, then hot stretching at 160°C to 90 % without any relaxation (0 %) (Johnson (2000)).

Figure 2.17 is a plot of the Gurley number (the Gurley number is an indication of the permeability of the membrane and is defined as the time required for 10 mL of air to pass through one inch square section of film at a constant pressure of 12.2 inches of H_2O based on the ASTM D726) versus cold stretching.

Each time one of process variables changed to observe the effect on Gurley number while the rest of other variables were kept constant in standard condition. What was referred to as standard conditions were: free annealing at a temperature equal to 205°C for 20 min, followed by cold stretching at 70°C to 50 percent extension, then hot stretching at 160°C to 90 percent extension without any relaxation

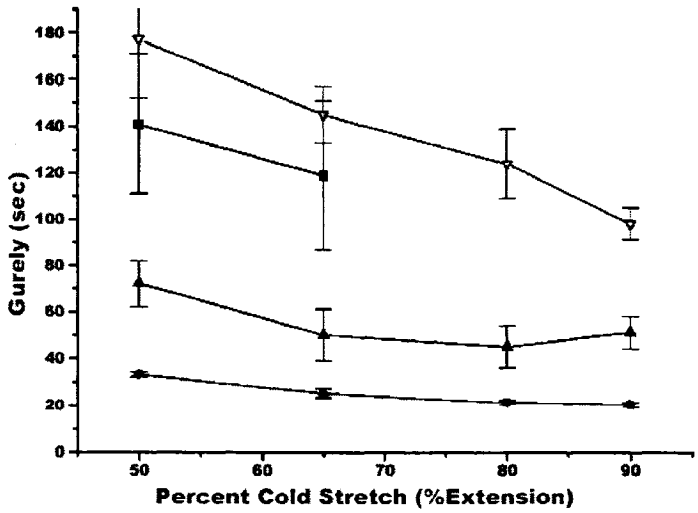

Figure 2.17 Effect of the cold stretching parameters (T_{co} and %CS) on the Gurley number for PMP stretched films (■) T_{co} = 40°C, (●) T_{co} = 70°C, (▲) T_{co} = 80°C, and (▼) T_{co} = 90°C (Johnson et al. (2000)).

Each curve also provides results for a constant value of cold stretching temperature. As the specific extension level was increased from 50 to 90 %, the Gurley number decreased. However, if the Gurley number was normalized by the final film thickness (not shown here), it would be observed that there is a slightly higher normalized Gurley for a film cold stretched at 90 % versus those stretched at either 65 or 80 %. The local minima in the normalized Gurley number would occur at approximately 80 % of the cold stretching. Johnson (2000) found that the temperature of cold stretching (up to the 70°C) improves the permeability as the Gurley number decreases. The films produced using the cold stretching temperature of 90 °C possessed the lowest permeability (largest Gurley number) for constant % CS (cold stretching) values. They concluded that the pore nucleation was improved as a result of higher cold stretch levels and more uniform pores and larger number of the micro pores will be found in the final membrane.

The dependence of the Gurley number on both the hot stretch (HS) parameters (T_{hs} and %HS) is shown in Figure 2.18. Indeed, the Gurley number decreased as the specific extension level is increased. However, if the Gurley numbers were normalized versus membrane thickness, the film produced using the highest level of hot stretch extension (90 %) had an equal if not a slightly larger normalized value versus the % 80 HS (80% hot stretching) film.

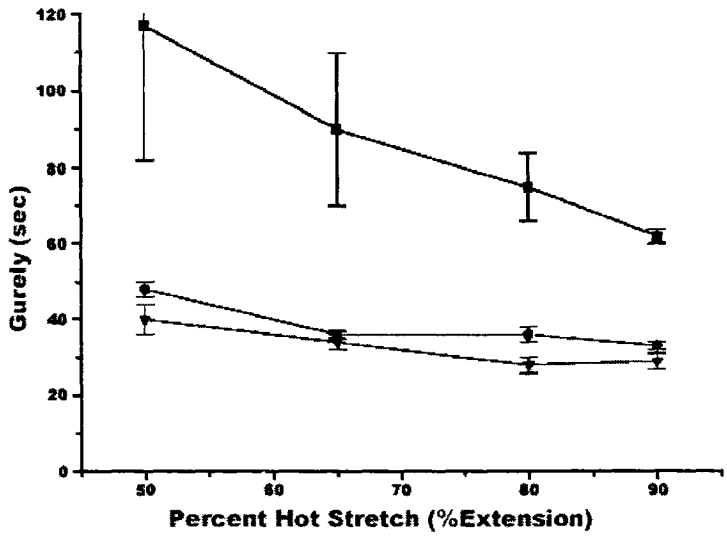

Figure 2.18 Effect of the hot stretching parameters (T_{hs} and %HS) on the Gurley number for PMP Stretched films (■)T_{hs}=120°C, (●)T_{hs}=160°C and (▼)T_{ca}=180°C (Johnson et al. (2000)).

It was also observed that the hot stretch temperature, T_{hs}, influenced the Gurley number. For a constant hot stretch level, the Gurley number decreased as the specific hot stretching temperature increased. This occurred regardless whether or not normalization of the Gurley number to film thickness was done because of a constant total extension. The stretching ratio for each stage and the associated Gurley numbers are shown in Table 2.4.

Table 2.4 The Gurley numbers for PMP at different stretching ratios. (Johnson et al. 2000).

%HS (%Extension) \ %CS (% Extension)	50	65	80	90
50	100% 48 ± 5	115% 35 ± 3	130% 34 ± 2	140% 30 ± 2
65	115% 36 ± 2	130% 30 ± 2	145% 28 ± 3	155% 24 ± 1
80	130% 36 ± 2	145% 27 ± 1	160% 23 ± 2	170% 19 ± 2
90	140% 33 ± 1	155% 25 ± 2	170% 21 ± 1	180% 20 ± 1

The influence of the stretching temperature on the Gurley number and pore size were also studied. As shown in the Table 2.5, when the cold stretching temperature increased from 40 to 70 °C, the Gurley number decreased. However, upon increasing the temperature above 70 °C, the Gurley number increased.

Table 2.5 The effect of different T_{cs} and T_{cs} combinations on the resulting *PMP* micro porous film Gurley number – all other annealing/stretching parameters remained constant with the standard condition. (Johnson 2000).

T_{hs} (°C) \ T_{cs} (°C)	40	70	80	90
120	NP	62 ± 2 sec	88 ± 14 sec	NA
160	141 ± 30 sec	33 ± 1 sec	66 ± 10 sec	177 ± 25 sec
180	86 ± 16 sec	29 ± 2 sec	34 ± 4 sec	67 ± 12 sec

NP: Sample was not able to produced because of rupture in cold stretching
NA: The test was not attempted

The initial decrease in the Gurley number with increasing cold stretch temperature is a result of greater mobility within the amorphous phase rather than that of the crystal phase. This is because at 40 °C a difference of only 5 °C exists between the cold stretch

temperature and the PMP glass transition of 35°C. The more limited amorphous mobility at 40 °C also accounts for the greater frequency of film rupture during stretching relative to higher cold stretch temperatures. However, upon stretching at higher cold stretch temperatures, the chain axes are able to move through the crystal more readily as a result of greater activation of the α relaxation.

While chain slippage in the crystalline phase is not desirable for the cold stretching step, it is exactly the desired factor in the hot stretching step. This resulted in greater lamellae separation as a consequence of larger drawing. As displayed in Table 2.5 one the Gurley number was the lowest for a hot stretch temperature of 180 °C. At lower hot stretch temperatures, the Gurley values were not as low when compared with films hot stretched at 180 °C, when all other variables were equal. A problem with annealing was also pointed out that for a very high annealing temperature (215 °C): permeability began to decrease. It was speculated that this possibly was a result of macroscopic lamellar melting during annealing, which would adversely affects the lamellae separation upon stretching.

The results for POM are not covered here since almost similar trends as PMP were observed.

2.6 Membranes from polypropylene by stretching

Chen et al. (1994) analyzed the micro porous membranes of the CELGARD Company made of polypropylene and polyethylene. They found that the degree of orientation in the PE and PP melt-extruded films was a critical parameter in controlling the pore

structure in membranes. Birefringence measurements showed that both annealing and higher extrusion speed promoted orientation in films. STM (scanning tunneling microscopy) and FESEM (field emission electron microscopy) images clearly showed the lamellar structures, which were found to be more pronounced and more aligned with respect to the machine direction and to the film plane normal in the annealed films, than in the outstretched extruded films. Lamellar structures in the PP film precursors were more difficult to observe by SEM than in the PE film precursors. This difference in lamellar structures in the film precursors resulted in the different surface pore morphologies between PE and PP of the CELGARD membranes. The PP membranes exhibited non-significant three dimensional surface topography and hence it was very difficult to be observed by electron microscope. SAXS (small angle x-ray scattering) results showed increases in lamellar spacing as well as improvement in the distribution order of lamellar spacing upon annealing. Annealing also resulted in a slight increase in crystallinty. Higher molecular weight was also found to increase lamellar thickness.

Kim et al. (1994) used a melt spinning method to make microporous fibers from the polypropylene of molecular weight of 200 kg/mol. They used a counter current type air quencher for effective cooling at the die. The samples were first annealed at 140 °C for 30 min and then cold stretched in three steps consequently to reach the total stretch ratio of 154 %. Heat setting steps were applied at 140 °C between the cold stretching stages for 1 min. A porosity of 53 % was measured by mercury porosimetery and the average pore dimension of 0.3× 0.1 (length× width) was reported.

CHAPTER 3

METHODOLOGY AND MATERIALS

3.1Originality of the work

The literature review showed very few investigations concerning the development of membranes by stretching through the lamellae separation. In our search an extensive work to investigate the individual stages for the development of microporous polypropylene membranes by stretching is absent.

Polypropylene possesses good mechanical properties and can be found in different forms and grades. It also shows a better thermal stability in comparison to polyethylene. The study of each individual step in the process of membrane development and understanding the role and influence of the involved parameters on membrane structure could lead us to a better control of process and to the development of membranes of better properties.

3.2 Objective

The objective of this project is to develop microporous membranes from polypropylene by stretching and study each individual stage in terms of effective involved parameters.

3.3 Methodology

The methodology to tackle the mentioned objective has been presented in form of individual steps in the following flow chart:

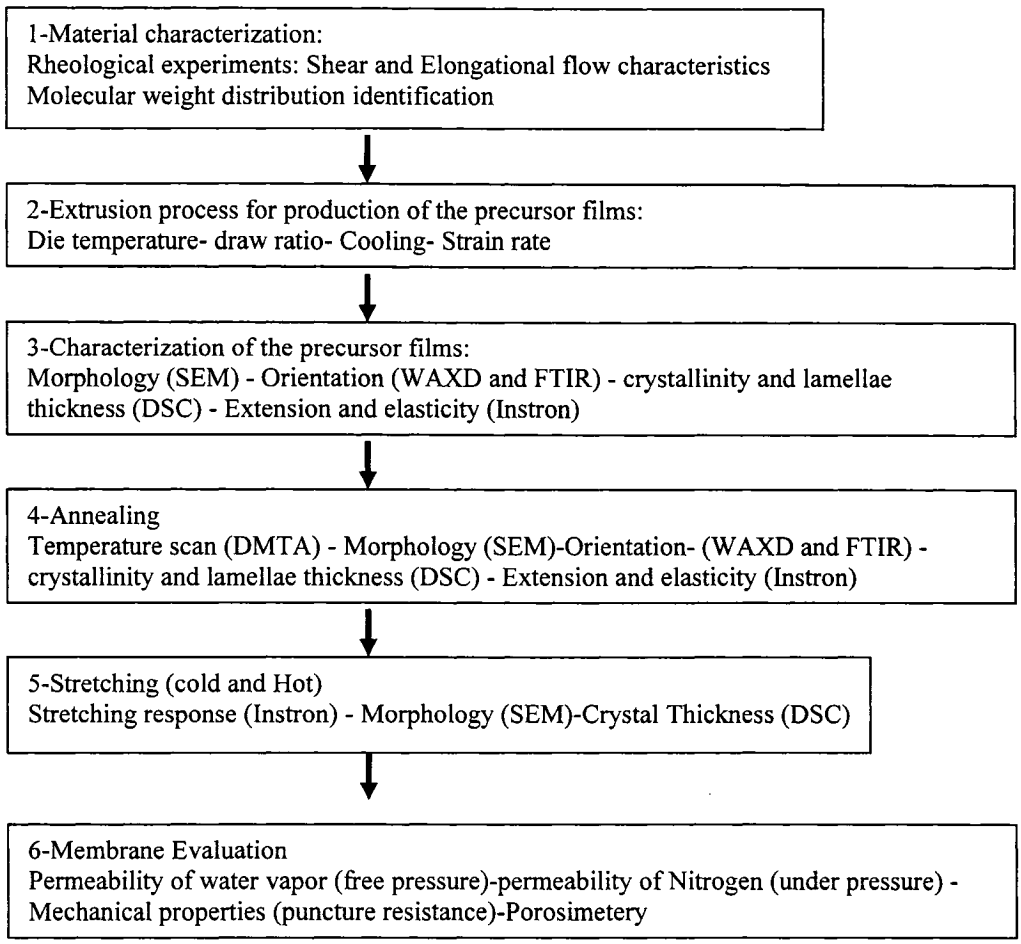

In our methodology initially a material characterization in term of melt rheology was carried out. Then the precursor films from the resin were prepared by cast extrusion. The films were analyzed in terms of orientation and physical properties. Annealing was performed on the films and then stretching was performed to form membrane.

The membranes obtained from the process were evaluated for the performance trough permeability and porosimetery tests.

3.4 Materials

Polypropylenes different in MFI (melt flow index) and molecular weight were selected to study the effect of molecular weight on the structure of the membranes. The effect of molecular weight firstly is observed in the extrusion process. As we discussed in the literature review, the precursor films should be produced under efficient cooling conditions (in this project two air jets were used to quench the film within 1 cm from the die) and a large draw ratio (between 40 to 70).

For the material side the presence of the long chains are needed to create elongated threads for the nucleation stage, but a very high number of them has two destructive effects. First, it reduces the processability and second it will alter the membranes performance since it generates very long and thick threads binding the lamellae strongly together. The strong connection by threads makes the lamellae separation difficult.

For this project five polypropylenes were selected as their properties provided by suppliers are presented in Table 3.1. A group of low and high molecular weight homo polypropylene was chosen to investigate the effect of molecular weight and structure on the properties of the precursor films and final obtained membranes.

Table 3.1. Polypropylene grades used

Resin Code	Company	MFI 230°C/2.16 kg	Nomenclature in this work
PDC1280	Basell	1.2	PP12
Pro-fax 6823	Basell	0.5	PP05
Pro-fax 814	Basell	2.8	PPB
PP4292E1	ExxonMobil	2.0	PP20
PP4612E2	ExxonMobil	2.8	PP28

PDC1280 is a general purpose grade and Pro-fax 6823 possess the lowest MFR in the Basell company list and assumed to have the highest molecular weight. Pro-fax 814 (Pf814) is a long chain branched polypropylene. It was selected because of the effect of branched chains on the relaxation time of molten polyolefins. PP4292E1 and PP4612E2 are the grades used for the production of oriented films according to ExxonMobil. The manufacturer reports these two resins as homopolymers which have a bimodal distribution of molecular weight. An FTIR test was carried out and no trace of ethylene was found in the absorption spectrum of the resins, or at least the amount of ethylene is very low that cannot be detected through FTIR.

3.5 Material Characterization

3.5.1 Rheology

For rheology characterizations thermal stability of the resins is a matter of concern since polypropylene is prone to degradation through chain scission reaction. As it is seen a combination of high temperature and oxygen will create radicals, which consequently split in two smaller macromolecules:

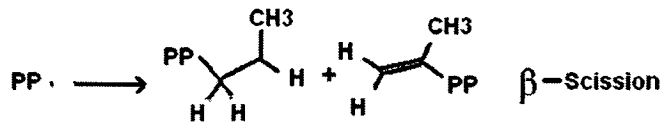

(3.1)

The chain scission for polypropylene will result in a drop in molecular weight and decrease in viscosity. Most of the commercial PPs have already some antioxidant included (the type and content depends on the producer company), but there is a shelf life for the efficiency of this antioxidant. Normally 1 year after the production date, the efficiency of this antioxidant should be verified again.

For the rheological experiments we added 0.2% of antioxidant (B-225 Irgonax) to the resins to make sure of thermal stability during the tests. To verify this we monitored the complex viscosity versus time through a time sweep test, as shown in Fig. 3.1.

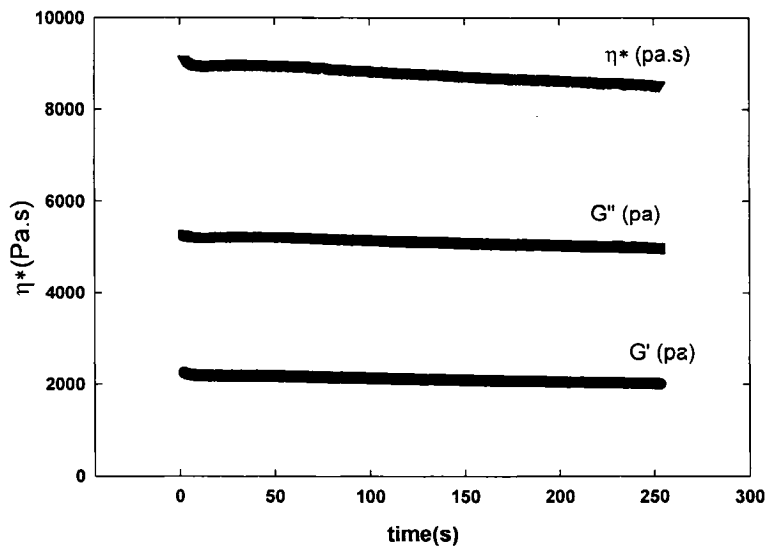

Figure 3.1 Time sweep test for the PP12 at 230°C

The change in viscosity was less than 7% during 4 hours test at 230°C that is acceptable for our experiments. The linear viscoelastic behavior was obtained using a Rheometric

Scientific SR-5000 controlled stress rheometer with 25 mm diameter parallel plates. Stress sweep tests were performed to determine the linear viscoelastic region and the frequency sweep tests were carried out within the linear region.

G' and *G''* were obtained through the frequency sweep tests at 230 °C. In the plot of *G'* and *G''* versus frequency, the cross over point also could give an idea about domination of elastic modulus over loss modulus. The graph for the resins at 230°C has been shown in the Fig. 3.2. The cross over happens first for PP05 followed by PP12, PP20 and PP28 which seems to follow the molecular weight trend. The case for PPB is different since negligible differences between the two modules are observed and it can be said that above the frequency of 30 (rad/s) the modules are approximately equal.

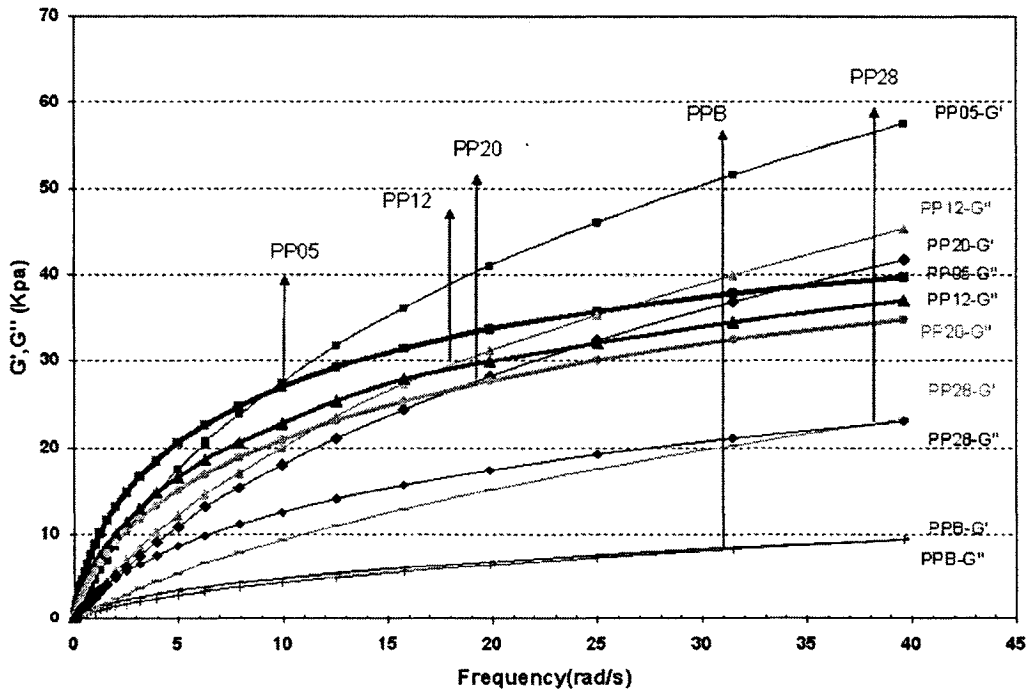

Fig.3.2 *G'* and *G''* for the resins obtained from small amplitude oscillatory shear tests at 230°C

The die temperature (extrudate temperature) can be set from 190 to 240°C for our case. To verify this effect, we studied the impact of temperature on the relaxation spectrum. We selected two resins: PPB and PP28 (low molecular weight PP) as they have been shown in Fig.3.3. It is clear that lowering temperature enhances the relaxation time (peaks at longer times in the weighted relaxation spectra).

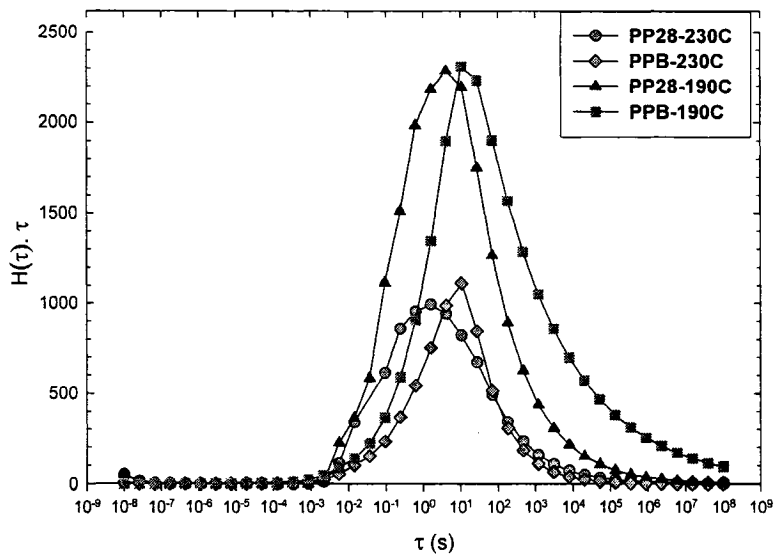

Fig.3.3. Relaxation spectra for PPB and PP28 at two temperatures 190 and 230°C.

3.6 Process

Two processes were used for production of the films in this project. The blown film and cast film extrusion lines both available in IMI (Industrial Material Institute, Boucherville-QC). The blown film line, Fig.3.4 (a), was equipped with a fan that blows air to film surface creating a frost line between 8 and 15 cm (depending on applied process conditions). The extrusion temperature was set from 180 to 230°C. The range of flow rate was 8-15 kg/h and the opening gap for cooling was adjusted between 20 to

100%. The films were picked up with speed of 0.06-0.3 m/s and final draw ratio was between 20 and 50. For cast film extrusion as is shown in Fig.3.4 (b) a simple twin screw extruder with L/D=32 was employed and extrusion temperature was set 190 to 220°C. Flow rate was much lower (1-2 kg/h) and die temperature was set on 220°C and the films were picked up with draw ratio of 20 to 65 that corresponds to roll speed (V2) of 0.02-0.1 m/s .

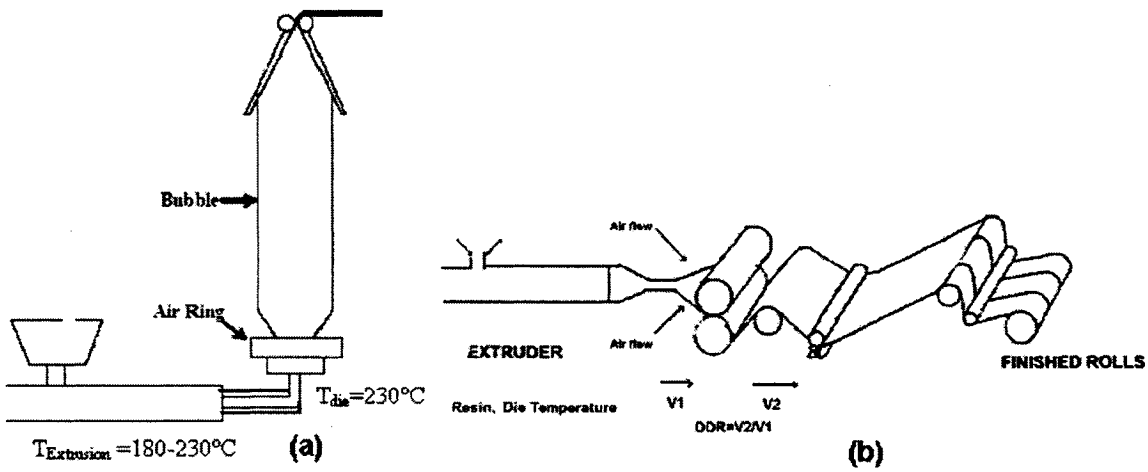

Fig.3.4.The sketch of the processes used for the production of precursor films

Chapter 4

ORGANIZATION OF ARTICLES AND THESIS STRUCTURE

Chapters 5 to 7 give the main results of this thesis and corresponding scientific findings. Each of these chapters consists of an article. The following is a brief description of each chapter and the link between them:

- Chapter 5 explains the conditions for obtaining a row nucleated lamellar structure for polypropylene
- Chapter 6 studies the obtained lamellar structure from physical and mechanical points of view.
- Chapter 7 covers the stretching of the precursor films leading to the formation of porous structure and evaluation of the performance of such porous structure.

Chapter 8 is a general discussion and summary of the results obtained in this study. Finally, a conclusion and recommendations for the future work are presented in Chapter 9.

CHAPTER 5

Study of Polypropylene Morphology Obtained From Blown and Cast Film Processes: Initial Morphology Requirements for Making Membrane by Stretching*

5.1 Presentation of the article

The objective of the first article was to study the appropriate conditions for the generation of a row-nucleated lamellar structure that is the first step for membrane formation. These conditions include resin and process parameters. We selected polypropylenes of different molecular weights and structure and for the process two methods (blown and cast film) were used. It was found that relaxation time of the polymer chain is an important factor in obtaining a row nucleated lamellar structure. From process points of view, cooling system was found to be a key element in generation of such crystalline structure.

J. Plastic Film Sheet, 21, 199-216 (2005)

5.2 Study of Polypropylene Morphology Obtained From Blown and Cast Film Processes: Initial Morphology Requirements for Making Membrane by Stretching

F.Sadeghi[1], A. Ajji[2] and P.J. Carreau[1]
1) Center for Applied Research on Polymers and Composites, CREPEC, Ecole Polytechnique, Montreal, QC, Canada
2) Industrial Materials Institute, CNRC, Boucherville, QC, Canada

5.2.1 Abstract

Four different polypropylene resins were extruded using the tubular and the cast film processes. The resin's morphology was observed by SEM and the effect of extrusion processing variables on the morphology was investigated. Melt rheological experiments were also carried out to characterize the polymer melt. It was found that the molecular weight distribution and the chain structure as well as the processing conditions have important effects on the morphology. Efforts focused on developing a lamellar morphology from polypropylenes through the control of processing conditions. The possibility of generating a porous membrane from the initial lamellar morphology using a stretching technique was evaluated. It was found that the initial lamellae arrangement of the precursor films and the stretching conditions play a significant role in obtaining a porous structure.

5.2.2 Introduction

The importance of polymeric materials in separation applications can be easily illustrated from the progress made in polymeric membrane technology for the past three decades. One of the most widespread applications of this type is membrane from polymers.

There are different methods for making membranes from polymers, among them, film stretching followed by voids creation has been in focus recently since it is inexpensive and more environmentally friendly [1,2]. The main idea of the process is formation of a two-phase structure that upon stretching creates stress concentration on the interface, which results in phase separation and voids creation. The two phase structure can be: two immiscible polymers, a polymer containing inorganic filler or a semi-crystalline polymer whose crystals are in lamellar form. A membrane obtained by stretching a neat unfilled polymer has a number of advantages when compared to other methods. The most important one is the use of a single material, thus eliminating the need for blending or dissolution and solvent removal.

Generally, membrane formation proceeds through three main stages:

- Production of the precursor film with lamellar morphology
- Annealing of the film to thicken the lamellae
- Film stretching at a low temperature to create voids and then at a higher temperature to enlarge the voids as illustrated in Fig. 5.1.

Understanding the mechanisms of micropore formation in the stretching process and the effect of the processing parameters on the pore size will guide us in developing

membranes with different pore sizes, size distributions and porosities. It has been shown that an initial lamellar morphology with high crystalline orientation function is necessary for making such a membrane [3]. Polyethylene and polypropylene are regarded as suitable materials because of their crystalline structure, their low cost and wide range of grades. Polypropylene (PP) is usually favored because of its higher temperature resistance and better mechanical properties when compared to polyethylene.

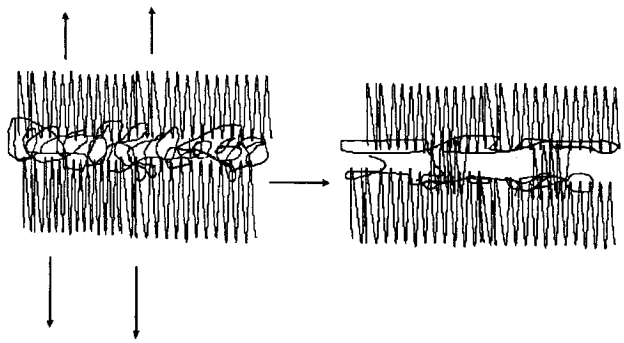

Fig. 5.1. Schematic of pore creation by stretching; the applied stress will separate the blocks from each other.

In this work the variations of PP morphology with processing conditions and resin properties are examined. A special emphasis is put on conditions leading to lamellar structure formation and then morphology of porous membranes made by stretching

5.2.3 The role of initial morphology

Polypropylene morphology can be defined as the final crystal structure and amorphous phase in the solidified state. Arrangement, form and crystalline phase content are controlled by the polypropylene molecular structure and process conditions. There are

three main crystal structures available for polypropylene. The spherulitic structure is formed in a quiescent state (or low stresses) and will result in the arrangement of crystal blocks in spherical shapes that make an isotropic configuration. The lamellar structure is formed when the polymer is crystallized under high or moderate stresses and the fibrillar structure is formed when the material is stretched to a high degree when the crystal blocks break and are embedded into fiber crystal formed in the stress direction. The first step in this work is to generate a lamellar morphology for polypropylene, which involves understanding the relationship between the material, processing conditions and morphology.

In the lamellar morphology development, the stresses applied during crystallization extend the polymer chains that act as initial nuclei and crystallization follows in lamellae blocks perpendicular to the extended chains [4]. Extended chains are necessary for the achievement of a lamellar morphology, especially at the beginning of the crystallization process to act as nucleating sites. Noglas et al. [4] have studied the shear-induced crystallization of isotactic polypropylenes with different molecular weight distributions. They found that the development of the oriented morphology in the resin having higher molecular weight is much faster than for the one with lower molecular weight. The presence of the long chains increases entanglements between the chains, which then increase the relaxation time; hence, the chance for the extended chains to relax before crystallizing decreases.

On the other hand, it has been shown that the PP microstructure such as crystallinity, crystal size and crystal type can be related to mechanical properties [6]. It has also been

shown that the yield strength is related to the degree of crystallinity, lamellar thickness or both. A linear relationship between the tie molecule fraction and yield strength was developed [7].

5.2.4 Experiments

5.2.4.1 Materials

Table 5.1 The four different polypropylene (homo polymer) grades used were:

Resin Code	Company	MFI 230°C/2.16 kg
PDC1280	Basell	1.2
Pro-fax 6823	Basell	0.5
Pro-fax 814	Basell	2.8
PP4292E1	ExxonMobil	2.0

Pro-fax 814 (PF 814) is a branched polypropylene with long chain branches. It was selected because of the effect of branched chains on its relaxation time. PP4292E1 is a grade apparently used for producing oriented films according to the Company. PP1280 is a general purpose grade and PP6823 possesses the lowest MFI in the homo polypropylene list introduced by Basell Company.

5.2.4.2 Sample preparation

Two production systems were used to obtain the precursor films: film blowing and cast film extrusion. The controllable processing parameters for blown film were: 1) frost line height, related to the cooling rate of the film; 2) draw down ratio (DDR), which is the ratio of take-up speed to the average velocity of the extrudate at the exit of the die and

represents the amount of stretching in the machine direction; 3) blow-up ratio (BUR), which is the ratio of the bubble diameter to the diameter of the die and 4) die temperature, which affects the temperature profile of the film below the freezing height and consequently the melt relaxation mechanism. The processing conditions are shown in Table 5.2; the die temperature was 230°C and die gap kept at 1.1mm for the all blown film samples.

Table 5.2. Summary of films produced by the film blowing process.

No.	Resin	DDR	BUR	Thickness (μm)	Die temperature (°C)	Die gap (mm)	Cooling gap (%)
1	PP1280	22	1.9	50	230	1.1	37
2	PP6823	22	1.9	50	230	1.1	50
3	PP6823	45.3	1.7	25	230	1.1	100
4	PF814	45	1.7	25	230	1.1	50
5	PP4292E1	44	1.7	25	230	1.1	60

For the cast film, a slit die was used and the die temperature was fixed at 220°C. The key parameters were the chilled roll temperature and take-up rolls speed. A fan was also installed to supply air to the film surface to improve the cooling. In that case, the cooling process was mainly controlled by the fan speed and air temperature. The cast film samples were prepared at different draw ratios (different thicknesses) as shown in Table 5.3.

Table 5.3. Summary of films produced by cast extrusion process.

No.	Sample	Draw Ratio	Die temperature (°C)	Thickness (μm)
1	PP4292E1-1	21	220	92
2	PP4292E1-2	40	220	46
3	PP4292E1-3	83	220	25
4	PP6823	80	220	26
5	PP1280	82	220	25

5.2.4.3 Characterization

The linear viscoelastic behavior was obtained using a Rheometric Scientific SR-5000 stress controlled rheometer with parallel plates of 25 mm diameter. Stress sweep tests were performed to determine the linear region and the frequency sweep tests were carried out within the linear region at 230°C.

Field emission scanning electron microscope (FESEM- Hitachi S4700) was employed for observation of the films. The samples were etched with a solution of 60% H_3PO_4, 40% H_2SO_4 mixed with approximately 0.5 wt % potassium permanganate. The etching time was 25 min and the samples were rinsed off and washed with a dilute solution of sulphuric acid, hydrogen peroxide and distilled water.

Crystalline orientation measurements were carried out using a Bruker AXS X-ray goniometer equipped with a Hi-STAR two-dimensional area detector. The generator was set up at 40kV and 40mA and the copper CuK_a radiation (λ=1.542 Å) was selected using a graphite crystal monochromator. The sample to detector distance was fixed at 8 cm.

Prior to measurements, careful sample preparation was required to get the maximum diffraction intensity. This consisted of stacking several film layers (about 180 layers) in order to obtain the optimum total thickness.

A standard test for tear resistance of plastic film based on ASTM D1922 was used to obtain MD and TD tear resistance.

5.2.5 Results and discussion

The relaxation spectrum is particularly sensitive to the molecular structure and can likely be employed to investigate the presence of high molecular weight chains with high relaxation times, responsible for the lamellar morphology. The viscosity curves and relaxation spectra are shown in Figs. 2 and 3, respectively. The relaxation spectrum from the modulus data (G',G'',ω) was calculated using the NLREG (non-linear-regularization) computer software [8]. The structure features of polypropylene are influenced by melt rheological characteristics. PP1280 and PP4292E1 exhibit a similar behavior in frequency sweep test. PP6823 shows a higher complex viscosity and the zero-shear plateau is not reached at the lowest frequencies (Fig.5.2). This is indicative of a larger average molecular weight. The complex viscosity curve of PF814 is similar to that of PP6823, but with much lower viscosity values and the shear thinning behavior for this resin is less pronounced that that of PP6823. Its relaxation spectrum is skewed with respect to the spectra of the other PP resins and its peak shifted to a higher relaxation time (Fig.5.3), which could be due to the branched structure of PF814.

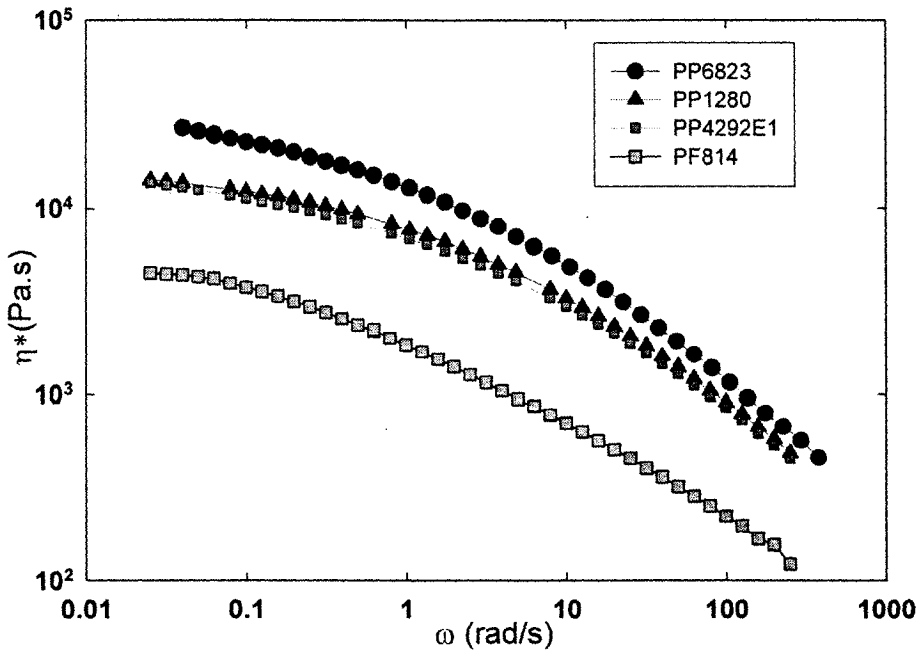

Fig. 5.2. Frequency sweep tests for the resins at 230°C

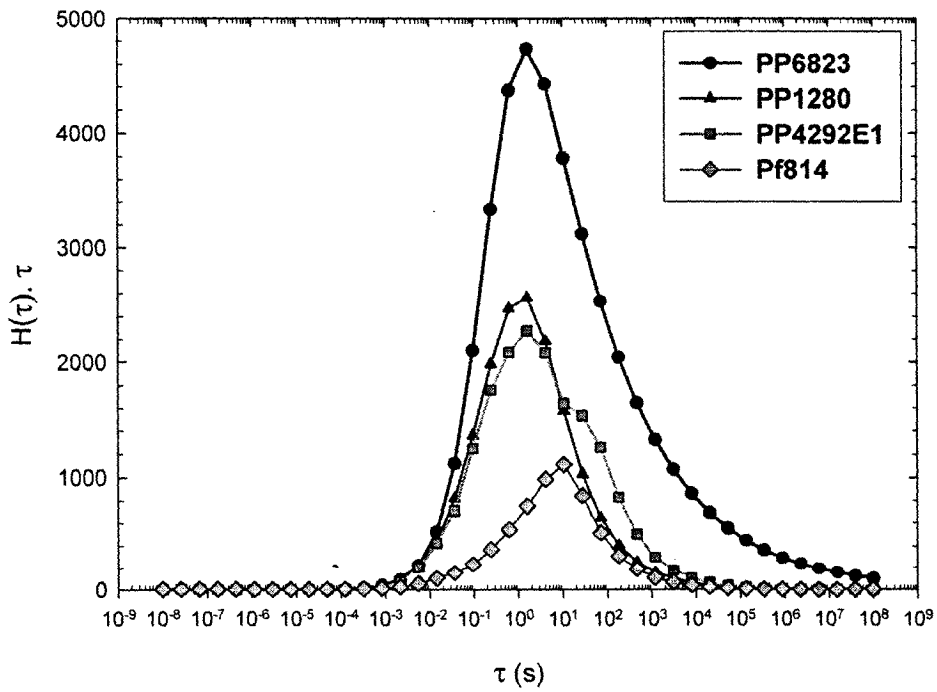

Fig.5. 3. Relaxation spectra for the resins at 230°C.

To achieve a lamellar morphology by film blowing, it is important to approach a blow up ratio of one. This improves the uniaxial orientation of chains at the beginning of the crystallization. The minimum blow-up ratio that we obtained with our blown film line was 1.7 for polypropylene. This limitation arises from the particular bubble shape and also because of polypropylene's low melt strength in comparison to polyethylene. The processing parameters for the film blowing were selected in a way that promotes the conditions for lamellae formation. High draw ratios, blow-up ratios as close as possible to 1 and fastest possible cooling rates are considered to be the desirable conditions.

Figure 5.4 shows the morphology of the film surface. Initially a spherulitic form with crosshatched structure is observed for PP1280. Fig. 5.4(b) shows the spherulitic structure for PP6823, the resin that possesses the largest zero shear viscosity. It was attempted to change the processing conditions to the highest draw ratio and cooling rate for this resin. Larger draw ratio will enhance the extension of the chains in the melt state and faster cooling will preserve the extended form of the chains for the crystallization before they relax [7]. Even for the maximum allowable processing conditions a spherulitic structure was obtained for PP6823 as shown in Fig. 5.4(c). By contrast, a lamellar morphology was observed for PF814 (Fig. 5.4 (d)). We believe this is due to the long branched chains, which increase the mean relaxation time. For PP4292E1 a disrupted lamellar structure with a tendency to spherulitic was observed in Fig. 5.4(e). As a conclusion for this part, it can be said that the key parameter is the chain relaxation time, which is controlled by the polymer structure and cooling process.

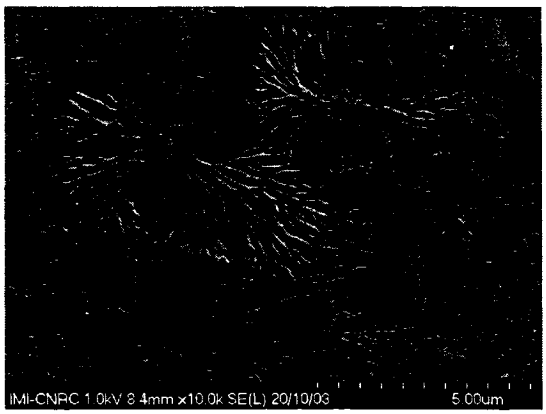

(a) PP1280 Blown film Table 5.1 #1

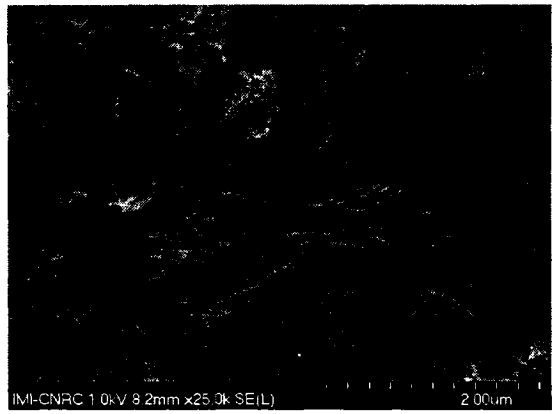

(b) PP6823 Blown film Table 5.1 #2

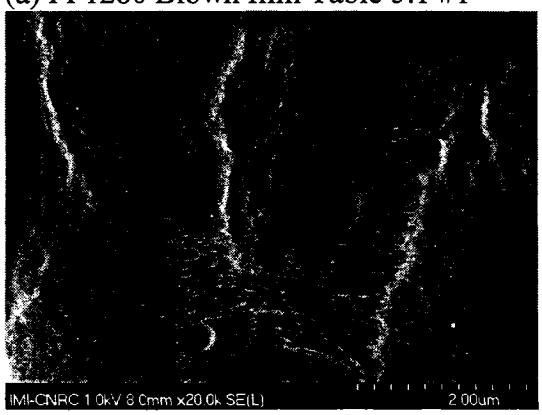

(c) PP6823 Blown film Table 5.1 #3

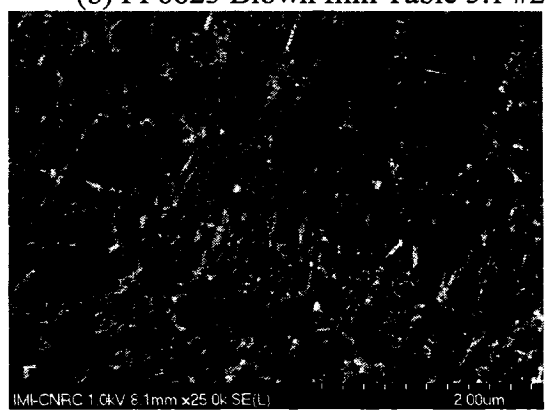

(d) PF 814 Blown film Table 5.1 #4

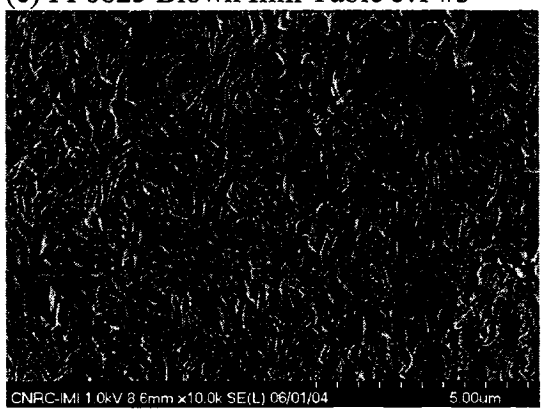

(e) PP4292E1 Blown film Table 5.1 #5

(f) PP4292E1 Cast film Table 5.2 #3

Fig. 5.4. SEM pictures of the samples (a) PP1280, (b) PP6823, (c) PP6823, (d) PF814, (e) PP4292E1 (f) PP4292E1(cast film)

Our results suggest the existence of a relationship between the draw ratio and drawing rate and relaxation time.

The lamellar structure (lamellae thickness) and the mechanical properties of the final film obtained from PF814 were very weak for post extrusion stretching. In order to obtain a lamellar morphology for all the resins, the process was changed to cast film. The advantage of cast film extrusion is the possibility of using a higher cooling rate and also of obtaining pure uniaxial deformation. The freezing for thin films (25 μm) could be achieved within 1.5 cm from the die exit. Fig. 5.4(f) shows the lamellar morphology in the form of stacked lamellae obtained via this process for PP4292E1.

Tensile tests were carried out to reveal the response of the two different morphologies. Fig. 5.5(a) shows the stress strain curve for a PP4292E1 film obtained by film blowing. A yield point is clearly observed, and right after that, the spherulites break-up through a shear-yielding mechanism. Strain hardening at the end of the curve is believed to result from the uniaxially oriented fiber network structure of the crystals. The lengths of the fibers are not clearly defined, but the fibers are connected together at their ends by the amorphous phase. A different behavior is seen for PP4292E1 with a lamellar structure in Fig. 5.5(b). Strain-hardening starts right after the yield point and this may be due to the orientation of the noncrystalline part between lamellae. Some voids are created at this stage and finally the larger lamellae separation ends up with the sample failure. The same behavior has been reported in the literature [9].

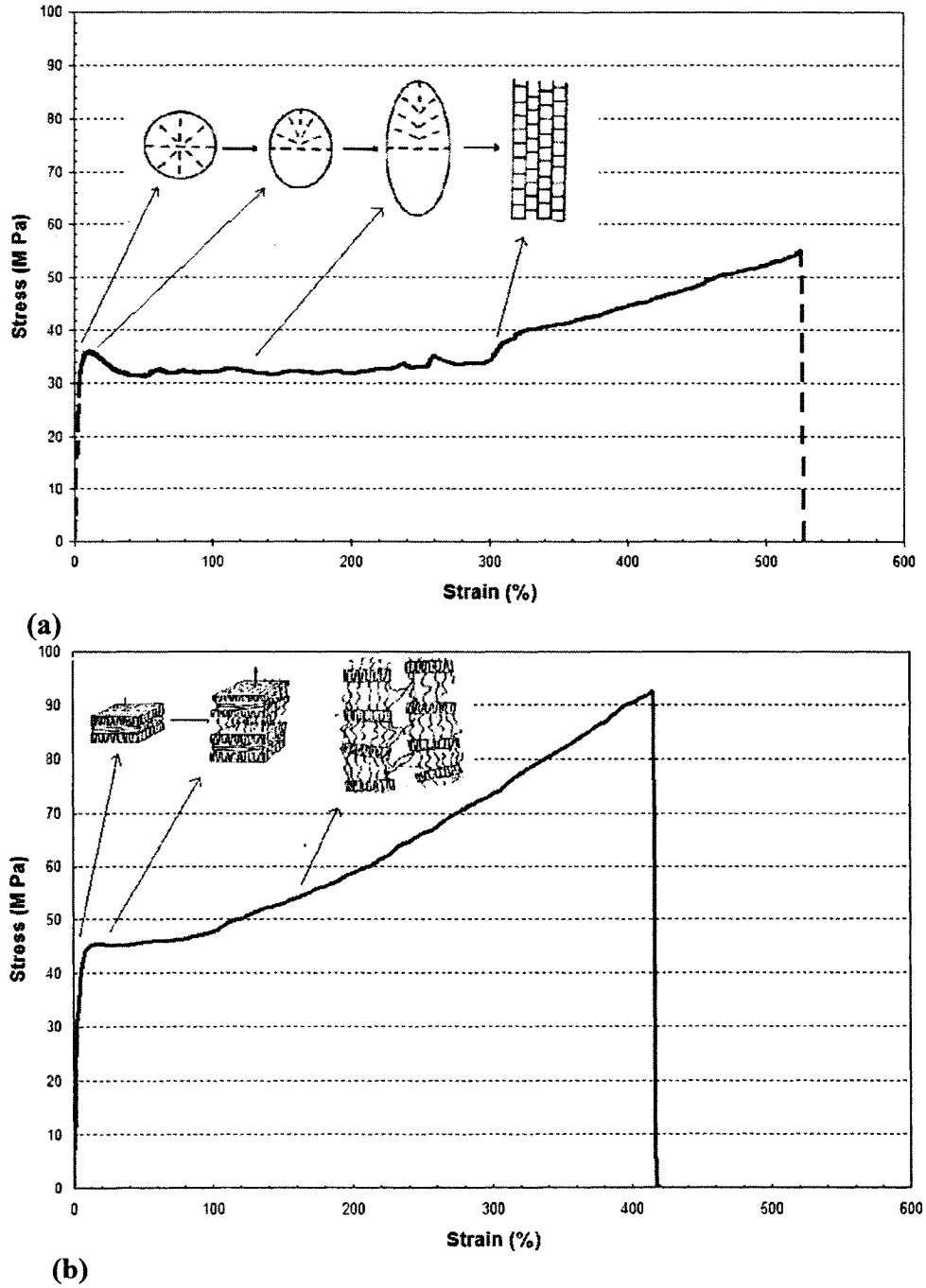

Fig.5.5. Tensile strength tests for PP4292E1 samples obtained by (a) film blowing (spherulitic structure) (b) cast film (lamellar structure)

Figure 5.6 shows the orientation parameters for PP4292E1 films. Crystalline orientation functions were obtained from the pole figures of (110) and (040) reflection plan. Herman's orientation functions were derived from (110) and (040) pole figures using the Bruker analytical system software. The *c*-axis of the isotactic polypropylene unit cell is parallel to the helical axis of the PP molecule in that cell while the three crystallographic axes in a monoclinic unit cell are not mutually perpendicular (the angle between *a* and *c* axis in isotactic PP is 99° 20′), so a modified coordinate system is utilized for the calculation of orientation parameters. Since the *b* axis of unit cell is perpendicular to its (040) planes, its orientation relative to reference (stretch) direction can be measured directly, that is $\cos^2\beta = \cos^2\phi_{040}$, where β is the angle between the stretch direction (machine direction) and the b-axis of the crystal, this value ($\cos^2\phi_{040}$) is measured experimentally and with replacement in Herman's equation [11], the orientation for b-axis will be determined:

$$f_b = f_{040} = f = \frac{3Cos^2\phi_{040} - 1}{2} \qquad (5.1)$$

On the other hand f_c (orientation of the *c*-axis) with respect to MD is determined by the combination of data of two planes for the polypropylene which are (040) and (110), [10]:

$$Cos^2\phi_c = 1 - 1.099\left(Cos^2\varphi_{110}\right) - 0.901\left(Cos^2\varphi_{040}\right) \qquad (5.2)$$

Substituting this result in Herman's equation, the orientation factor for the *c*-axis will be also obtained. The other orientation factor, (*a*-axis), can be calculated from the orthogonally relation:

$$Cos^2\phi_a = 1 - \left(Cos^2\phi_c\right) - \left(Cos^2\phi_b\right) \qquad (5.3)$$

Figure 5.6 presents the orientation parameters $Cos^2\bar{\phi}_a, Cos^2\bar{\phi}_b, Cos^2\bar{\phi}_c$ for PP4292E1 samples prepared using the cast film process. It can be observed that the *c*-axis moves toward the machine direction as the draw ratio increases from 20 to 80 (Figs. 5.6a-5.6c), while the *a*- and *b*-axes take a position between the TD and the normal (ND) direction. The results for other resins showed the same trend. The orientation factor for the *c*-axis in the MD direction almost correlated linearly with the drawing ratio as it is seen in Fig. 5.7 The higher orientation function of PF814 is likely attributed to its long chain branching structure. In a certain range of draw ratio, the orientation factor of PP4292E1 is larger than those of PP1280 and PP6823. It has been shown that a certain orientation is likely needed to develop lamellar structure for the precursor film in a way that can be used into stretching process for making membranes from polyethylene [3]. Based on our experiments an orientation factor larger than 0.3 in the cast film was needed for polypropylene.

The membranes were made for samples 3, 4 and 5 of Table 5.3. The samples were initially annealed at 145°C resulting into a 3% extension of their initial length and then cold stretched for about 35% at room temperature.

a)

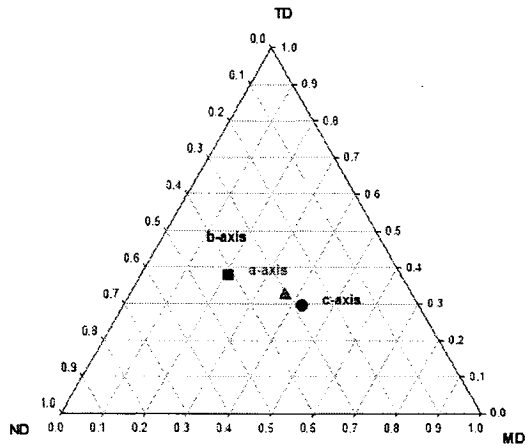

(b)

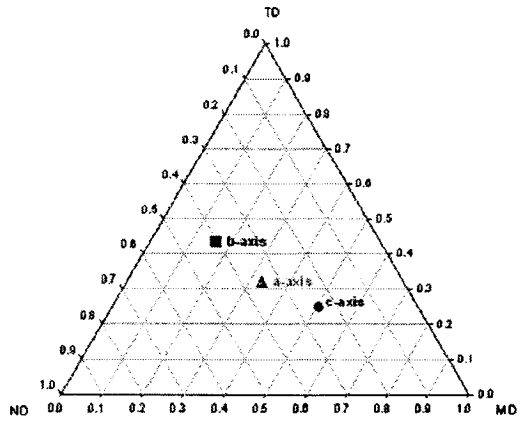

(c)

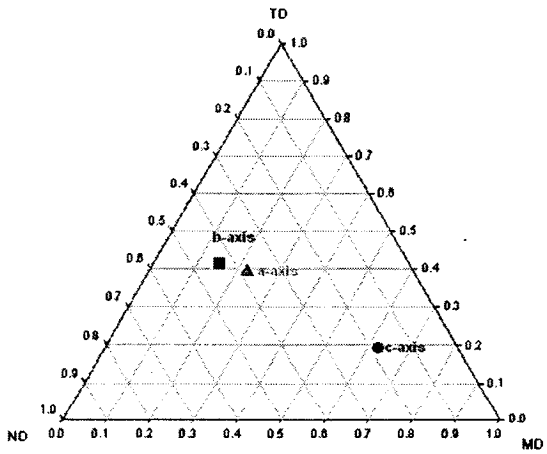

Fig. 5.6. Orientation parameters $Cos^2\bar{\phi}_a, Cos^2\bar{\phi}_b, Cos^2\bar{\phi}_c$ for PP4292E1 sheets (a) No.1 (b) No.2 (c) No.3 (as listed in Table 5.2).

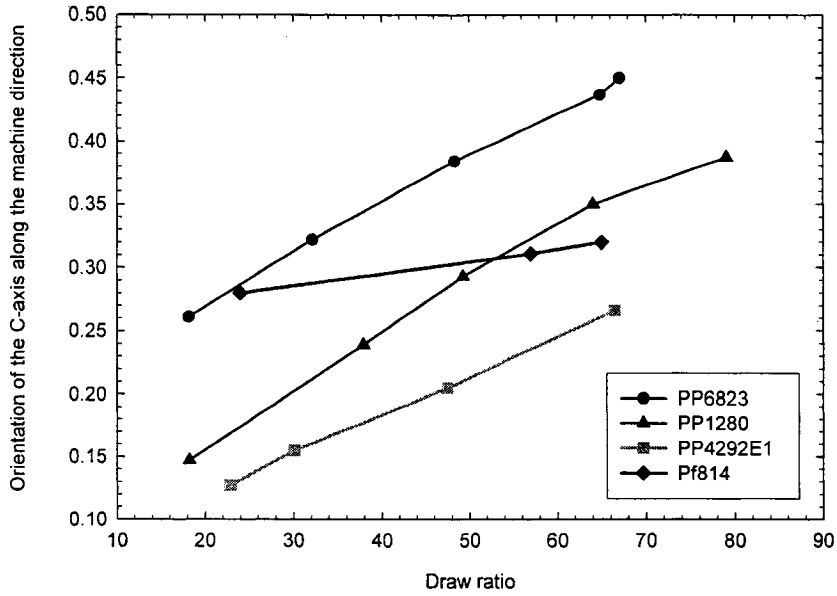

Fig 5.7. Orientation factor for samples produced by cast film process

This was followed by hot stretching to about 45% at 145°C. Figure 5.8 compares the structure obtained for three different polypropylene resins. The pore distribution and porosity are somewhat more uniform for PP4292E1. We believe this is due to the larger orientation factor of the precursor film. The larger orientation function likely comes from the entanglement density in the melt state and cooling conditions, which in turn improves the chain stretch ability and crystallization for the row nucleated crystal structure. It should be noted that the crystallization kinetics and involved parameters like isotacticity are important as well. It has been shown that for drawn polypropylene samples the characteristic length (thickness of lamella and amorphous part together) increases with draw ratio. Increases from 14.4 to 32.4 nm have been reported for samples uniaxially stretched 5 times [5].

(a)

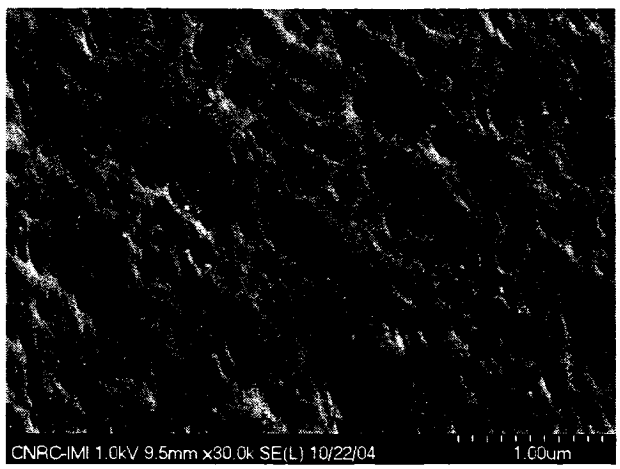

(b)

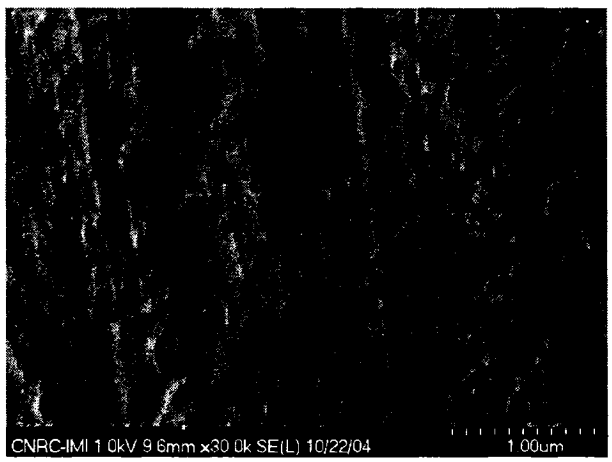

(c)

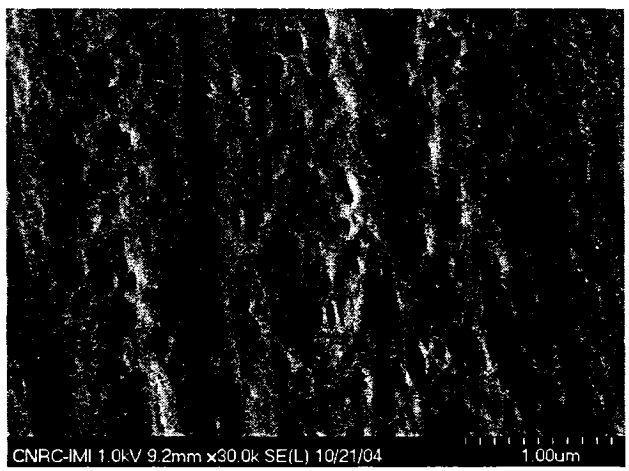

Fig.5.8. SEM pictures of membrane surfaces, (a) PP4292E1, (b) PP1280 and (c) PP6823

At this stage we believe that thinner samples that experienced larger draw ratio and faster cooling rate posses the larger orientation function, and hence show a better lamellae separation configuration for the pore creation stage.

Table 5.4 shows also the tear resistance for the same series of PP4292E1 films. The tear resistance is the most sensitive mechanical property to orientation. With increasing draw ratio, the tear resistance proportionally improves in the transverse direction (TD) while it diminishes in MD.

Table 5.4 Tear resistance of the samples PP4292E1 as listed in Table 5.3.

PP(4292E1)	Tear resistance g/μm (MD)	Tear resistance g/μm (TD)	Tear resistance TD/MD
1	0.33	14.8	44.4
2	0.44	23.5	53.3
3	0.24	18.1	76.4

5.2.6 Conclusion

A lamellar morphology for polypropylene can be achieved if optimum processing conditions are used. The most important processing factors for blown films are fast cooling, large draw ratio, followed by a low blow-up ratio. Different responses to tensile tests were observed for samples with spherulitic and lamellar structures. For the cast film process, an almost linear relationship between draw ratio and orientation factor was

observed. For a large orientation factor (greater than 0.3) a lamellar morphology suitable for membrane formation was obtained. Tear resistance in the transverse direction improved while it became worse in the machine direction as the orientation increased in MD with increasing draw ratio. Porous membranes were obtained with precursor films having a lamellar morphology and orientation factor of the *c*-axis in MD greater than 0.3.

5.2.7 Acknowledgements

Financial support from NSERC (National Research Council of Canada) and FQRNT (Fond Quebecois de Recherche en Nature et Technologies) is gratefully acknowledged.

5.2.8 References

1. Kundu P.P. and Choe S. 'Transport of moist air through microporous polyolefin films' J. Macrom. Sci., Part C-Polymer Reviews, C43: 143-186 (2003)
2. Wei Zhu,Xian Zhang, Chuntian Zhao, Wei Wu, Jianan Hou and Mao Xu, 'A Novel polypropylene microporous film', Polymer for Advanced Technologies, 7: 743-748 (1995)
3. Yu, T. H., 'Processing and structure-property behavior of microporous polyethylene from resin to final film', PhD thesis, Virginia Polytechnic Institute and State University, materials engineering science, May 1996

4. Nogales A., Hsiao B.S., Somani R.H., Srinivas S., Tsou A.H., Balta-Calleja F.J. and Ezquerra T.A., 'Shear-induced crystallization of isotactic polypropylene with different molecular weight distributions: in situ small- and wide-angle X-ray scattering studies', Polymer, 42: 5247-5256 (2001)
5. Seki M., Thurman D.W, Oberhauser J.P and Kornfield J.A., 'Shear-Mediated Crystallization of Isotactic Polypropylene: The Role of Long Chain-Long Chain Overlap', Macromolecules, 35: 2583-2594 (2002)
6. D. Ferrer-Balas, M.LI. Maspoch, A.B. Martinez, and O.O. Santana, 'Influence of annealing on the microstructure, tensile and fracture properties of polypropylene films', Polymer, 42: 1697-1705 (2001)
7. Koh-Hei Nitta and Mtowo Takayanagi, 'Tensile yield of isotactic polypropylene in terms of a lamellar-cluster model', Journal of polymer science : Part B polymer physics, 38: 1037-1044 (2000)
8. Honerkamp J., and Weese J., 'A non linear regularization method for the calculation of relaxation spectra', Rheol. Acta, 32: 65-73 (1993)
9. Th. Lupke, S. Dunger, J. Sanze and H.-J. radusch, 'Sequential biaxial drawing of polypropylene films ' , Polymer, 45: 6861-6872 (2004)
10. L. E. Alexander, X-ray Diffraction Methods in Polymer Science (Wiley, New York, 1969)
11. R. J. Samuels, 'High strength elastic polypropylene', Journal of polymer science : Part B polymer physics, 17: 535-568 (1979)

Chapter 6

Orientation analysis of row nucleated lamellar structure of polypropylene obtained from cast film

6.1 Presentation of the article

The objective of the second article was to study the orientation and arrangement of the crystal blocks in the films with row-nucleated lamellar structure. Orientation, position, thickness and connection of the crystal blocks control the process of lamellae separation in the stretching stage. Five polypropylenes were selected as presented in article 1 (chapter5) and were processed in cast film extrusion to produce precursor films with lamellar structure. It will be shown that orientation and position of the crystal lamellae are functions of the type of resin and applied process parameters.

* *Submitted to Poly. Eng. Sci,* July 2006

6.2 Orientation analysis of row nucleated lamellar structure of polypropylene obtained from cast film

Farhad Sadeghi[1], Abdellah Ajji[2] and Pierre J. Carreau[1]
1) **Center for Applied Research on Polymers and Composites, CREPEC, Ecole Polytechnique, Montreal, QC, Canada**
2) **CREPEC, Industrial Materials Institute, CNRC, Boucherville, QC, Canada**

6.2.1 Abstract

Five different polypropylene resins were characterized by rheology to study the effect of melt rheology on the row-nucleated lamellar structure development during the cast film process. The arrangement and orientation of the crystalline and amorphous phases were examined by WAXD (wide angle X-ray diffraction) and FTIR (Fourier transform infrared) methods. Tensile tests were carried out to examine the effect of orientation on the behavior of the samples. It was found that the molecular weight evaluated from rheology and the processing conditions played a crucial role on the orientation of the crystalline and amorphous phases and, in turn, affected significantly the tensile response. The molecular weight was the main parameter that controlled the orientation and it was found that the resin with a higher molecular weight had a tendency to form a planar crystalline morphology as the draw ratio increased. It was also observed that a planar morphology was associated with a suppression of the yield behavior in the tensile measurements.

6.2.2 Introduction

A row nucleated lamellar structure as an initial morphology has been a matter of concern0 for developing microporous membranes based on a three stage process (melt-extrusion/annealing/uniaxial-stretching) [1,2]. In this process illustrated in Figure 6.1 a precursor film with an appropriate row nucleated structure is first prepared, then by stretching at room temperature (cold stretching) voids are created due to lamellae separation and finally stretching in high temperature enlarge the voids resulting in a fairly regular distribution of the pores [1]. The preparation of a precursor film with the appropriate lamellar morphology is the most important issue. This structure is believed to be obtained by crystallization of the chains during melt stretching, which in literatures is called stress induced crystallization [1,3]. Nogales et al [3] studied the shear-induced crystallization of polypropylene and concluded that a certain amount of high molecular weight chains is necessary to develop an oriented structure in the melt state. They determined this critical molecular weight for polypropylene using gas permeation chromatography (GPC) and small angle X ray scattering (SAXS) experiments. They showed that this "critical molecular weight for orientation" was dependent on shear rate and temperature up to a certain shear rate, then, it would be unchanged at higher shear rates. They speculated that the high molecular weight chains (with long relaxation times) were the main cause for the formation of shear-induced nuclei that acted as the initial nucleation sites for crystal lamellae growth. It was shown that the development rate of the oriented structure morphology was much faster for a high molecular weight resin. It has also been pointed out that a certain shear rate was necessary for the extension of the

chains and this critical shear rate shifted to lower values as the molecular weight increased.

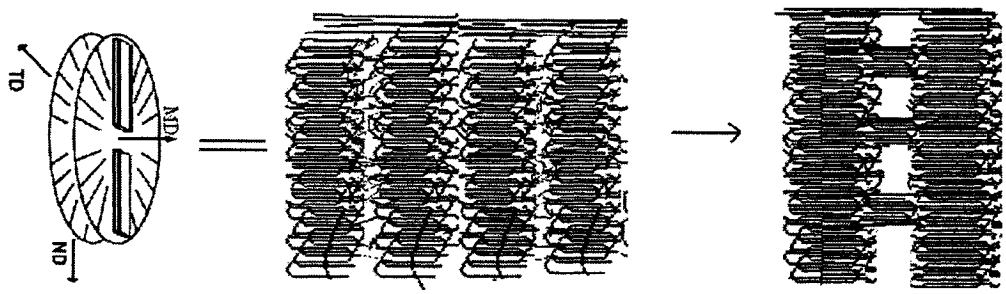

Fig.6.1 Schematic of a row nucleated structure lamellar morphology for making micro porous membranes. Stretching at room temperature (25°C), called cold stretching, initiates voids and consequently hot stretching develops a porous structure.

In polymer melt processing chain orientation in the melt state affects significantly the subsequent crystallization process. Chain orientation in the melt state enhances the crystallization kinetics, as shown in the detailed study of Kornfied et al. [4]. They found that the time for crystallization under stress is orders of magnitude faster than under quiescent conditions. The temperature dependence of the crystallization time was much less pronounced in shear-induced crystallization while for quiescent crystallization it rose drastically with temperature. They considered the turbidity of the melt as a criterion of crystallization initiation, and found that in quiescent state. the crystallization time was 10 000 s (at a temperature of 141°C) while under stress this reduced to 16 s. Under quiescent crystallization conditions over a wide range of temperature, the lower molecular weight materials crystallized faster owing to the higher crystal growth rate (higher mobility), but under shear-induced crystallization commenced with longer chains and the overall rate was larger. The increase in the crystallization rate was mainly

due to the increase in the flow-induced primary nuclei. In other words, the nucleation stage controlled the process, and the total crystallization rate was larger because of the faster nucleation rate.

In our previous paper [5], we have shown that a high chain orientation in the melt state can result in the generation of a row nucleated lamellar structure for polypropylene. In the current work, we analyze key factors that may control the orientation of the lamellae in the row nucleated structure for polypropylene. These factors include rheological characteristics, molecular weight and process conditions. We also make use of an FTIR method to detect the amorphous orientation between the lamellae. Finally, the influence of the orientation on the solid state tensile response of the samples is investigated. The effect of the lamellae orientation on the properties of membranes and their performance prepared by cold and hot drawing will be the topic of another paper.

6.2.3 Experimental

6.2.3.1 Materials

The five different polypropylene grades used in this study are listed in Table 6.1 PDC1280 (PP12) is a general purpose grade and Pro-fax 6823 (PP05) possesses the lowest melt flow rate (MFR) in the homo polypropylene list introduced by Basell. Pro-fax 6823 is a high molecular weight homo polypropylene of Basell. Pro-fax 814 (PPB) is a branched polypropylene with long chain branches. It was selected because of the effect of branched chains on the relaxation time of molten polyolefins. PP4292E1(PP20) and PP4612E2 (PP28) are the grades used for the production of oriented films according to

ExxonMobil. The manufacturer reports these two resins as homopolymers, An FTIR test was carried out and no trace of ethylene was found in the absorption spectrum of both resins.

Table 6.1. Polypropylene grades used

Resin Code	Company	MFR 230°C/2.16 kg	Nomenclature in this paper
PDC1280	Basell	1.2	PP12
Pro-fax 6823	Basell	0.5	PP05
Pro-fax 814	Basell	2.8	PPB
PP4292E1	ExxonMobil	2.0	PP20
PP4612E2	ExxonMobil	2.8	PP28

6.2.3.2 Rheological Characterization

The linear viscoelastic data were obtained using a Rheometric Scientific SR-5000 controlled stress rheometer with 25 mm diameter parallel plates. Stress sweep tests were performed to determine the linear viscoelastic region and the frequency sweep tests were carried out within the linear region at 230°C.

Measurements of the elongational viscosity were made with an elongational rheometer (Rheometrics RER 9000). The measurements were performed at 200°C and constant strain rate. The deformation of the molten specimen, immersed in a bath of hot silicone oil, was accomplished by exponentially varying the velocity of one end of the sample with time. The density of the oil was close to the density of the polymer to avoid buoyancy effects. The samples were carefully prepared so that all the residual stresses could be removed, to avoid deformation when the sample was melted. The granules were transfer-molded under vacuum using the Rheometric RSV-2100 sample

preparation kit in conjunction with a Yokogawa programmable temperature controller model UP25. The uniformity of the resulting cylinder-shaped specimens was verified, and the average diameter was found to be 6 mm. The sample length used in this study varied from 22 to 24 mm. The end surfaces of the molded specimens were cleaned and then fixed to aluminum ties using a high temperature epoxy (24 h curing).

6.2.3.3 Film Preparation

The films were prepared by cast film processing with a slit die at the temperature of 220°C. To improve cooling, a fan was installed to supply air to the film surface right at the exit of the die. The key parameters were the fan speed, take-up roll speed and air temperature. We worked at the maximum speed of the fan and constant die temperature, so the only variable was the take-up speed .The cast film samples were prepared at different draw ratios (roll speed to die exit velocity, thus implying different thicknesses) as shown in Table 6.2.

6.2.3.4 Orientation Features

Crystalline orientation measurements were carried out using a Bruker AXS X-ray goniometer equipped with a Hi-STAR two-dimensional area detector. The generator was set up at 40 kV and 40 mA and the copper CuK_a radiation (λ = 1.542 Å) was selected using a graphite crystal monochromator. The sample to detector distance was fixed at 8 cm. Prior to measurements, careful sample preparation was required to get the maximum diffraction intensity. This consisted in stacking several film layers in order to obtain the

optimum total thickness of about 2.5 mm. Poles figures of (110) and (040) crystalline reflections were measured and orientation factors determined from the measurements.

Table 6.2. Summary of the conditions for the cast films and their thicknesses.

No.	Sample	Draw Ratio	Thickness (μm)	No.	Sample	Draw Ratio	Thickness (μm)
1	PP05-1	23	55	6	PP20-2	65	22
2	PP05-2	65	23	7	PP28-1	23	56
3	PP12-1	23	55	8	PP28-2	65	22
4	PP12-2	65	23	9	PPB-1	23	55
5	PP20-1	23	56	10	PPB-2	65	23

6.2.3.5 Tensile Tests

Tensile tests were performed using an Instron 5500R machine, based on the D638-02a ASTM standard.

6.2.3.6 FTIR

Infrared spectra were recorded on a Nicolet Magna 860 FTIR instrument from Thermo Electron Corp. (DTGS detector, resolution 4 cm^{-1}, accumulation of 128 scans). The beam was polarized by means of a Spectra-Tech zinc selenide wire grid polarizer from Thermo Electron Corp.

6.2.4 Results and Discussion

The elasticity of the resins in the melt state is taken as the ratio of the storage modulus to the product of the loss modulus with frequency, $\lambda = G' /(G''\omega)$, which is also called a characteristic elastic time [6]. It should be pointed out that, generally in the low frequency region, the elastic response of a melt is more pronounced largely because of higher degree of entanglements. The small amplitude oscillatory data (SAOS) in terms of the complex viscosity and the characteristic elastic time of the resins as functions of frequency are shown at 230°C, in Figures 6.2 a and b, respectively. Since the elasticity response of material is more critical at low deformation rates only the data for the low frequency window are reported in Figure 6.2 b. The molecular weight of the linear homo polypropylenes can be evaluated through the zero-shear viscosity dependency of polymer melts to molecular weight [7]:

$$\eta_0 = KM_w^{3.4} \qquad (6.1)$$

The molecular weight, M_w, of one of the samples (PP12) obtained from GPC was used to calculate the K value. The zero-shear viscosity was determined from the complex viscosity data using the Carreau-Yasuda model [6]. For PP12, η_0 was found to be equal to 16 000 Pa.s at 230 °C. Then, the K factor was calculated to be 1.21×10^{-15} (Pa.s/ $(g/mol)^{3.4}$) , which is in agreement with results of the literature [7]. Table 3 lists the molecular weight of the linear resins calculated via Eq.6.1. For branched polypropylenes the zero-shear viscosity would show a stronger dependence on molecular weight than 3.4 [8]. For this reason, no attempt was made to estimate the molecular weight of PPB.

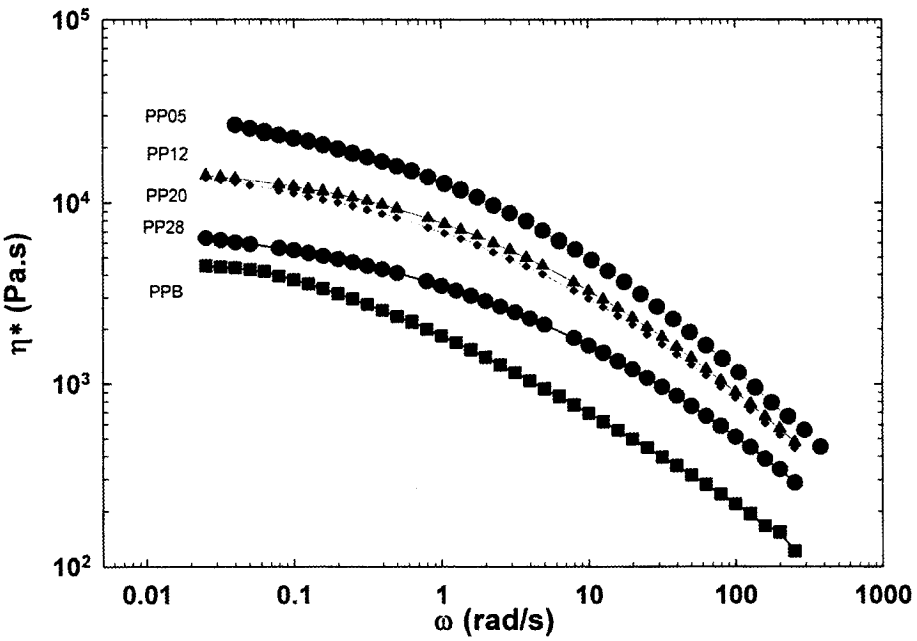

(a)

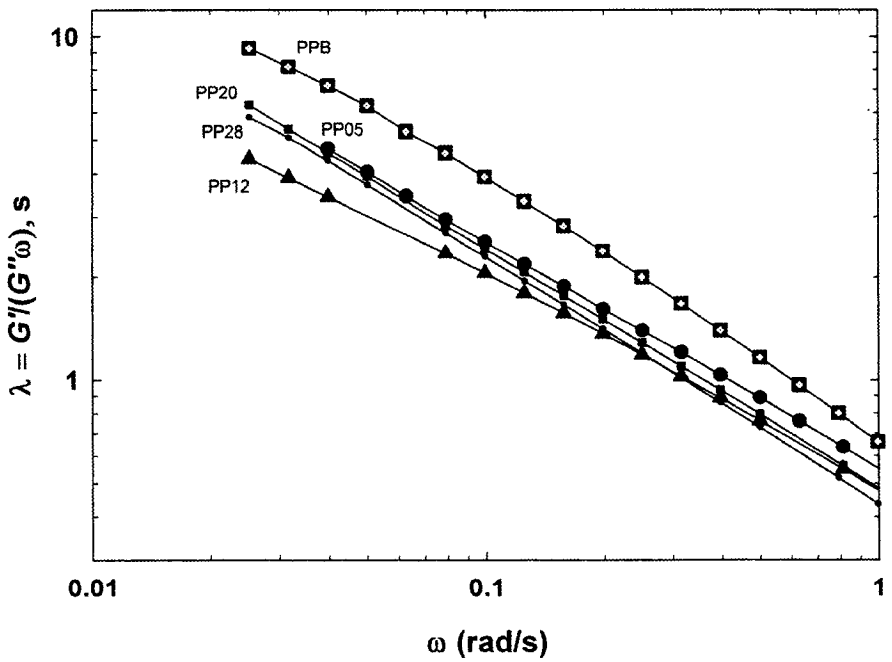

(b)

Fig. 6.2. Small amplitude oscillatory shear data for the resins at 230°C; a) complex viscosity, b) elastic characteristic time (low frequency range).

The rheological behavior of these resins is typical of that of molten polyolefins. However, it is interesting to note that the branched polypropylene (PPB), which exhibits the lowest viscosity, shows the longest elastic characteristic time at low frequency. The high elastic character of this resin is clearly related to its long chain branching structure and likely to its melt strength. The elasticity for the three resins, PP05, PP20 and PP28, is quite similar at 230°C and this suggests that the effect of molecular weight at high temperature is less important for these linear polypropylenes. The slightly larger values for PP20 compared to PP12 might come from a very small fraction of high molecular weight chains, although its weight average molecular weight is slightly lower than that of PP12. This portion of high molecular weight chains could be detected through the relaxation spectrum of the resin [5].

Table 6.3. Zero-shear viscosity at 230°C and calculated molecular weight of the PPs.

Resin Code	η_0 (Pa.s)	M_w (kg/mol)
PP12	16 000	420.5
PP05	31 000	510.8
PP20	15 500	416.5
PP28	8600	350.3

Figure 6.3 shows the transient elongational behavior of four polypropylene resins at 200°C for two elongational rates, 0.1 and 0.3 s^{-1}. The elongational behavior of PP20, PP12 and PP05 is quite similar and no strain hardening is observed. No elongational tests have been carried out for PP28, as its behavior was expected to be quite close to that of the first three linear resins.

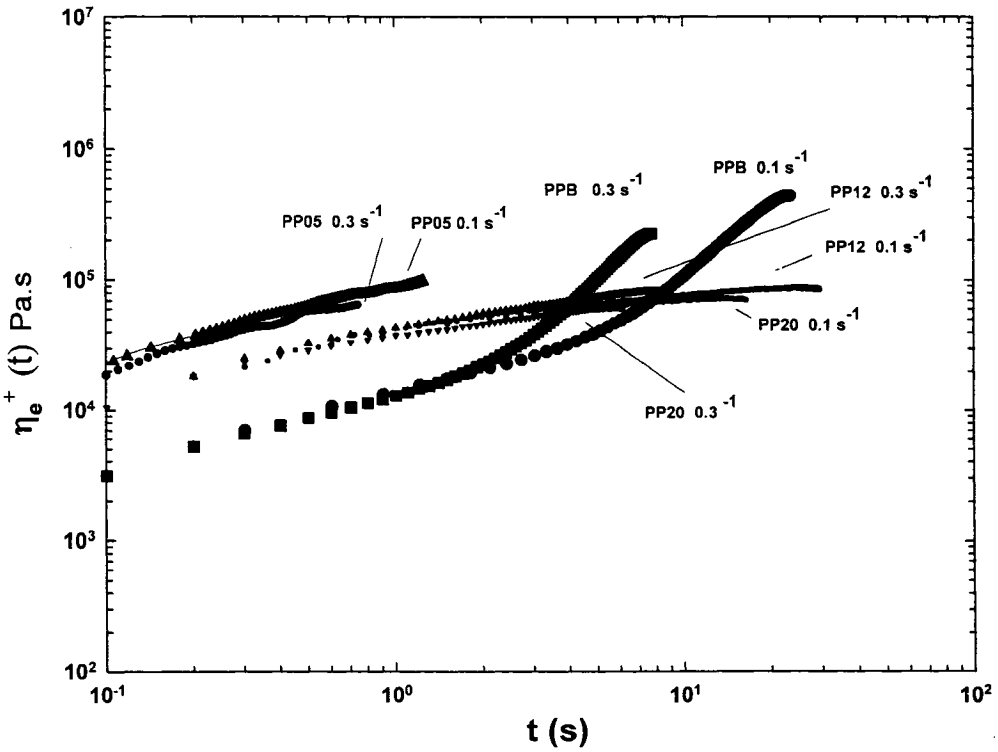

Fig.6.3. Transient elongational viscosity of four PP samples at 200° C.

The larger elongational viscosity for PP05 is attributed to its larger molecular weight (see Table 6.3). In contrast for PPB a highly strain hardening for both elongational rates is observed and starts at short times or small Hencky strains. The strain hardening for this material is very similar to that observed for low density polyethylene [9] and caused by the long branched chains.

Shear stress growth data were also obtained at very low shear rates and a good correspondence with the transient elongational viscosity data of Figure 6.3 was observed, except for the strain-hardening portion of PPB. However, the transient shear data are not presented to avoid crowding Figure 6.3. The films obtained by cast film extrusion were examined by WAXD (wide angle X-ray diffraction) to analyze the

orientation of the crystal reflections. To calculate the orientation functions we used the Herman equation:

$$f = \frac{3cos^2\phi - 1}{2} \qquad (6.2)$$

The details of the method have been mentioned in our previous paper [5] and the data collected from the WAXD apparatus give directly the Herman functions, *f*. In order to obtain a better perspective of the orientation feature, we report in Figure 6.4 the $\cos^2\phi$ values for all the samples where ϕ is the angle between the axes of the crystal blocks (*a*, *b* or *c*-axis) with respect to machine (MD), transverse (TD) or normal direction (ND). The determination of chain orientation in polymers is of great interest because it specifies the arrangement of crystal blocks in the bulk of the precursor film. This arrangement in turn is one of the important factors, which controls the physical and mechanical properties of the film. The high orientation of the crystal blocks is evidently a characteristic of a row nucleated lamellar structure and of a more significant order in the lamellae structure [5]. The higher molecular weight resin shows a larger orientation function of the *c*-axis along the machine direction. In all cases with increasing draw ratio, the *c*-axis moves toward the machine direction while the *b*-axis position almost stays in the TD-ND plane and the *a*-axis moves towards the TD-ND plane. A higher draw ratio will extend more chains in the machine direction, which means more nucleating sites for lamellar crystallization. A larger draw ratio also creates longer extended chains.

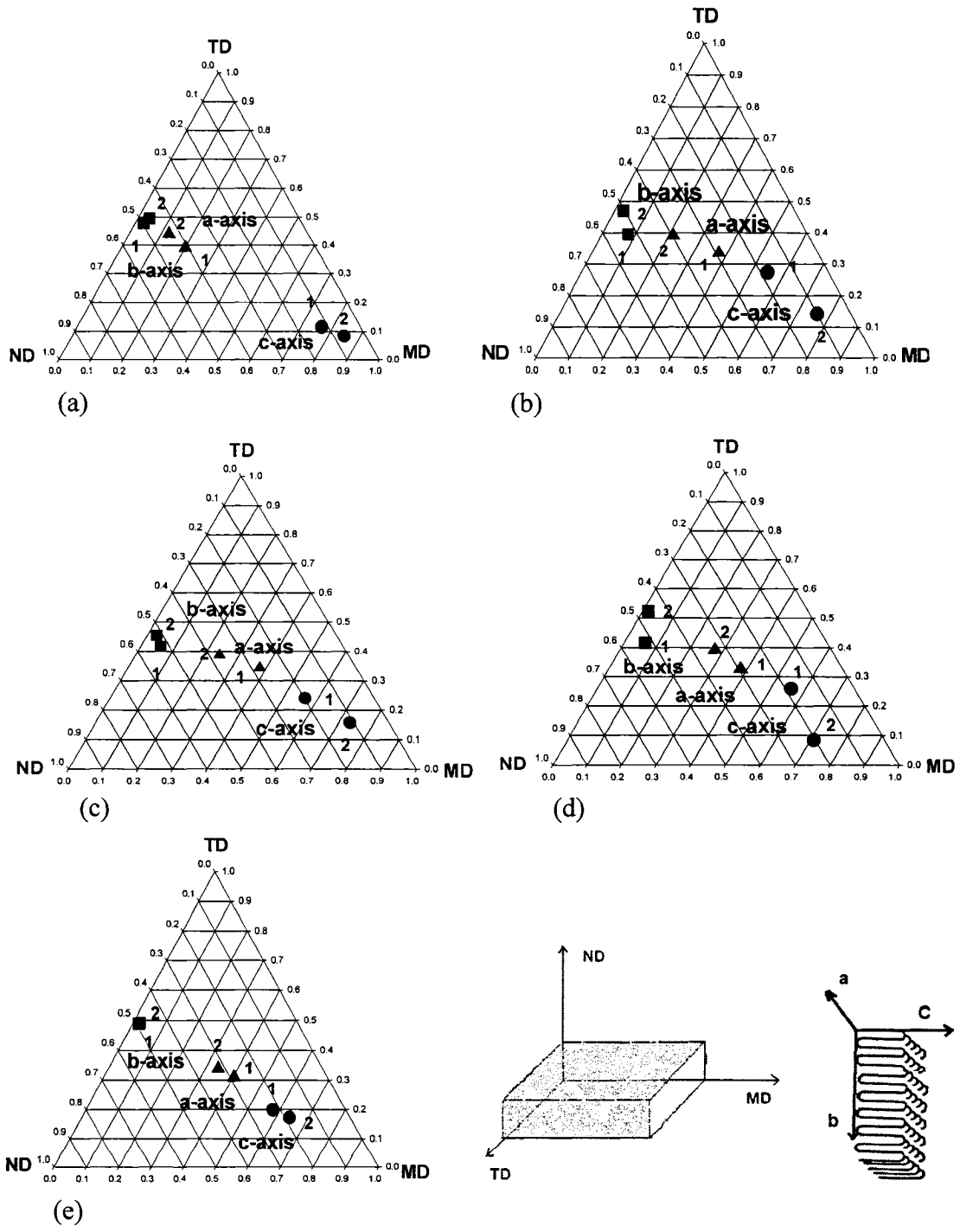

Fig.6.4. Orientation features, $cos^2(\phi)$ values, of the solid films: (a) PP05, (b) PP12, (c) PP20, (d) PP28 and (e) PPB.

It has been shown that a cluster of these long chains forms fibril crystals, which act as a base or support for the lamellar growth [4]. The effect of the draw ratio is more effective when the molecular weight is larger. The tendency of the *a*-axis to move towards the TD-ND plane increases for the higher molecular weight resins. The slightly higher orientation value for PP12 compared to PP20 is probably due to its larger molecular weight. For PPB and PP28 the values don't show a large orientation and this is likely due to their lower molecular weight.

The effect of molecular weight on shear induced crystallization of PP has been already studied in a series of experiments with different grades [10,11]. High, moderate and low molecular weight linear PPs were used to investigate the nucleation process in shear induced crystallization. It was found out that the nucleation of the crystal entities for the lower molecular weight resin occurred after a longer shearing time [11]. However, the effect of long chain branching complicates the shear induced crystallization mechanism. In PPB chain interlocking probably provides more stretched chains in the molten state, Moreover, it is not certain that at very high stretching rates (much beyond the maximum Hencky strain recorded by the extensional viscometer as reported in Fig. 6.3) applied in practical processing, the behavior will still remain the same or interlocking will be diminished. The second issue is lamellae defects and twisting that we believe are more severe for the lower molecular weight resins. The extended chains in the nucleation stage form extended fibrils that act as nucleating sites for the growth stage. It is speculated that PPB creates more stretched fibrils due to its long chain branches, but because of its lower molecular weight the fibrils are much shorter. This could result in

more units that can easily twist or tilt. Figure 6.5 shows schematically the idea: the long fibrils in the case of the high molecular weight resin form a longer and stronger scaffold for the lamellae to grow on them.

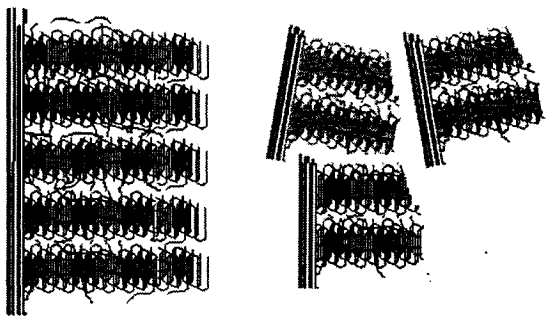

Fig.6.5. Schematic of two types of lamellar structure for polypropylene (a) high molecular weight, (b) low molecular weight polypropylene.

Annealing is one of the main processing stages in developing microporous membranes by stretching as it firstly removes defects in the crystalline structure and secondly increases the lamellae thickness [12]. We annealed one of the samples (PP05-2) for which the original orientation is illustrated in Figure 6.4a to see the effect on the crystal orientation. The annealing was carried out under an extension of 2% with respect to the initial length at 145 °C for 35 min. Figure 6.6 shows the orientation results for the annealed sample. As can be observed, annealing pushes the *a*-axis towards the TD-ND plane (a random distribution of *a* and *b* in the TD-ND plane), and this is an approach to the formation of a planar morphology. This kind of morphology is also desirable for improving the elastic behavior of the films. By conducting tests with other PPs it was observed that annealing is more effective for higher molecular weight resins.

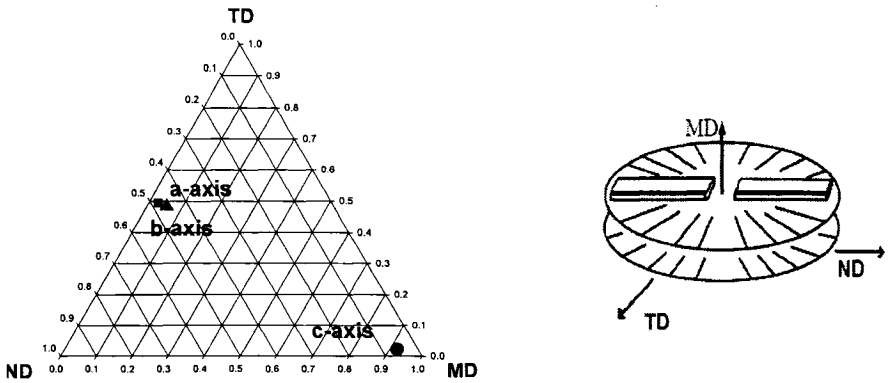

Fig.6.6. Orientation feature of the annealed PP05-2 sample and a schematic of the planar morphology.

We didn't study the effect of isotacticity (steroregularity of the chains) of PP on its crystallization. This important issue in film and fiber production has been discussed by other authors [13]. The rate of crystallization and crystalline chain-axis orientation for resins with higher isotacticity was significantly greater than for lower isotacticity resins. It was shown that, for the resin with high tacticity, an increase in the spinline stresses increases f_c while f_a and f_b decrease and all reach finally a plateau. For resins of lower tacticity the trend was not simple and a maximum for f_c was observed [13].

Fourier transform infrared spectroscopy was carried out to detect the amorphous phase orientation. The method is based on differences in the magnitude of infrared beam absorption along the machine and transverse directions. For an isotropic sample the absorbance is the same in both directions, but as the draw ratio increases the chains are likely more oriented in the machine direction and this causes higher density of the chains in that direction, which leads to higher absorbance. The Herman orientation function is

used to describe the orientation of given molecular axis with respect to the sample direction [14]:

$$f_{i,j} = \left(\frac{S_j}{S_0} - 1\right)\frac{1}{3\cos^2 \alpha_i - 1} \qquad (6.3)$$

where S_j is the intensity of the peak in the spectrum obtained in MD, TD or ND, and $S_0 = (1/3)(S_{MD} + S_{TD} + S_{ND})$, α is an angle related to the configuration of the bonds. For polypropylene the absorption values at the wave numbers of 998 and 972 cm^{-1} are considered as the contribution of the crystalline part for the first and the combination of both crystalline and amorphous parts for the second. For both states the angle, α, will be equal to 90° and in the case of the uniaxial orientation ($S_{TD} = S_{ND}$) the above formula can be modified as:

$$f_{i,MD} = \left(\frac{(S_{MD}/S_{TD}) - 1}{(S_{MD}/S_{TD}) + 2}\right) = \left(\frac{D-1}{D+2}\right) \qquad (6.4)$$

where D is the ratio of the absorbance in the machine (parallel) to the transverse (vertical) direction. For the orientation function of the crystal phase, f_c, the band 998 cm^{-1} is considered so D will be $(A_{II}/A_{\perp})_{998}$, where A is the absorbance. For measuring the total orientation that includes both the crystalline and the amorphous phase orientations the band at 972 cm^{-1} is selected and f_{av} (average orientation) is calculated based on $(A_{II}/A_{\perp})_{972}$. The orientation of the amorphous phase, f_a, can be determined from these two values by:

$$f_{av} = X_c f_c + (1 - X_c) f_a \qquad (6.5)$$

where X_c is the degree of crystallinity determined through DSC (differential scanning calorimetry). The results for the orientation functions vs. draw ratio are plotted in Figure 6.7 for all the linear PPs. The trend for the orientation of the crystalline phase is in accordance with the WAXD results. However, the orientation function values are slightly lower than the WAXD values.

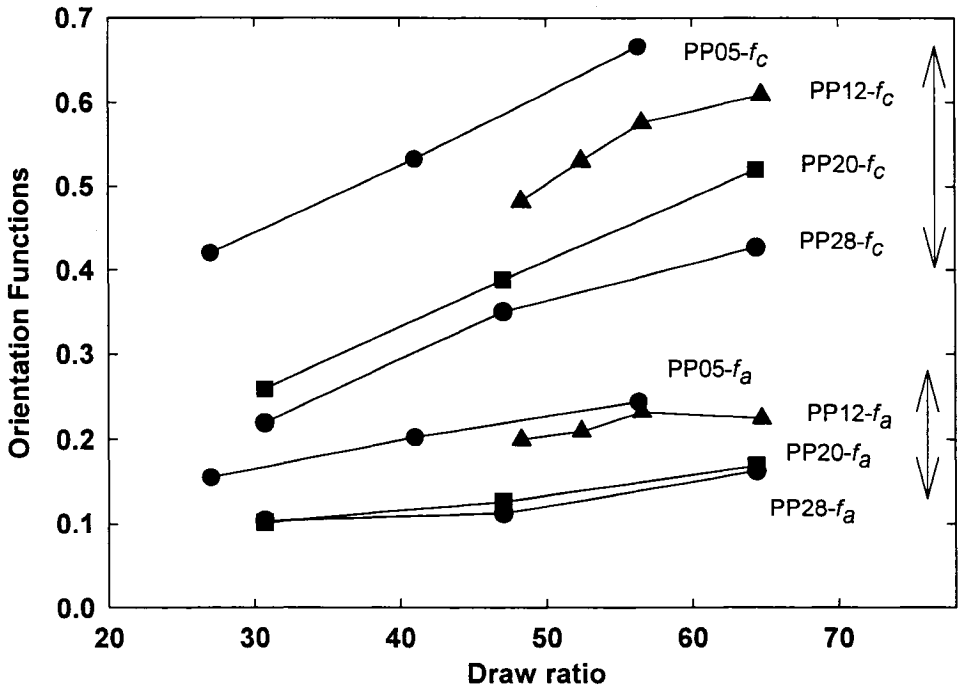

Fig.6.7. Orientation functions of the crystalline and amorphous phases for the all the linear resins versus draw-down ratio.

As expected, the orientation increases with draw ratio, but the increases for the crystalline phase are much more significant, with a clear influence of the molecular weight. Almost the same order for PPs is observed for amorphous orientation but less influence of the draw ratio is seen and the values are closer to each other compared with the crystalline orientation functions.

Tensile tests have been carried out to analyze the response of the solid films to extension and the results are presented in Figure 6.8.

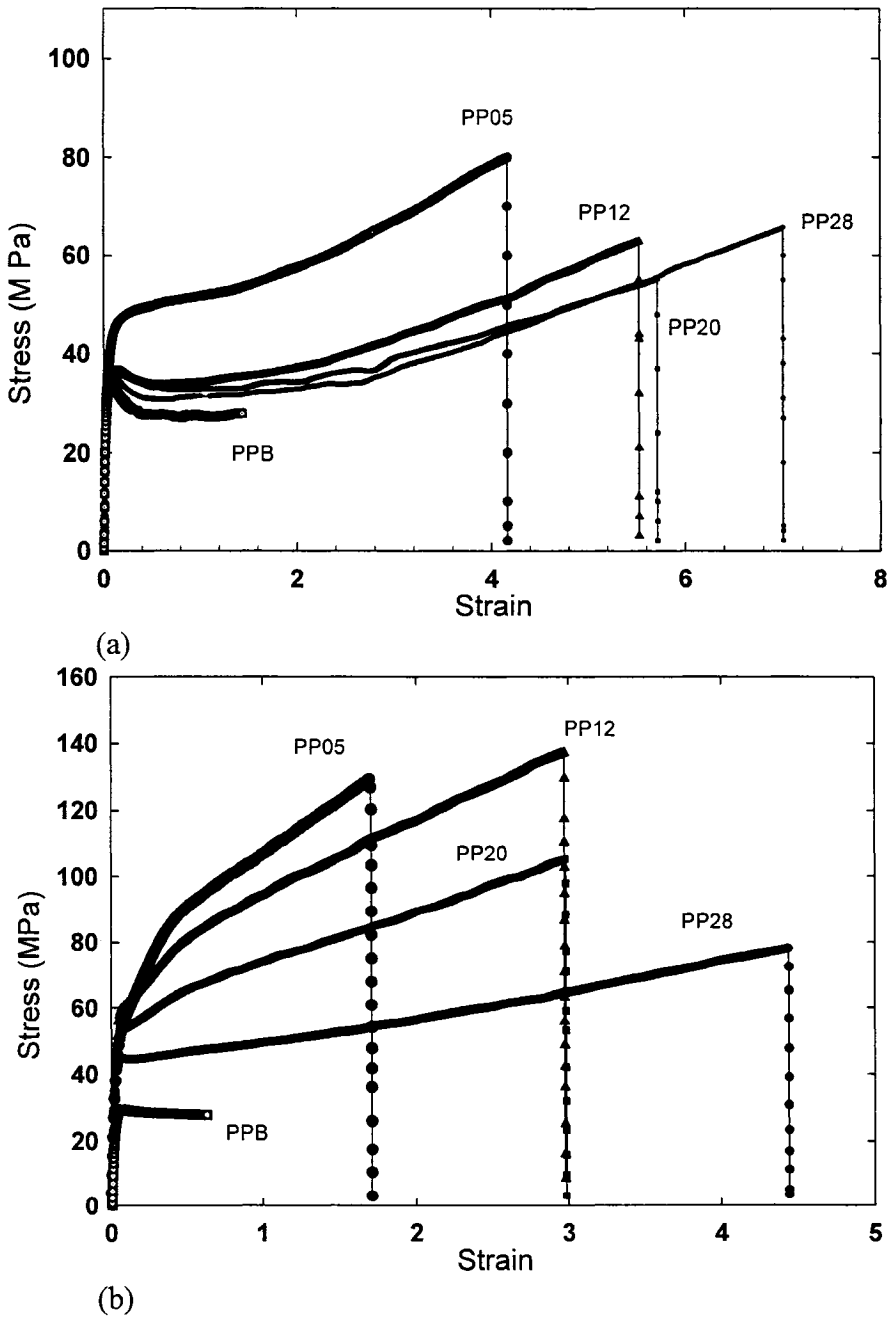

Fig.6.8. Tensile results for the solid PP film samples produced under (a) small draw ratio (DR=23), (b) large draw ratio (DR=65).

It is likely that for the larger draw ratio all the resins develop a lamellar structure while for smaller draw ratio the structure is not fully oriented with a tendency to form twisted lamellae and also a high density of cross hatching [5]. All film samples prepared at the smaller draw ratio, except PP05, show a clear yielding behavior (Fig. 6.8a), whereas the samples prepared at the larger draw ratio show no significant yielding (Fig. 6.8b). The higher yield strength for PP05-2 in comparison to PP05-1 can be attributed to the higher orientation function. A part of this also could be due to the larger number of active tie chains between the crystal blocks. A direct relationship between the yield strength and the fraction of the tie chains has been assumed by Nitta and Takayanagi [15]. For highly oriented samples that may possess more active tie chains the stresses are mostly concentrated in the space between the crystal blocks and are spent to stretch the tie chains. For low oriented samples the stresses are mostly spent to deform the crystal blocks (shear yielding) and orient them in the stretching direction. Hence, we believe that for highly oriented samples the role of tie chains is more critical as their number and orientation can influence the strength significantly [16].

6.2.5 Effect of the applied strain rate

The applied strain rate at the die exit is an important issue for generating a lamellar structure [5]. Larger strain rate generate more stretched chains to develop shishs upon crystallization. Although solidification takes place rapidly, enough time should also be provided for crystallization of the rest of the chains to form stable kebabs perpendicular

to the shishs. To study the effect of strain rate we lowered the extrusion flow rate and the film pick-up speed by half. The total draw ratio was the same while strain rate that comes from the difference between the speeds at the die and pick-up became almost half. It should be noted that an apparent strain rate can be calculated by dividing the difference between the pick-up speed and the extrudate velocity in the die by the drawing distance, which was kept constant. Figure 6.9 shows the DSC for these two samples of PP12 with draw ratio of 65.

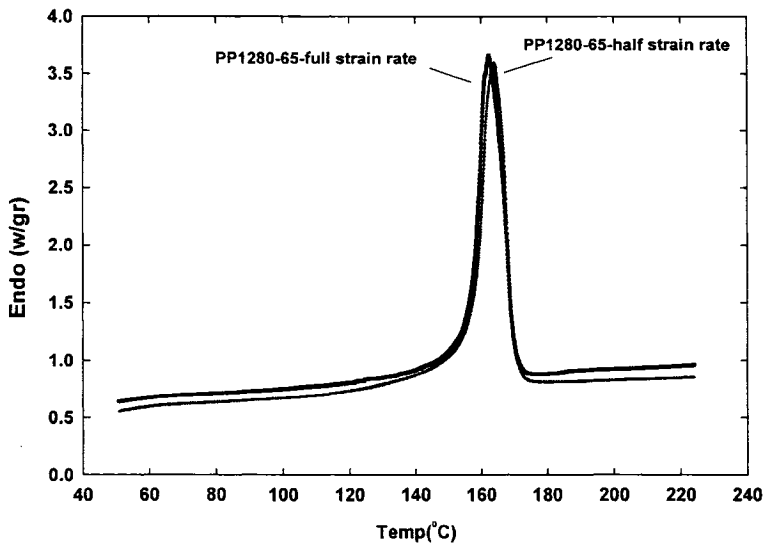

Fig. 6.9. DSC results for two precursor PP12 film samples (with draw ratio of 65), one prepared with the full strain rate and the other with the half strain rate.

While the overall crystallinity did not change, the DSC result reveals slightly thinner lamellae for the sample processed under full strain rate.

Figure 6.10 reports the tensile results for two samples and we observe a net improvement of the tensile properties when stretching the sample at full strain rate. We believe that more shishs are formed at high deformation rate, which improves the tensile

strength. We also examined these two samples by wide angle X-ray scattering to reveal the orientation. As it is shown in Table 6.4, the orientation functions of the samples are in the same range.

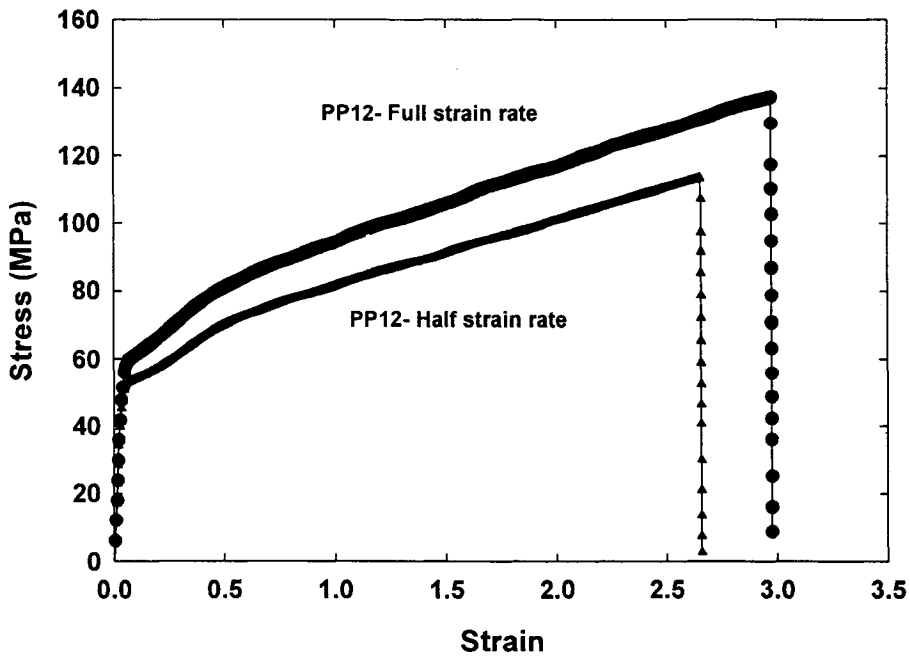

Fig.6.10. Tensile results for two precursor PP12 film samples (with initial draw ratio of 65), one prepared under full strain rate and the other under half strain rate.

6.2.6 Effect of Annealing

Annealing under low tension is the first stage for making a microporous membrane from the precursor film. Annealing has a significant effect on the orientation as shown above and on the thickness of the crystal lamellae as well [12]. The improvement of orientation and thickness may be the result of the crystallization of the trapped end chains between

the lamellae and also the melting of very thin lamellae and their recrystallization in the form of the thicker ones. Annealing at a temperature above the α transition will allow the crystalline blocks to move locally.

Table 6.4. Orientation for precursor PP12 films (DR=65) : Sample (a) prepared under full strain rate and Sample (b) prepared under half strain rate.

f (Herman orientation function)	*a*-axis		*b*-axis		*c*-axis	
	a	b	a	b	a	b
MD	0.215	0.207	-0.475	-0.467	0.690	0.674
TD	0.136	0.083	0.239	0.219	-0.375	-0.302
ND	0.079	0.123	0.235	0.253	-0.314	-0.376

This local sliding removes some defects in the crystalline structure of the lamellae and reorients them in the direction of the applied tension. This may explain the increase in orientation as shown in Figure 6. The tensile behavior of one of the precursor films obtained from PP12 (PP of moderate molecular weight) under a medium draw ratio of 48 is compared in Figure 6.11 with that of the annealed sample (performed at 145 °C and for 25 min.). As the test proceeds the sample passes the initial elastic region that is believed to be due to the stretching of the short tie chains. Following the elastic response region the second part coincides with voids creation as a result of chain scissions of the already stretched short chains. Pores are created between the lamellae and are enlarged as the stress increases linearly. With scission of short tie chains the stress is transferred to the longer tie chains causing them to be stretched out. Stretching of the longer tie chains will result in a local crystallization,

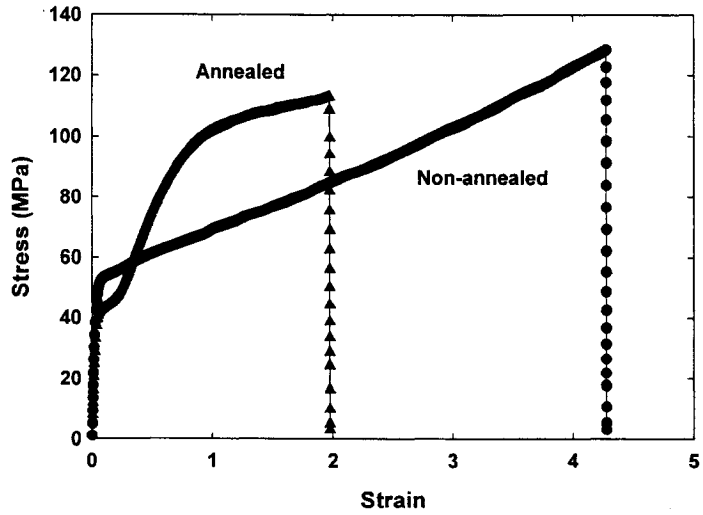

Fig.6.11. Tensile results for two precursor film samples of PP12, one annealed at 145°C and the second regular (non-annealed) sample.

which explains the strain hardening behavior observed in Figure 6.11. Local crystallization creates bridges between the crystal blocks as it is shown in Figure 6.12 (micrograph for the sample before the breaking point). Stretching will continue until the stress reaches a value large enough to breakdown the bridges and then rupture happens. The rupture for the annealed sample occurs at much shorter strain than for the non-annealed sample. It should also be noted that the initial orientation of the crystal blocks for the non-annealed precursor film is far from that of a planar morphology. Instead of a series stacked aligned lamellae there will be some lamellae tilting. For the non-annealed sample, in the second region of Figure 6.11, a part of the stress is consumed for reorientation of the crystal blocks. This contribution is the largest for the less oriented samples and the smallest for the annealed and highest molecular weight PP sample (compare Figs. 4b and 6). This sample possesses a planar morphology associated with the highest orientation of the *c*-axis along the machine direction and the stress is largely

concentrated in the crystal blocks and spent to separate them. That may also explain a sharper rise of the stress with strain. The larger strength for the annealed sample is likely due to the presence of thicker lamellae and also a direct concentration of the stress in the crystal blocks. The shoulder in the tensile curve for the annealed sample is attributed to the load transition to the long tie chains and also to voids formation.

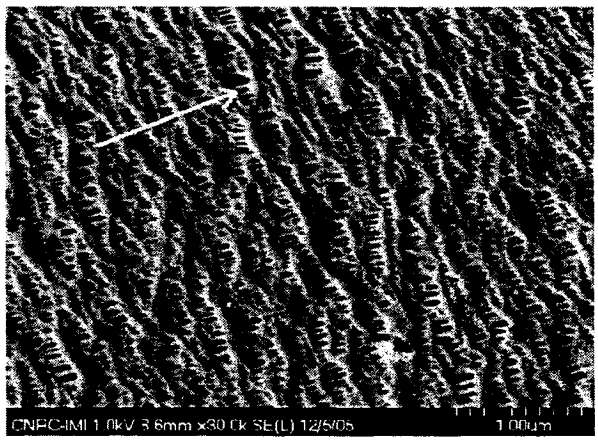

Fig.6.12. Micrograph of the surface of the stretched annealed sample of Fig. 10 before breaking point (the arrow indicates the direction of stretching).

6.2.7 Conclusion

Five different polypropylene resins have been characterized by rheology and the row-nucleated lamellar structure development during the cast film process has been investigated. The orientation of crystal blocks appears to be controlled by the molecular weight of the resins, as indirectly deduced from the melt index and the rheological properties (zero-shear viscosity) for the linear PPs. The behavior of the branched PPB was found to be totally different with a much longer elastic characteristic time at low frequency with respect to its melt index and strain-hardening effects under elongational

flow.A row-nucleated morphology for polypropylene can be achieved via cast film extrusion under efficient cooling. The orientation of the *c*-axis of the crystalline lamellae along the machine direction improved with draw ratio and this was more pronounced for the higher molecular weight resin. The strain-hardening and the larger elasticity for the branched PPB did not favor the orientation of the crystalline phase. The film samples showed different responses to tensile tests. The tensile properties were shown to increase with increasing draw ratio of the cast films. Except for the high molecular weight resin, a necking behavior was observed for samples prepared under a low draw ratio. For samples prepared under a high draw ratio non-significant yielding was observed and the tensile strength values were much larger than those for the low draw-ratio samples. Annealing the precursor film under a slight tension improved the orientation and significantly affected the tensile response. Two distinct regions were detected: the first was the typical elastic region attributed to the stretching of the short tie chains, while the second region was due to the contribution of the stretching of the longer tie chains, voids creation and reorientation of crystal blocks.

6.2.8 Acknowledgements

Financial support from NSERC (Natural Science and Engineering Research Council of Canada) and from FQRNT (Fonds Québécois de Recherche en Nature et Technologies) is gratefully acknowledged.

6.2.9 References

[1] T. H. Yu., PhD thesis, Virginia Polytechnic Institute and State University (1996)

[2] R.W. Callahan, R.W. Call, K. J. Harleson and T.-H. Yu, US Patent No.6602593 (2003)

[3] A. Nogales, B.S. Hsiao, R.H. Somani, S. Srinivas, A.H. Tsou, F.J. Balta-Calleja, and T.A. Ezquerra, *Polymer*, 42, 5247 (2001)

[4] J.A Kornfield, G. Kumaraswamy and A. Issaian, *Ind. Eng. Chem. Res.*, 41, 6383 (2002)

[5] F. Sadeghi, A. Ajji and P.J. Carreau, *J. Plastic Film Sheet*, 21, 199 (2005)

[6] P.J. Carreau, Daniel C.R. De Kee, and R.P. Chhabra, Rheology of Polymeric Systems: Principles and Applications, Hanser (1997)

[7] M. Fujiyama and H. Inata, *J. Appl. Polym. Sci.*, 84, 2157 (2002)

[8] F. A. Morrison, Understanding Rheology, Oxford University Press (2001)

[9] M.H. Wagner, S. Kheirandish and M. Yamaguchi, *Rheol. Acta*, 44, 198 (2004)

[10] A. Nogales, B.S. Hsiao, R.H. Sommani, S. Sirinivas, A. H. Calleja, and T.A. Ezquerra, *Polymer*, 42, 5247 (2001)

[11] F. Jay, J.M. Haudin, and B. Monasse, J. *Mat. Sci.*, 34, 2089 (1999)

[12] L. E. Alexander, X-ray Diffraction Methods in Polymer Science, Wiley, New York (1969)

[13] D. Choi and J. White, *Polym. Eng. Sci*, 44: 210 (2004)

[14] I.M. Ward, P.D. Coates, and M.M. Dumoulin, eds., Solid Phase Processing of Polymers, Hanser (2000)

[15] K.H. Nitta and M. Takayanagi, *J. Polym. Sci.: Part B Polym. Physics*, 38, 1037 (2000)

[16] M. Takayanagi, K.H. Nitta, and O. Kojima, *J. Macrom. Sci., Part-B,* B4, 1049 (2003)

Chapter 7
Analysis of Microporous Membranes Obtained from Polypropylene Films by Stretching

7.1 Presentation of the article

The objective of the third article was to present a detailed vision of membrane formation. For this purpose we ran elongational viscosity tests at the rate similar to the practical production case for the films and studied the response of the melt. The effect of annealing of the precursor films on orientation are discussed in detail. The cold and hot stretching stages leading to formation of the porous structure are reviewed and mechanisms for the structure formation are presented. Finally, the performance of membrane is shown by permeability and puncture tests.

* *Submitted to Journal of Membrane Science Aug.2006*

7.2 Analysis of Microporous Membranes Obtained from Polypropylene Films by Stretching

Farhad Sadeghi[1], Abdellah Ajji[2] and Pierre J. Carreau[1]

1)Center for Applied Research on Polymers and Composites, CREPEC,
Ecole Polytechnique, Montreal, QC, Canada
2)CREPEC, Industrial Materials Institute, CNRC, Boucherville, QC, Canada

7.2.1 Abstract

Five different polypropylene resins were selected to develop microporous membranes through melt extrusion and stretching (cast film process). The effect of the polymer melt rheology on elongation and on row-nucleated lamellar crystallization was investigated. The arrangement and orientation of the crystalline and amorphous phases were examined by WAXD (wide angle X-ray diffraction) and FTIR (Fourier transform infrared) methods. The extrusion and cooling parameters were adjusted properly to obtain uniform precursor films with appropriate morphology. Annealing, cold and hot stretching were consequently employed to generate and enlarge the pores. It was found that molecular weight was the most important material factor that controlled the membrane structure. The role of annealing and stretching parameters was also investigated. The permeability to water vapor (under atmospheric condition) and nitrogen (under elevated pressure) was measured. It was observed that permeability increased with increasing pressure and went through a transition from Knudsen diffusion to Poiseuille flow.

7.2.2 Introduction

Membranes are increasingly employed for separation processes. From energy and processing points of view, they are progressively competing with the conventional separation processes such as distillation. Polymers are among the best candidates for the development of membranes covering a broad range of applications from microfiltration to reverse osmosis.

There are several techniques used for the fabrication of membranes and most of them are based on solution casting followed by phase separation. Solvent contamination and costly solvent recovery are two drawbacks for solution casting, although some improvements have been made in the recent decade [1]. One technique, which is applicable to semicrystalline polymers, is based on the stretching of a thin film with a row nucleated lamellar structure [2]. In this case pores are created as a result of lamellae separation. This method is relatively less expensive and there is no solvent contamination but the major disadvantage is the low tear resistance in machine direction, due to the highly oriented structure of the film.

The fabrication of membranes by stretching is carried out in three main consecutive stages: 1) production of the precursor film with a lamellar morphology, 2) annealing of the film to thicken the lamellae, and 3) stretching of the film at low temperature to create voids and then stretching at high temperature to enlarge the pores [2]. One of the main issues in this process is the generation of a proper initial row nucleated structure. The polymer type and applied extrusion conditions are key factors for this method [3]. These factors determine the orientation and position of crystal

blocks. Annealing will, in turn, partially remove the defects in the crystalline phase. The defects could be disruption of chain folding in the blocks or plane slippage. Annealing also improves the long spacing (the total thickness of the crystalline and amorphous phases that is almost periodically repeated) and uniform the lamellae thickness distribution [4]. Consequently cold and hot stretching determine the configuration and properties of the obtained membrane. The parameters that affect the crystalline structure of the precursor films can be classified into material and process categories. The molecular weight and molecular weight distribution of the resins are the main material parameters controlling the crystalline lamellae and amorphous structures.

In this work, different polypropylene (PP) resins have been selected to study the effect of molecular weight on crystalline structure and membrane formation. High molecular weight resins possessing long chains are good candidates for the generation of a proper row nucleated lamellar since they form long fibrils (threads) that act as sites for lateral lamellae crystallization [5]. If the amount of the long chains is large, the number of threads goes up and they get very close to each other and lamellae impingement happens quickly [6]. Longer fibrils also improve orientation by keeping a strong scaffold for later crystallization. In contrast, for a small amount of long chains, there will be less threads and the longer distance between them can cause lamellae twisting [5].

The extrusion and production of the precursor films is a delicate process since the samples should be produced under high draw ratio and cooling rates. Although the presence of long chains is important for improvement of drawability and crystalline structure, a very large number of long chains can cause problems. For example, the

stick-slip phenomenon [7] was observed for a high molecular weight PP studied in our preliminary tests. The presence of low molecular weight tail (short chains) is generally undesirable for the formation of a row nucleated structure since it affects adversely the chain relaxation, but it improves melt processability via smoother extrusion [8,9]. Obtaining a very uniform film is a major concern since any non uniformity and thickness variations cause irregularities in the stress distribution.

Yu et al [2] studied the development of high density polyethylene (HDPE) membranes. They used two grades of HDPE with identical M_n but differing in molecular weight distribution. The resin with a broader molecular weight distribution showed more elongated fibrils. As a result of more fibrils, the precursor film showed a larger modulus and better mechanical properties in comparison to the resin with the narrower molecular weight distribution. They also showed that annealing under a slight tension (3%) was more effective for lamellae thickening. They observed a reduction in permeability with increasing cold draw ratio beyond 40%. The microporous structure was found to be more uniform for the resin of broader molecular weight distribution, and this was attributed to the higher inter-lamellar tie chain density or fibril nuclei. They also observed that annealing at 120°C in comparison to 105°C could significantly increase the long period of the film structure.

Johnson et al [6] studied the process for the production of microporous membranes from Poly (4-methyl-1-pentene) (PMP), and polyoxymethylene (POM) by stretching. They used the Gurley number (time required for 10 mL of air to pass through one square inch section of film at a constant pressure of 12.2 inches of H_2O) to examine

the permeability of their membranes. Lower Gurley numbers correspond to higher permeability. For PMP, cold stretching decreased the Gurley number while for a normalized Gurley number (time/thickness) the minimum Gurley occurred around a stretching of 80 %. Also, the cold stretching temperature was shown to be optimum around 70 °C. Rising the hot stretching temperature up to 160°C decreased the Gurley number, while there would be a possibility for structure deformation at very high temperature. They concluded that the initial decrease of the Gurley number with increasing cold stretch temperature was the result of a greater mobility within the amorphous phase rather than of the crystal phase (the PMP glass transition is 35°C).

Polypropylene is widely produced in different grades and structures and, in comparison to polyethylene, PP shows better thermal stability and mechanical properties. Hence, it could be a more suitable candidate for the fabrication of microporous membranes. Although this material is commercially used in membrane development, very few articles have been published on this topic [10]. In this work we have investigated the role of material properties and process parameters on the structure and performances of PP porous membranes obtained by stretching of films.

7.2.3 Experimental

7.2.3.1 Materials

The five different polypropylene grades used in this study are listed in Table 7.1.

Table 7.1. Polypropylene grades used

Resin Code	Company	MFR 230°C/2.16 kg	Nomenclature in this paper
PDC1280	Basell	1.2	PP12
Pro-fax 6823	Basell	0.5	PP05
Pro-fax 814	Basell	2.8	PPB
PP4292E1	ExxonMobil	2.0	PP20
PP4612E2	ExxonMobil	2.8	PP28

PDC1280 (PP12) is a general purpose grade and Pro-fax 6823 (PP05) possesses the lowest MFR (melt flow rate, high molecular weight) in the homo polypropylene list introduced by Basell. Pro-fax 814 (PPB) is a branched polypropylene with long chain branches (its molecular weight is unavailable). It was selected because of the effect of branched chains on the relaxation time of the molten polyolefin. In this paper, we refer to these materials as PP12, PP05 and PPB. PP4292E1 (PP20) and PP4612E2 (PP28) are ExxonMobil grades used for the production of oriented films. The manufacturer reports these two resins as homopolymers with bimodal molecular weight distributions. An FTIR test was carried out and no trace of ethylene was found in the absorption spectrum of both resins.

7.2.3.2 Rheological Characterization

The extensional viscosity was measured via the new SER universal testing platform from Xpansion Instruments. The model used in our experiment was SER-HV-A01,

which is a dual windup extensional rheometer and has been specifically designed for the ARES rheometer platform and is capable of generating elongational rates up to 20 s^{-1} under a controlled temperature up to 250°C.

7.2.3.3 Film Preparation

The films were prepared by cast film processing with a slit die at the temperature of 220 °C. To improve cooling, a fan was installed to supply air to the film surface right at the exit of the die. The key parameters were the fan speed, take-up roll speed and die temperature. We worked at the maximum speed of the fan and constant die temperature, so the only variable was the take-up speed. Since the extrudate velocity in the die was constant the pick speed determined the draw ratio for the film production.

7.2.3.4 Film and membrane characterization

Crystal orientation measurements were carried out using a Bruker AXS X-ray goniometer equipped with a Hi-STAR two-dimensional area detector. The generator was set up at 40 kV and 40 mA and the copper CuK_a radiation (λ = 1.542 Å) was selected using a graphite crystal monochromator. The sample to detector distance was fixed at 8 cm. Prior to measurements, careful sample preparation was required to get the maximum diffraction intensity. This consisted in stacking several film layers in order to obtain the optimum total thickness of about 2.5 mm.

Tensile tests were performed using an Instron 5500R machine equipped with a chamber for running tests at elevated temperatures. The procedure used was based on the D638-02a ASTM standard.

For FTIR measurements, infrared spectra were recorded on a Nicolet Magna 860 FTIR instrument from Thermo Electron Corp. (DTGS detector, resolution 4 cm^{-1}, accumulation of 128 scans). The beam was polarized by means of a Spectra-Tech zinc selenide wire grid polarizer from Thermo Electron Corp. The crystalline and amorphous orientations were measured based on the method that has been explained in detail in Ref. [3].

The DSC (differential scanning calorimetry) tests were carried out on a TA Instruments Q1000, with the heating rate of 20 °C/min.

Permeability of water vapor was measured via a MOCON PERMATRAN-W Model 101K at room temperature. For nitrogen the flow of gas transmitted through the membrane was measured with a photo flowmeter (Optiflow520). The set-up for nitrogen permeability was built in our lab.

For porosimetery, the pore size distribution and porosity were evaluated using a mercury porosimeter (Pore Sizer 9320-Micromeritics).

7.2.4 Results and Discussion

7.2.4.1 Extrusion and materials

Figure 7.1 shows the stress-strain curves for the melts obtained from the extensional viscosity measurements at a temperature of 200 °C and an elongational rate of 5 s^{-1}. The strain rate was similar to the value applied to the molten extrudate at the exit of the die

while for temperature we couldn't conduct the experiment at a higher temperature because of sagging of the samples.

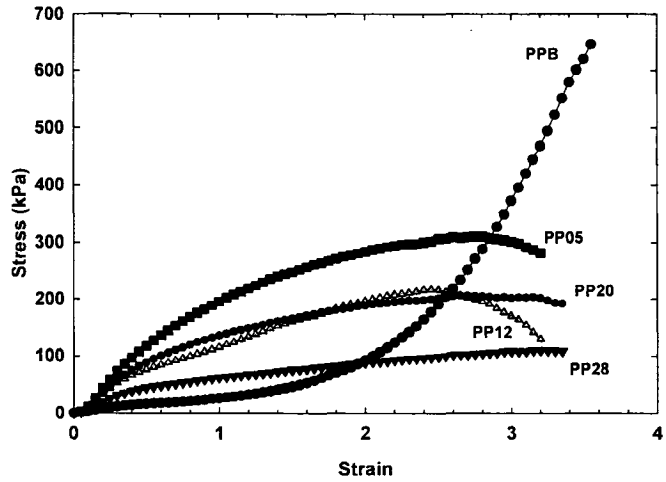

Fig.7.1 Stress-strain obtained from the elongational tests at the elongational rate of 5 s^{-1} and 200°C.

The decreases of the stress at high strain for the homopolymers are indicative of sample failure. As expected the largest molecular weight resin (PP05) exhibits the largest extensional properties among the homopolymers and its stress increases smoothly up to a strain value close to 3, which is slightly larger than for the general purpose grade (PP12). For the two bimodal resins, PP20 and PP28, the stress is increasing further up to a strain of 3.4. The behavior is totally different for PPB, which shows a rapidly ascending trend. This is the result of strain hardening, which occurs for a resin with long chain branches. While PPB shows a good melt strength, its lower molecular weight results in poor drawability [8] and also mechanical properties for the films.

It should be noted that the effect of the extrudate temperature at the die exit is not trivial. A lower temperature more likely preserves the initial state of polymer chains but it

affects the extrusion process. A lower die temperature also reduces the mobility of the chains to be extended at high draw ratios at the die exit and also influences the mobility of the shorter chains for secondary crystallization.

7.2.4.2 Crystallization and solidification

The stress induced crystallization is influenced, in addition to material parameters, by strain, strain rate and cooling conditions. These parameters control the lamellae structure such as crystal thickness, orientation and type of the crystals. DSC tests were performed on the precursor films prepared with a draw ratio of 65 and under maximum cooling rate (except for PP05 for which 70% cooling rate was used). The key results are presented in Figure 7.2a. The DSC results for PP20 and PP28 were quite similar to those of PP05 and, hence, are not presented in Figure 7.2a. Since the melting peaks of all samples (except PPB) did not change much, it was assumed that the lamellae thickness was of the same order. Hence the major difference in the crystalline structure of the precursor film is thought to come from orientation of the crystal blocks and configuration of tie chains connecting crystal blocks (tie chain density, length and orientation). We believe that the samples from a very high molecular weight resin possess a larger amount of strong threads, which makes lamellae separation difficult. We observe in Figure 7.2a a slight shoulder at higher temperature for the film of PP05 (also for the films of PP20 and PP28 not shown). WAXD results (discussed later) show only one crystalline form (α) for the precursor films and no trace of β crystalline form could be observed. Since the resins

are all considered homopolymers the shoulder peak is only attributed to lamellae distribution (thinner and thicker lamellae).

Cooling is a critical controlling factor in the formation of precursor films [4]. Although very efficient cooling conditions are necessary to prevent chains relaxation at the die exit, rapid cooling might affect the secondary crystallization (lamellae growth). Therefore there should be optimum cooling conditions to obtain the appropriate lamellae structure.

We didn't have any mean to measure the crystal growth under stress, but we studied the spherulitic growth for these resins under quiescent crystallization conditions. Apparently the stress conditions mostly affect the nucleation stage while the spherulitic growth proceeds through secondary crystallization (similar to lamellae growth) and is controlled by the cooling conditions. As it can be seen from Figure 7.2b the spherulitic growth rate, given by the slope of the curves, is almost the same for the four resins.

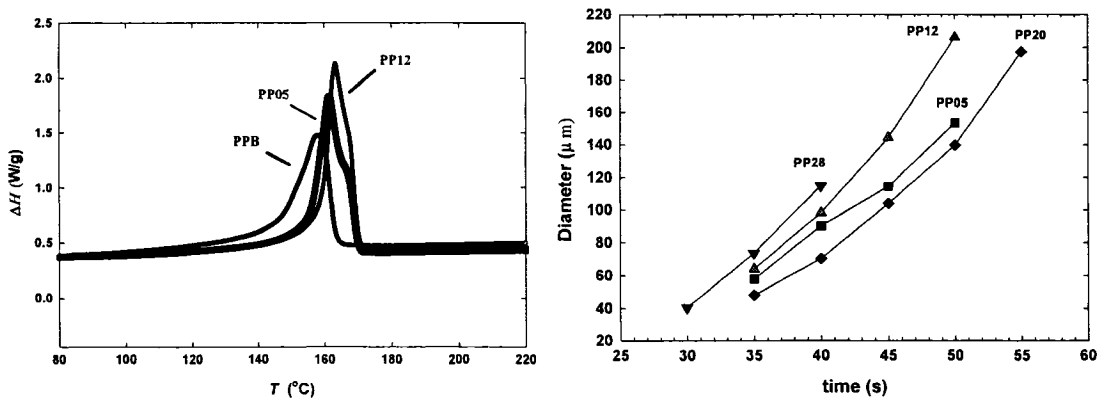

Fig.7.2. (a) DSC of the PP films (heating rate of 20°C/min) and (b)Spherulite growth versus time (cooling rate of 20°C/min).

The results for PPB (long chain branched PP) are not shown in Figure 7.2b because they showed a large amount of very tiny spherulites, smaller than the range of our measurement accuracy.

7.2.4.3 Annealing

Annealing is performed at a certain temperature that is the beginning of the mobility in the crystalline structure (T_α) [6]. This annealing removes the defects in the crystalline structure, thickens the lamellae and finally improves lamellae orientation and uniformity [11]. Although annealing usually takes place in a short time, its role is critical in membrane production. The three controlling factors are annealing time, annealing temperature and applied stress during annealing. Some authors found that a slight tension during annealing is effective [2], improving orientation, but in our case we didn't observe any significant improvement. Annealing increases the long period (total thickness of the crystal and amorphous phases) [12]. It is estimated that much of the long period improvement is due to the increasing of the lamellae thickness. We observed that for polypropylene under quiescent annealing (in absence of stress) the efficient annealing time was 10 min at 140 °C and beyond that, the structure parameters remained constant. This has also been reported for PE films [2].

The annealing temperature is probably the most important factor here. It should be noted that increasing temperature to a high degree might deteriorate the initial lamellar crystalline structure through local partial melting and recrystallization. Figure 7.3 compares the DSC results for the annealed and non-annealed samples of a precursor

PP28 film. A small peak is observed around 140 °C after annealing, as it has also been reported by other authors [13].

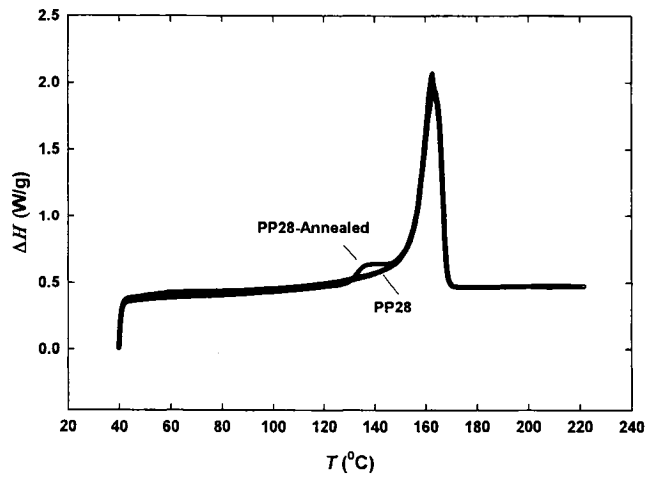

Fig.7.3. DSC of the PP28 annealed and non-annealed samples (annealing time of 10 min at 140°C; heating rate of 20°C/min).

It can be observed that the area under the curves is also increased after annealing, which means an improvement in crystallinity. The position of the peak didn't change significantly suggesting that the crystal thickness change was negligible. We observed that annealing improved the orientation significantly as shown in Table 7.2 [3].

The same trend was observed for all other films. The improvement in crystal orientation after annealing has been addressed elsewhere [11]. Annealing provides a possibility for the lamellae to be rearranged in machine direction resulting in orientation improvement. Since tie chains are connecting the lamellae, rearrangement and improvement in the orientation of the lamellae would affect the tie chains as well. That could be an explanation for the rise in amorphous orientation. We didn't anneal any PPB samples

since the film couldn't be stretched for membrane development due to its low molecular weight.

Wide angle X-ray diffraction measurements were carried out on the annealed samples. Figure 7.4 shows the diffraction patterns for two PP films (high and low molecular weight PP samples). The first ring represents the 110 and the second one is the 040 crystalline plane. The normal to the 110 plane is the bisector of the *a* and *b* axes and 040 is along the normal of the *b*-axis of unit crystal cells, as shown in the sketch of Figure 7.44 (d).

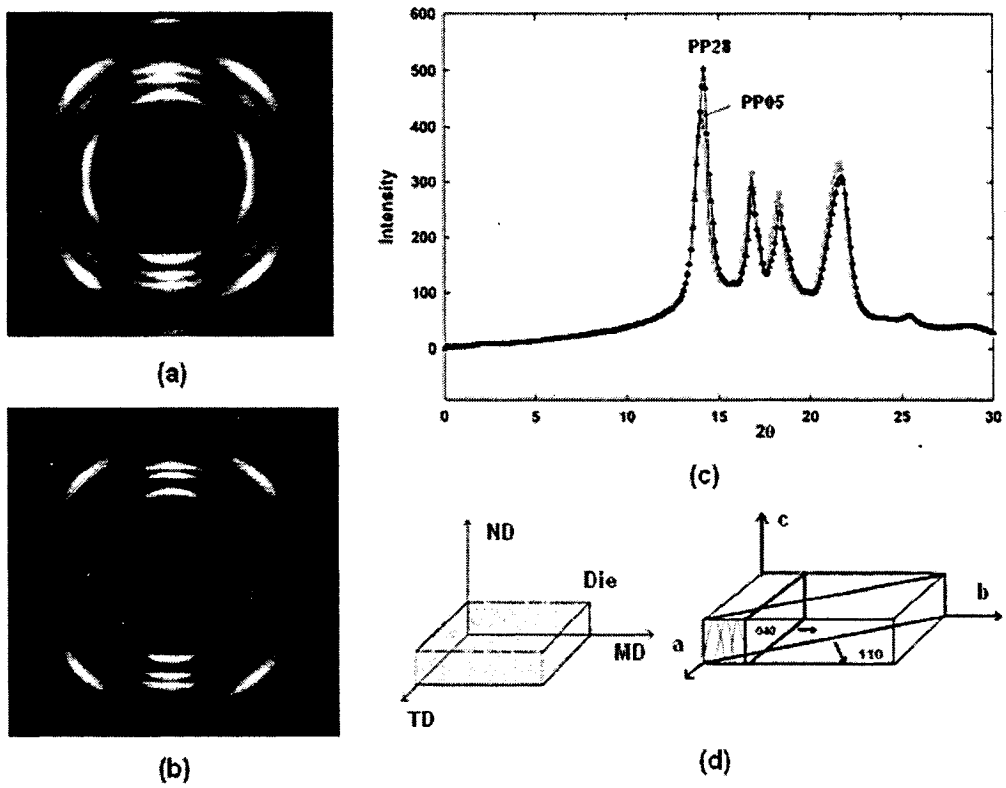

Fig.7.4. WAXD patterns of the annealed precursor films (a) low and (b) high molecular weight resins with initial draw ratio of 65, (c) diffraction spectrum with integration throughout the circles and (d) the crystal plans with respect to fixed coordinate.

The arcs are sharper for PP05 (the resin of highest molecular weight) and more concentrated while no major difference is observed for the WAXD spectrum (intensity versus 2θ). With respect to the Scherrer equation [12] and the inverse dependency of the width of the half maximum of a peak on crystal thickness, a conclusion can be drawn that the lamellae thickness doesn't change at least along the *a* and *b* axes. Hence, it is assumed that the effect of molecular weight is more pronounced on the orientation of lamellae as it will be shown later.

The orientation and position of the crystal blocks in the precursor films determine the lamellae separation process, which results in pores formation. The orientation of the amorphous and crystalline phases (*c*-axis with respect to MD) of the samples has been measured by Fourier transform infrared spectroscopy and the results are presented in Table 7.2. The orientation function was calculated as [14]:

$$f_{i,MD} = \left(\frac{D-1}{D+2} \right) \qquad (1)$$

where D is the ratio of the absorbance in the machine (parallel) to that in the transverse (perpendicular) direction. For the orientation function of the crystal phase (*c*-axis with respect to MD), f_c, the band 998 cm^{-1} is considered so D will be $(A_{II} / A_{\perp})_{998}$, where A is the absorbance. To measure the total orientation that includes both the crystalline and the amorphous phase orientations the band at 972 cm^{-1} was selected and f_{av} (average orientation) was calculated based on $(A_{II} / A_{\perp})_{972}$. The orientation of the amorphous phase, f_a, can be determined from these two values by:

$$f_{av}=X_c f_c+(1-X_c) f_a \qquad (2)$$

where X_c is the degree of crystallinity. We have shown that the *c*-axis crystal orientation measured by FTIR is in reasonable agreement with the values obtained from the WAXD results [3]. The processing conditions have also been listed in Table 7.2 along with the results for the orientations of the crystalline and amorphous phases.

Table7.2. Orientation of crystalline and amorphous phases

Resin	DDR	f_c	f_{av}	f_a
PP05*	65	0.710	0.517	0.381
PP05-An**	65	0.769	0.568	0.427
PP12	48	0.512	0.374	0.277
PP12-An	48	0.584	0.435	0.33
PP12-An-150 °C	48	0.667	0.498	0.379
PP12	65	0.623	0.448	0.325
PP12-An	65	0.721	0.534	0.402
PP12-Half strain rate	65	0.608	0.439	0.319
PP20	65	0.556	0.390	0.272
PP20-An	65	0.698	0.522	0.398
PP28	65	0.484	0.348	0.259
PP28-An	65	0.569	0.424	0.328

*As it was mentioned there were more noticeable thickness variations for the PP05 precursor film. For this case the measurement was made for a sample taken from the middle of the film

** Annealing was performed for 1 h and at 140 °C unless other conditions are mentioned.

Annealing improves the amorphous orientation along the machine direction. This is likely due to the participation of disrupted amorphous chains (end chains) in the crystallization and also the partial motion of the crystal blocks, which results in a slight stretching of the tie chains along the lamellae thickness. The effect of temperature and strain rate is also shown in Table 7.2. The annealing temperature significantly improves orientation while reducing the strain rate applied at the die decrease the orientation for both crystalline and amorphous orientation.

7.2.4.4 Cold stretching

After annealing, the precursor films were stretched at room temperature for lamellae separation and pores creation. The tensile properties for tests carried out with a recovery response following an applied strain of 1 are presented in Figure 7.5. The speed of stretching was 200 mm/min and the same speed was used in the recovery to return to the initial length. It should be noted that in our process for making membranes we usually considered a strain of 0.4 for cold stretching.

The recovery of the applied strain, which reflects the elasticity of the film, is controlled by factors such as crystal thickness, tie chain density and orientation. The whole process is governed by stretching of two types of tie chains. Initially, the short tie chains are stretched out and are finally broken apart (end of the elastic region) resulting in pores creation [11]. However, at the end of this region the sample can recover most of the initial strain (if relaxed) because of the connection of long tie chains. After this point the stress is transferred to the long tie chains. The enlargement of the pores proceeds with

stretching of the long tie chains. The stretched long tie chains could go then through crystallization in a later hot stretching step to form strong interconnected bridges [11]. As shown in Figure 7.5, PP05 failed around a strain of 1 (the ultimate limit for the tie chain stretching). We believe this could be due to larger amount of extended fibrils that strongly connect the lamellae together. High molecular weight chains promote orientation through the creation of long fibrils. On the other hand, long fibrils limit the mobility of the lamellae for separation in stretching. PP28 showed a maximum recovery in comparison with the other resins, which could be the result of less pores formation (lower structure damage) and also more flexibility in the lamellae motion. The use of a larger draw ratio in the precursor films, as shown in Figure 7.5 by comparing results for PP12-48 and PP12-65, also improved the strain recovery. The improvement could be due to higher orientation of the structure.

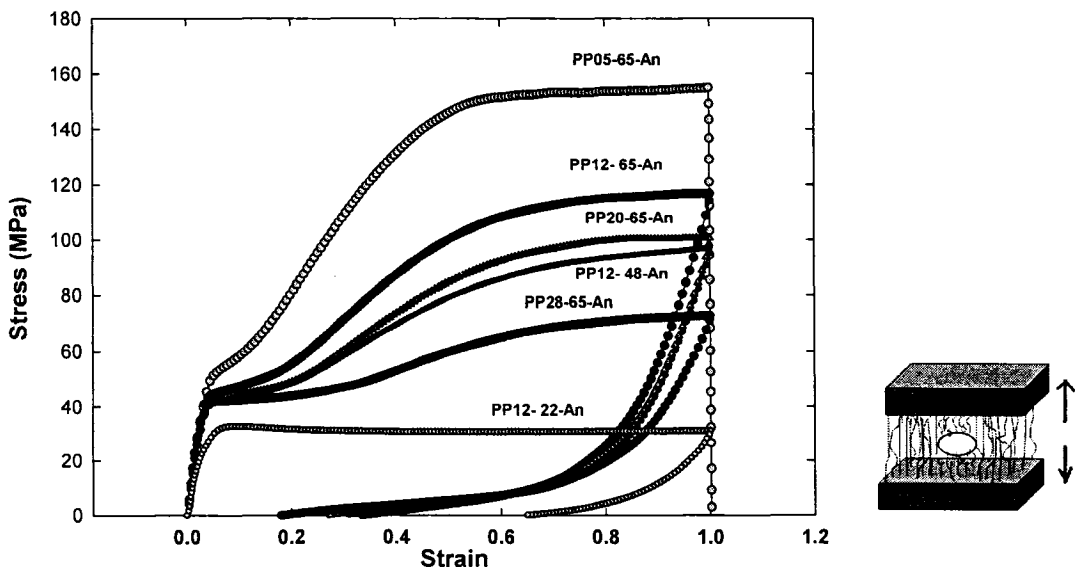

Fig.7.5. Tensile properties of annealed samples; stretching and recovering were performed at a speed of 200 mm/min.

The annealed samples were cold stretched to 40 % at 25 °C and heated up to 140 °C for 20 min for heat setting. Figure 7.6 presents the SEM micrographs of the samples after cold stretching. It is clear that the pores size does not vary significantly from one resin to the others. The pores are more uniformly distributed for PP20 and less uniform for PP05. As these images were taken from the surface, the important issue is the interconnection state between the pores along the thickness, which controls the permeability.

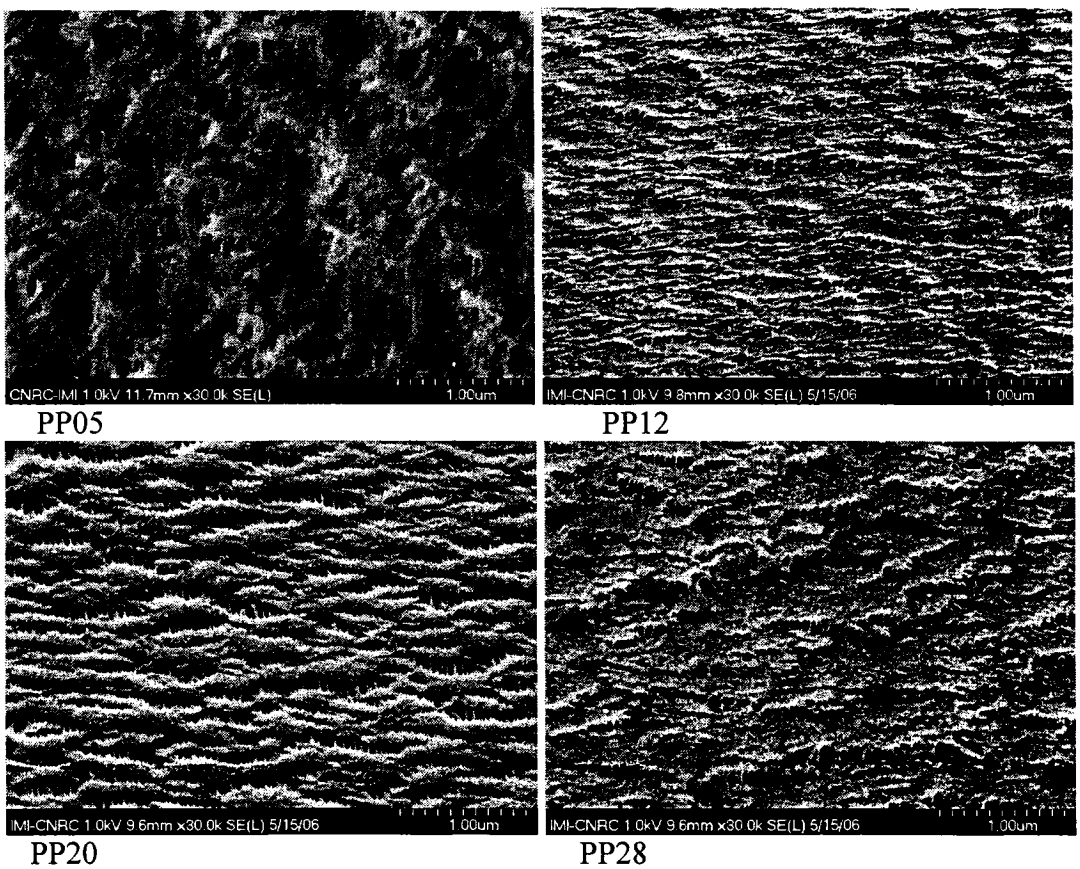

Fig.7.6 SEM micrograph of the surface of PP (initial draw ratio of 56.5) samples cold stretched to 40% and heated up to 140 °C for 20 min for heat setting.

In fact, interconnected pores determine the membrane performances. The effective factors in this case are the orientation of the crystal blocks and also the structure uniformity along the width of the film. As already mentioned, even though PP05 showed a good orientation of the crystal blocks, strong interconnection between the lamellae confines the lamellae mobility. Thickness variations (as a result of lower applied cooling rate) and non uniformity along the width did not allow for a uniform stress distribution in the cross-section.

7.2.4.5 Hot stretching

After cold stretching and formation of pores, samples that were not heat set were stretched again to 40 % at an elevated temperature (140 °C) to enlarge the pores. For a constant hot stretch level it has been shown that the permeability improved as the specific hot stretch temperature is increased [5]. Figure 7.7 depicts the pore structure of two samples, for which the surface structures are shown in Figure 7.6 after cold stretching. It seems that for PP20 the pores are a little larger. The pore diameter changed after hot stretching but not dramatically. We could consider an average of 120 nm to 200 nm for PP20, while for PP12 the pore size is smaller. However, comparing the pore sizes from micrographs should be done with caution. In fact the interconnection (created channels along the thickness) between the pores determines the effective pore diameter.

We believe that in the hot stretching stage, some lamellae are melted and recrystallized in the form of interconnected bridges. This is a complex process, but it is

the most probable phenomenon that could happen as suggested by the observation of a decrease in the lamellae thickness along with creation of more interconnecting bridges. The unraveling of folded polymer chains and their complete reorientation have also been reported elsewhere [11].

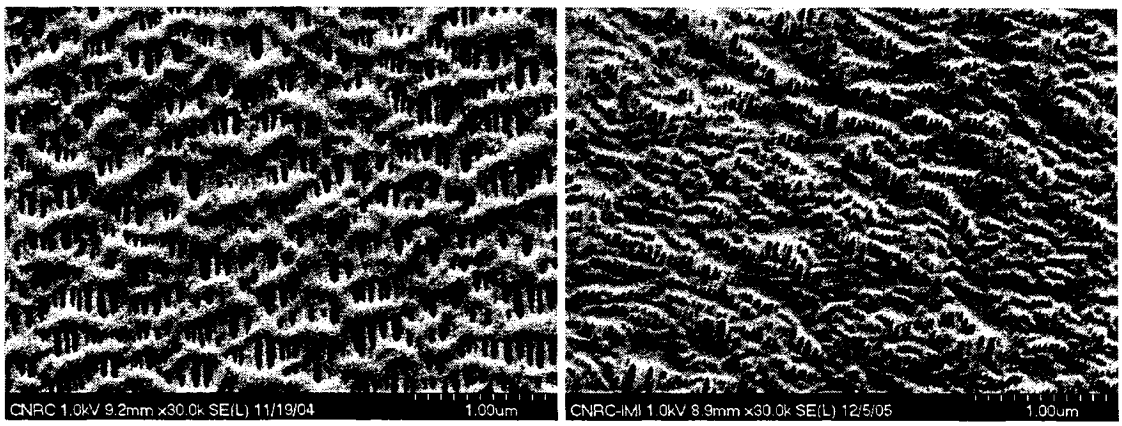

PP20 (hot stretched) PP12 (hot stretched)

Fig.7.7. SEM micrographs of the two hot stretched (40% at 140°C) samples already presented in Figure 7.6

In the other hand some pores that are invisible after the cold stretching as initiated pores are enlarged during the hot stretching process. These phenomena could explain the increase in the number of pores during the hot stretching stage as well. Figure 7.8 shows the stress consumption in the samples at 140°C during an Instron tensile test (with a similar speed as applied during the hot stretching of the samples). The stress consumption increases with the initial draw ratio and the molecular weight. The stress at this stage is mostly spent: i) to separate the lamellae to a larger extend and ii) to stretch the tie chains with simultaneous crystallization of some of them, which increase the number of interconnected bridges. There is also a possibility for reorientation and

motion of the crystal blocks in the stretching direction, which requires a larger share of the stress for the samples with lower orientation.

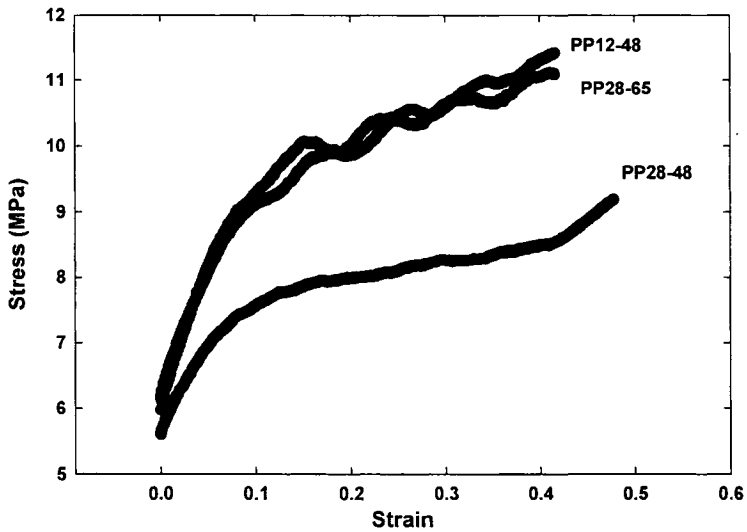

Fig.7.8. Tensile properties for three samples at 140°C

DSC of the produced membranes provides us with some information regarding the lamellae thickness distribution. Figure 7.9 shows the DSC results for the final PP20 membrane compared with the previous annealed film.

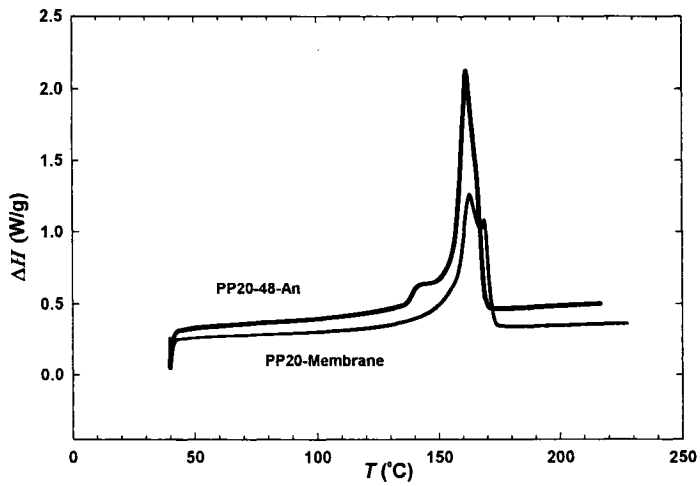

Fig.7.9. DSC of the final PP20 membrane (with initial draw ratio of 48) compared with the annealed sample.

The evolution in the crystalline structure can be seen after final stretching. The two distinctive peaks suggest two types of lamellae distribution. It is assumed that one of these peaks corresponds to crystals of the interconnected bridges between the lamellae and the other reflects the lamellae crystals.

7.2.4.6 Permeability

Permeability of the produced membranes was evaluated by water vapor and nitrogen. Water vapor permeability was performed under atmospheric conditions (no pressure applied) and with cross flow configuration while for nitrogen, a pressured system was used to monitor the flow rate versus pressure. Table 7.3 reports the water vapor permeability for the membranes. The permeability results are in accordance with the orientation results presented in Table 7.2 except for PP05. The lower permeability for PP05 could be due to two factors: first, there was a non uniformity observed along the width of the precursor film as mentioned before, which disturbed the stress distribution and, second, the presence of a large number of long chains for this resin resulted in many long thick threads that didn't lead to an easy lamellae separation. The SEM micrograph of this sample (Figure 7.6) shows the non uniformity of the pores distribution. It is observed for PP20 that increasing the cold temperature from 25 to 50 °C improves slightly the permeability. The PP12 sample obtained under a larger initial draw ratio shows a 25 % increase in permeability whereas the PP12 sample prepared at a lower strain rate but under the same draw ratio of 65 (as mentioned in the extrusion section) shows a 18 % drop in permeability. This is probably due to a weaker row

nucleated lamellar structure, even though the orientation stays almost constant for the sample (Table 7.2).

Table 7.3. Permeability of the membranes prepared using different processing conditions.

Resin	Conditions: DR = draw ratio t = membrane thickness	Permeability at the end of cold stretching stage (g/m^2.day) (Error: ± 5 %)	Permeability of final membranes (at the end of hot stretching) (g/m^2.day) (Error: ± 5 %)
PP05	DR = 56.5, t = 24 μm Cooling = 70 %*	2200	12 000
PP12	DR = 56.5, t = 24μm	12 700	23 800
PP20	DR = 56.5, t = 24μm	14 100	21 000
PP28	DR = 56.5, t = 24μm	8700	17 750
PP20	$T_{\text{Cold stretching}}$ = 50°C	**	25 050
PP12	DR = 65, t = 22 μm	**	29 800
PP12	DR = 65 produced under half strain rate, t = 22 μm	**	25 400

*As we mentioned previously for obtaining a stable and uniform sample we had to use 70 % of the cooling (fan speed) used for the other resins.
**Not measured.

Figure 7.10 presents the permeability to N_2 under pressure of the membranes. The ranking of the membrane permeability to N_2 is the same as the ranking for the permeability values to water vapor reported in Table 7.3. Two distinguishable regimes are observed: at low pressure, the behavior reflects the Knudsen diffusion process (no pressure effect) and at high pressure this is the Poiseuille flow regime (linear pressure effect) [15]. The two regimes can be distinguished by the difference in slopes as a function of pressure, which depends on the diffusion mechanism.

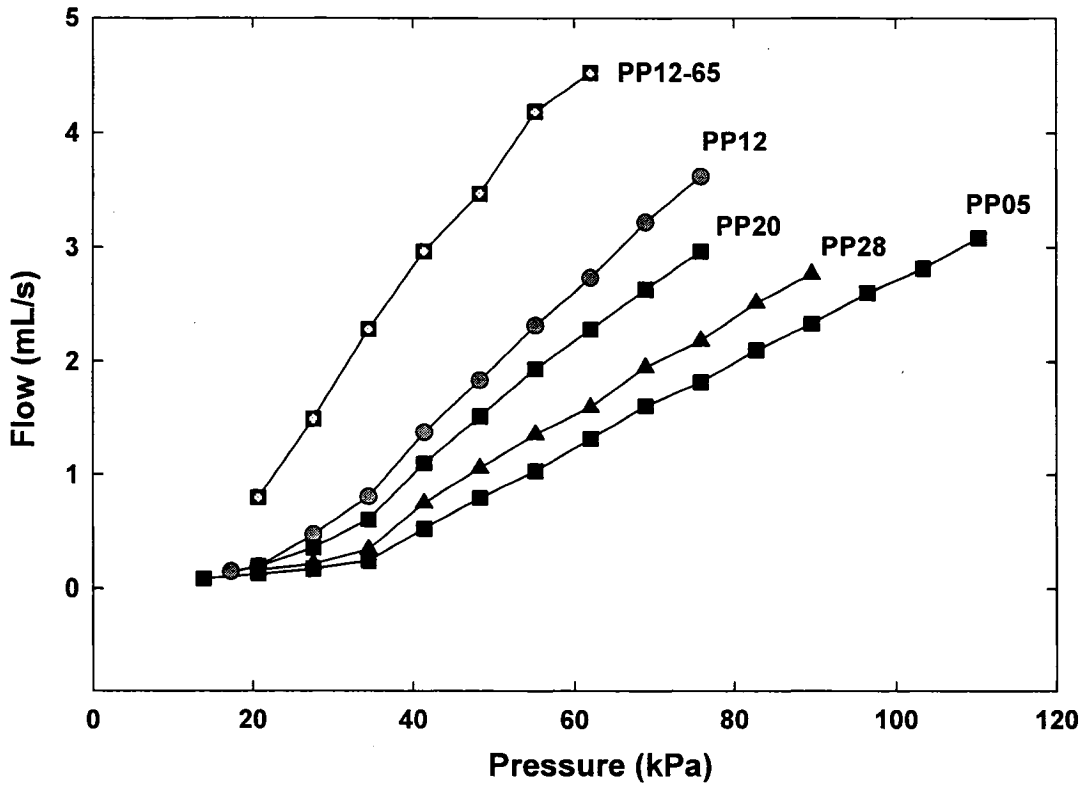

Fig.7.10. Flow versus applied pressure for nitrogen for the membranes produced with initial draw ratio of 56.5 (as presented in Table 7.3) and for one membrane prepared at a draw ratio of 65.

The transition between the Knudsen regime and Poiseuille flow occurs around a pressure of 0.35×10^5 Pa. The transition is less pronounced for the membranes with higher permeability. The higher permeability is a result of larger orientation that improves the interconnection between the pores. In the case of lower orientation the pores interconnection is weak and the porosity is decreased. However, the effect of thickness

also should be considered here since both high orientation and smaller thickness intensify this effect.

7.2.4.7 Mercury porosimetry

The porosity and pore size distribution from mercury porosimetery are reported in Figure 7.11 for two microporous PP12 and PP28 films, with initial precursor film draw ratio of 56.5. For PP12 (high permeability) a peak in the pore size distribution around 0.15 μm is observed while for PP28 (lower permeability), the whole curve shifts to the lower values with a peak around 0.10 μm.

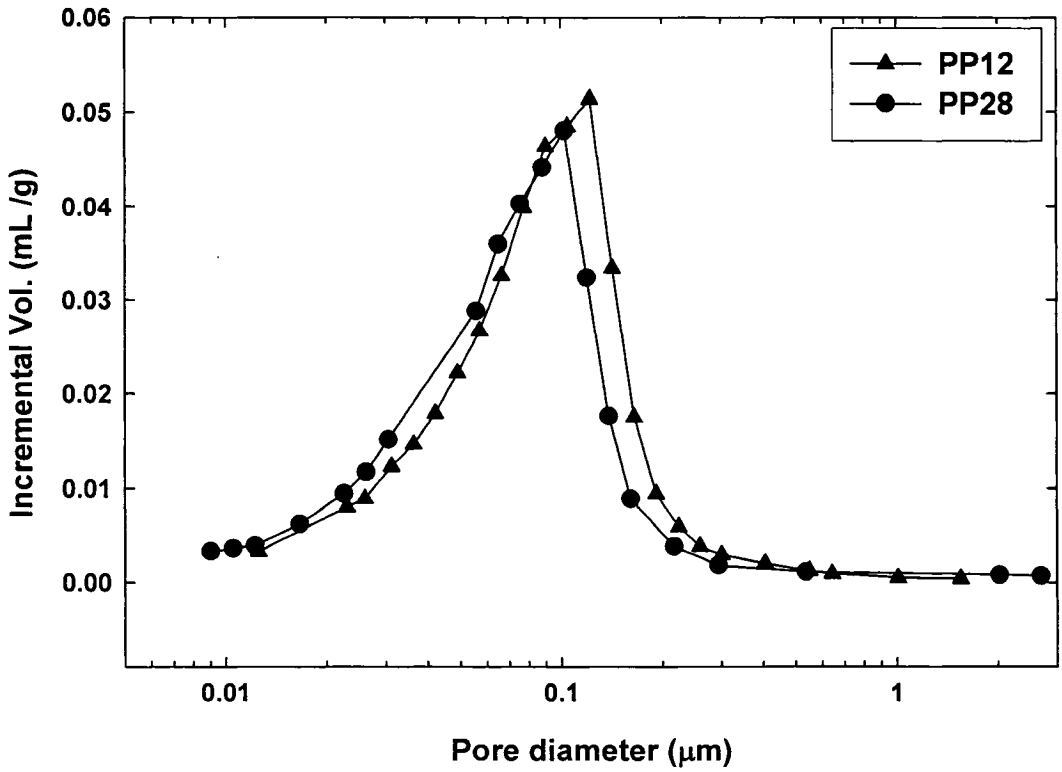

Fig.7.11 Pore size distribution for two microporous PP12 and PP28 membranes, with initial precursor films prepared under a draw ratio equal to 56.5.

The porosity was evaluated as 47 and 41 % for PP12 and PP28 films, respectively. Although the SEM micrographs of the surface of PP12 and PP20 samples are quite different (see Fig. 7.7), their pore size distribution and porosity are about the same (results not shown for PP20). The intrusion volume of mercury is directly related to pore size and porosity for interconnected pores. Lower effective pore size for the resin with smaller molecular weight could be attributed to lower orientation resulting in less pores interconnection.

7.2.5 Conclusion

The process for developing microporous membranes covers several stages, which are precursor film production, annealing, cold and hot stretching. The molecular weight of the base resin seems to be one of the key parameters for predicting membrane performances provided that the proper extrusion process is employed. In this work, five different PP resins have been investigated. These resins of distinct molecular weights showed different melt behavior during stress relaxation as well as uniaxial elongation. DSC results showed a change in lamellae distribution in each step starting from the precursor films to membranes. The lamellae thickness didn't show a large dependency on molecular weight while most impact of molecular weight was revealed on the orientation and connectivity of lamellae. The most effective parameter in annealing was temperature, which highly improved the crystal phase orientation, while it had a much weaker effect on the amorphous phase. It was found that cold stretching also initiated

some pores, which might not be visible in cold stretched samples, but would appear in the hot stretching step.

Membranes prepared from the resins were tested for permeability. The water vapor permeability, which reflects the pores interconnection, depended on molecular weight and orientation in the samples. The permeability to N_2 under pressure showed two distinguishable regimes. A change from Knudsen to Poiseuille flow was observed as the pressure was increased. The behavior of the samples with high orientation in the precursor films was mainly controlled by Poiseuille flow. The larger high permeability PP12 membrane had pores around 0.15 μm and porosity of 47 % whereas the lower permeability PP28 membrane had smaller pores of 0.10 μm and porosity of 41 %.

7.2.6 Acknowledgements

Financial support from NSERC (Natural Science and Engineering Research Council of Canada) and from FQRNT (Fonds Québécois de Recherche en Nature et Technologies) is gratefully acknowledged.

7.2.7 References

[1] M. Cheryan, Ultrafiltration and Microfiltration Handbook, second edition, CRC Press LLC, Boca Raton, Florida (1998)

[2] T. H. Yu, PhD thesis, Virginia Polytechnic Institute and State University, (1996)

[3] F. Sadeghi, A. Ajji and P.J. Carreau, 'Orientation analysis of row nucleated lamellar structure of polypropylene obtained from cast film', submitted to Polymer Engineering Science (2006)

[4] H. D. Noether and I. L. Hay, 'Small-angle X-ray diffraction studies and morphology of microporous materials and their 'hard' elastic precursors', J. Appl. Cryst. 11, 546 (1978)

[5] F. Sadeghi, A. Ajji and P.J. Carreau, 'Study of polypropylene morphology obtained from blown and cast film processes: Initial morphology requirements for making porous membrane by stretching', J. Plastic Film and Sheeting, 21, 199 (2005)

[6] M.B. Johnson, PhD thesis, Virginia Polytechnic Institute and State University, September 2000

[7] H. Münstedt, M. Schmidt, and E. Wassner, 'Stick and slip phenomena during extrusion of polyethylene melts as investigated by laser-Doppler velocimetry' , J. Rheol. , 44, 413 (2000)

[8] M. Dupire and J. Michel, 'Polypropylene with high melt strength and drawability', US patent 6,723,795 (2004)

[9] Z. Bashir, J. A. Odell and A. Keller, 'Stiff and strong polyethylene with shish kebab morphology by continuous melt extrusion', J. Materials Sci., 21, 3993 (1986)

[10] J.J Kim, T.S Jang, Y.D Kwon, U.Y. Kim and S.S Kim, 'Structural study of microporous polypropylene hollow fiber membranes made by the melt-spinning and cold-stretching method', J. Membrane Sci. 93, 209 (1994)

[11] I. K. Park and H. D. Noether, 'Crystalline "Hard" Elastic Materials', Colloid &Polymer Sci. 253, 824 (1975)

[12] L. E. Alexander, X-ray Diffraction Methods in Polymer Science, Wiley, New York (1969)

[13] D. Ferrer-Balas, M.LL. Maspoch, A.B. Martinez and O.O. Santana, 'Influence of annealing on the microstructural, tensile and fracture properties of polypropylene films', Polymer 42, 1697 (2001)

[14] I.M. Ward, P.D. Coates, and M.M. Dumoulin, eds., Solid Phase Processing of Polymers, Hanser (2000)

[15] R. B. Bird, W. E. Stewart and E. N. Lightfoot, Transport Phenomena, 2nd Edition, John Wiley & Sons Inc. (2001)

Chapter 8

General Discussion

Generating a row nucleated lamellar structure is the first step in membrane production from semi crystalline polymers by stretching. The process for the formation of such a lamellar structure is based on the elongation of the chains in the melt state followed by a rapid crystallization. It is obvious that the chains should preserve their elongated form to be able to act as initial nuclei. The relaxation time of the chain is the most important factor for this stage. Although very long or branched chains seem better options, other factors such as melt processability and properties of produced films need be considered. Hence, molecular weight and molecular weight distribution need to be adjusted to obtain the appropriate precursor films.

In the extrusion process the cooling rate is the most effective parameter, which could prevent the chain relaxation. Cooling conditions need to be adjusted: low cooling rate will create a weak lamellar structure with non-uniformity along the width of the film. In other hand, high cooling rate might adversely affect the crystallization of the lateral lamellae.

The die temperature (the extrudate temperature) is important since it has a major influence on the stability and properties of the film. Low temperature will slow down the chain relaxation while it will diminish the quality of the film at the die where the stretching can not proceed properly. An optimum temperature need to be selected for each polymer. We found the overall effect of moving towards lower temperature is more deteriorating than processing at higher temperature.

Strain rate and melt velocity applied at the die is also an important issue. Low strain rate produce less elongated chains resulting in a smaller amount of fibrils. The strain rate for a constant die gap is controlled by the melt and pick-up speeds. The ratio of pick-up speed to the melt velocity determines the draw ratio. It is possible to produce samples with two different strain rates but of equal draw ratios. Raising the draw ratio improved the orientation along machine direction. A minimum Herman's orientation factor of 0.3 (c-axis with respect to the machine direction) for the crystalline phase of the precursor film was necessary to develop a microporous structure in the later stretching process. A linear relationship was revealed between the orientation function and draw ratio while the dependency was smaller for the amorphous phase orientation. Tensile tests were performed on the samples showed a significant change in the response as the draw ratio increased. Increasing the draw ratio suppressed the yield point and strain hardening starts right after yield point. It is obvious that very low draw ratios (in our case less than 35) caused a deformed spherulitic structure while above 45 the structure turned into a lamellar structure. It should be noted that the molecular weight of the resin was also a determining factor in the behavior of the tensile response.

After production of the precursor films with a proper structure and orientation, annealing should be performed. This stage has two main functions: 1-Removing the defects in crystalline structure and improving the orientation and 2- increasing the long period (total thickness of crystal and amorphous phase). Two key factors in this stage are time and temperature of the annealing. The temperature was more effective and we found that the film structure would be set after annealing time of 10 min. Further annealing didn't

change the structure any more. Some studies suggested keeping a slight tension on the film during annealing but we didn't observe a significant difference in the orientation parameters.

Strain recovery tests can provide some information regarding the orientation and crystalline structure of the precursor films. When the sample goes under higher stretching (passing the elastic region) the total stress (or energy) can be spent in:

1-Stretching of the tie chains during the lamellae separation.

2-Rotation and orientation of the crystal blocks, which are not initially oriented (or partially oriented).

3-Motion of the oriented crystal blocks along the machine direction.

Fig.8.1 shows the effect of the annealing on the response of the sample PP28 to the recovery test.

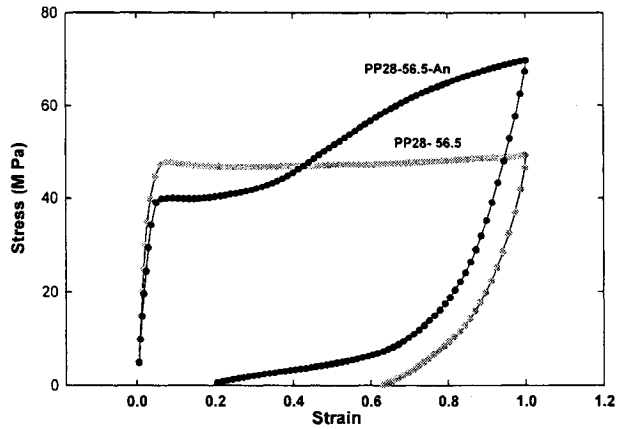

Fig.8.1 The recovery strain test for PP28-DR=56.5

As it can been seen that annealing significantly improves the recovery. The increase in recovery could be due to the improvement in orientation during annealing. A larger recovery means that the deformation is mostly takes place in the space between lamellae

for the tie chains. We stretched the annealed sample of PP12 (prepared with initial draw ratio 65) to different extension ratios and studied the strain recovery. Fig.8.2 shows the effect for four extension degrees.

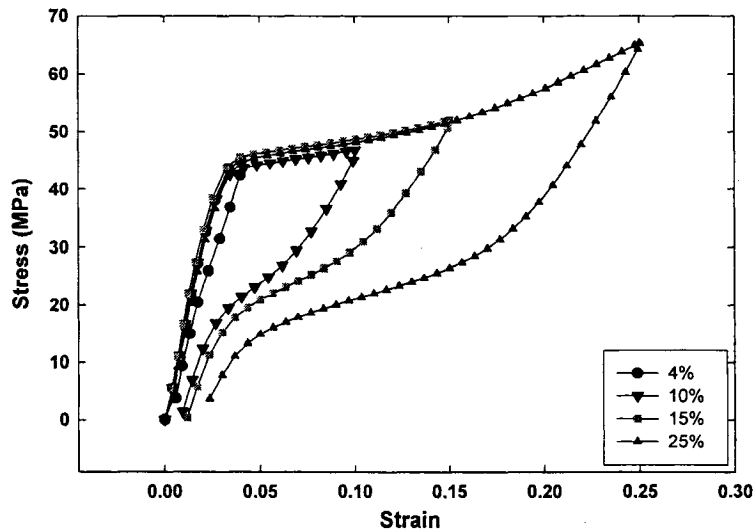

Fig.8.2. The elastic recovery for different stretching ratio for PP12-65-An

It seems that after the strain of 0.25 (25% stretching) the recovery value diminishes noticeably. This could be the result of larger amount of voids creation and partially orientation of the initially non oriented crystal blocks.

The behavior in cold stretching in comparison to that in hot stretching is different since the temperature is low. In hot stretching the lamellae can move more easily while the crystallization also can take place. However, both processes are very complicated since a combination of events happens simultaneously and it is hard to predict which one

exactly is dominating. In this part we will address the events that could happen in cold and hot stretching:

1- With the stretching of the tie chains, chain scission happens for the short tie chains and voids are created and they get larger as the load will be taken by longer tie chains.

2- Rotation and reorientation of the crystal blocks happen, and this becomes more important if the precursor film posseses a lower initial orientation for the lamellae. The stress rotates the lamellae and orients them in the stretching direction.

3-Some crystallization happens as a result of chain stretching. This crystallization will take a very small share in cold stretching and in larger extend in hot stretching.

4-Going into higher temperature for the hot stretching will melt some surface layers of the lamellae and some will recrystallize under stress on the fibrils, as shown in Fig.8.3.

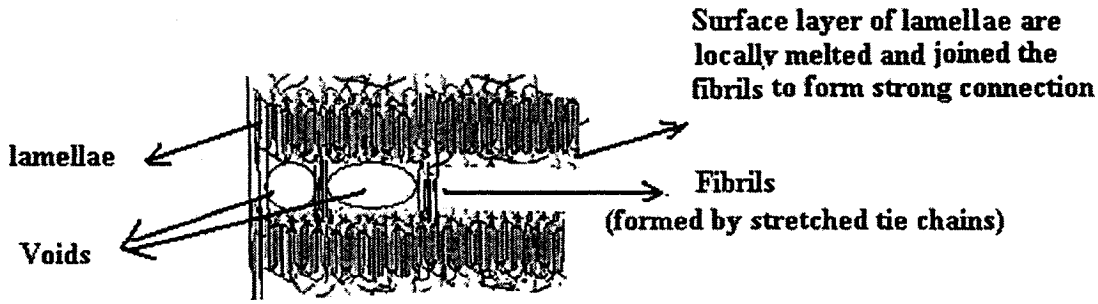

Fig. 8.3 The schematic of the formation of voids and connected bridges

In hot stretching some surface layers of lamellae are believed to locally melted, detached and rotated to form interconnected bridges. This explains the increase in the number of interconnected bridges after hot stretching. The pore structure after this satge is set and stabilized. Membranes were afterward tested for permeability performance. The water

vapor permeability, which reflects the pores interconnection, depended on the orientation of the precursor films, which in turn was related to molecular weight. For the permeability under pressure, N_2 gas was used. In this case when the flow versus pressure was plotted two distinguishable regimes were observed. A change from Knudsen to Poiseuille flow was observed as the pressure was increased. The regimes are shown in Fig.8.4.

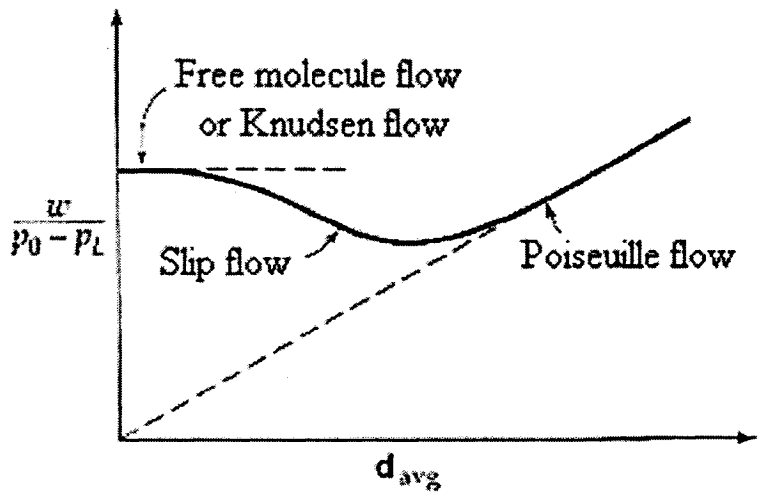

Fig. 8.4 The normalized flow (kg/s) with respect to pressure versus average density Bird et al. (2001).

CHAPTER 9

CONCLUSION AND RECOMMENDATIONS

9.1 Conclusions

In this dissertation the procedure for development of the microporous membranes from polypropylene by stretching was studied and following conclusions can be drawn from the work:

1-The method for the production of the precursor films with initial appropriate lamellar structure was established. The most important factors involved were relaxation time of the polymer chains and also the cooling rate of the molten film at the die.

2- For the precursor films to be used for the membrane production by stretching, the minimum orientation factor of 0.3 (*c*-axis along MD) is found to be the critical requirement. It was also realized that the orientation is mainly controlled by the resin molecular weight in the equal process conditions.

3-Annealing was found to be a crucial stage for the membrane production and it was observed that improved orientation for both crystalline and amorphous phases. It significantly affected the response of the sample to tension test.

4-Cold stretching separated the lamellae to create pores. It was concluded that the initial source of the pores was the chain scission of the short tie chains.

5-Enlargement of the pores was accomplished further with stretching at high temperature. The shape and size of the pores were stabilized at the end of this stage.

8-SEM pictures showed an increase of 70 % in the pore size (in average) from cold to hot stretching stage. This is based on the surface observation and effective pore size depends on the type of the resin and initial structure of the precursor film.

9-Tests for the water permeability showed almost a double fold increase from cold to hot stretching for most of the resins.

10- Porosimetry tests were carried out and the sample with larger water vapor permeability showed larger porosity.

11-Puncture resistance tests were performed and the sample containing the largest porosity showed the highest resistance.

9.2 Recommendations

For the future work we recommend two subjects:

1-Developing a blend system composed of two PPs to obtain the superior permeability results. This can be performed through the improvement in orientation of crystalline structure in a way that promotes the pore interconnection. We have already evaluated this idea with the blending of two PPs. Permeability was improved about 20 % in comparison to a regular commercial Celgard2400 polypropylene membrane. The puncture test also improved for the proposed blend.

2- Extending the method to some other semi crystalline polymers, which potentially can be employed to generate a lamellar structure. We have already examined the idea about PVDF. The porous structure was detected by lamellae separation by SEM. The

permeability of water vapor was also carried out to assure interconnectivity between the pores, the latest permeability of 1200 (g/m^2.day) was achieved.

REFERENCES

Agarwal P.K, Somani R.H., Weng W., Mehta A., Yang L., Ran S., Liu L., Hsiao B.S., (2003), 'Shear-Induced crystallization in novel long chain branched polypropylenes by in situ Rheo-SAXS and –WAXD', Macromolecules, 36, 5226-5235.

Aoyama M., Ito M., Tsuji S., Ishii, T., Tanaka T., (1990), 'Method of forming a porous polyolefin film', US 4921653.

Bird R. B., Stewart W. E., Lightfoot E. N., (2001), Transport Phenomena, 2nd Edition, John Wiley & Sons Inc.

Chen R. T, Saw C.K., Jamieson M.G, Aversa T. R., Callahan R.W., (1994), 'Structural characterization of CELGARD microporous membrane precursors: melt- Extruded polyethylene film', Journal of applied polymer science, 53, 471-483.

Cheryan M., (1998), Ultrafiltration and Microfiltration Handbook, second edition. CRC

Chu F., Yamaoka T., Ide H., Kimura Y., (1994),'Microvoide formation process during the plastic formation of beta-form polypropylene' Polymer; 35:,3442-3448.

Fujiyama M., Kawamura Y., Wakino T., (1988), 'Study on rough-surface biaxailly oriented polypropylene film', Journal of applied polymer Science, 36(V), 1035-1048

Johnson M. B. ,(2000), 'Investigations of the processing –structure-property relationship of selected semi crystalline polymers', PhD Thesis, Virginia Polytechnic Institute and State University, Chemical Engineering

Holman J. P., (2002), Heat transfer, 9th ed., McGraw-Hill, New York.

Keller, A., Kolnaar , J. W. H., (1993), 'Chain extension and orientation: fundamentals and relevance to processing and products', Progress in colloid polymer science), 92, 81-102.

Kim J.J, Jang T.S., Kwon Y.D, Kim Y.U., Kim S.S, (1994),'Structural study of microporous polypropylene hollow fiber membranes made by the melt-spinning and cold-stretching method', Journal of membrane science, 93, 209-215.

Kumaraswamy G., Issaian A.M, Kornfield J.A., (1999), 'Shear-Enhanced crystallization in isotactic polypropylene. 1. Correspondence between in situ rheo-optics and ex Situ Structure determination', Macromolecules, 32, 7537-7547.

Kundu P.P. and Choe S., (2003), ' Transport of moist air through microporous polyolefin films' Journal of macromolecular science part C-Polymer reviews, C43, 143-186.

Nagasawa, T., Matsumura, T. Hoshino, S., (1973) 'Film forming process of crystalline polymer: Microstructure' Applied polymer symposium, 20, 295.

Nago S., Nakamura S., Mizutani Y., (1992), 'Structure of microporous polypropylene sheets containing Caco3 filler', Journal of applied polymer science, 45, 1527-1535

Nogales A., Hsiao B.S., Somani R.H., Srinivas S., Tsou A.H., Balta-Calleja F.J., Ezquerra T.A.,(2001) 'Shear-induced crystallization of isotactic polypropylene with different molecular weight distributions: in situ small- and wide-angle X-ray scattering studies', Polymer, 42,5247-5256

Sadeghi F., Ajji A. and Carreau P.J., (2005) 'Study of Polypropylene Morphology Obtained from Blown and Cast Film Processes: Initial Morphology Requirements for Making Porous Membrane by Stretching' , Journal of Plastic Film and Sheeting , 21, 199.

Seki M., Thurman D.W, Oberhauser J.P, Kornfield J.A., (2002), 'Shear-Mediated Crystallization of Isotactic Polypropylene: The Role of Long Chain-Long Chain Overlap', Macromolecules, 35, 2583-2594.

Shi, G., Chu, F., Zhou, G. and Han, Z., (1989), 'Plastic deformation and solid-phase transformation in beta-phase polypropylene' Makromol. Chem., 190, 907-913

Sidiropoulos V., Vlachopolous J.J, (2005), 'Temperature Gradients in Blown Film Bubbles', Advances in polymer technology, 24, 83-90

Somani R.H., Hsiao B.S., Nogales A., Srinivas S., Tsou A.H., Sics I., Balta-Calleja F.J, Ezquerra T.A., (2000), 'Structure development during Shear Flow-Induced Crystallization of i-PP: In-Situ Small-Angle X-ray Scattering Study' Macromolecules,33,9385-9394.

William D., Jr. Callister, (1997), Materials Science and Engineering (An Introduction) 4th ed, New York ; Toronto : John Wiley & Sons

Yu T. H., (1995), 'Processing and structure-property behavior of microporous polyethylene-from resin to final film' Ph.D. Dissertation, Virginia Tech.

Appendix A

Study of the PE film morphology

Verification of the extrusion processing parameters

We selected polyethylene as another resin to observe the morphology of produced blown films. SEM observation of lamellar structure for PE is much easier and more reproducible. This is probably because of the better surface roughness discrimination between the crystalline and amorphous phases. The SEM method is basically based on the detached secondary electron originated from the surface of the sample. These electrons are highly sensitive to the topography of the surface. That could explain the better image contrast for polyethylene in comparison to polypropylene.

HDPE 6200 (supplied from Petromont Company) was used in the film blowing process to produce samples with different process conditions. Morphology of the surface was observed to see the effect of different process parameters. We studied 6 sets of process conditions presented from HD1 to HD6.

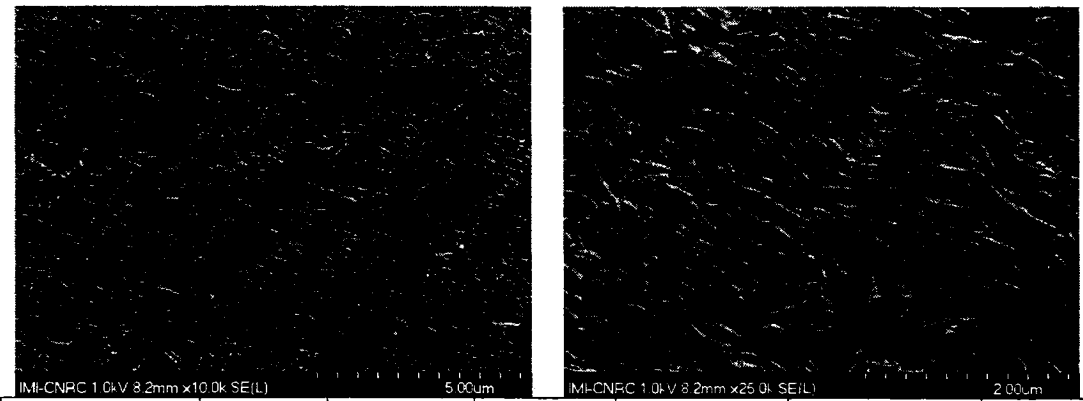

Cooling=31.1%	t=35μm	DDR=30.5	BUR=1.5	Die gap=1.1	Flow=12.4kg/h	Tdie=220°C

Fig.A-1- HD1

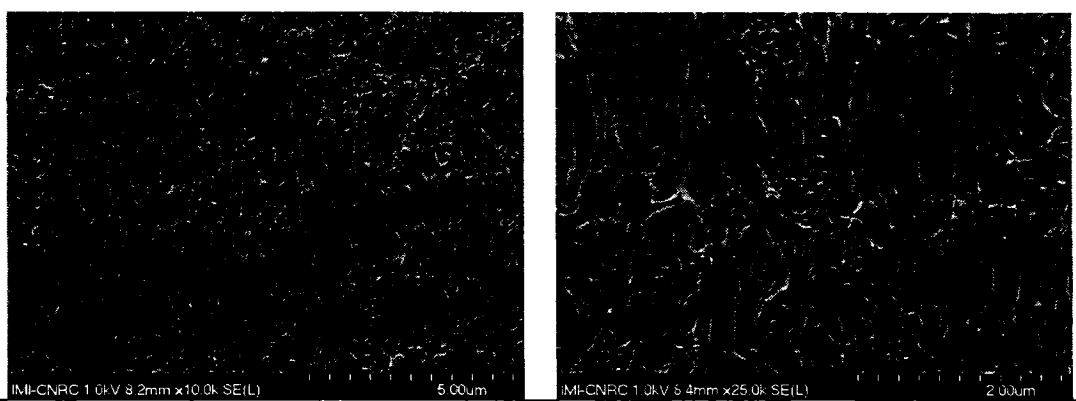

Cooling=41%	t=35μm	DDR=31	BUR=1.5	Die gap=1.1	Flow=12.4kg/h	Tdie=220°C

Fig.A-2- HD2

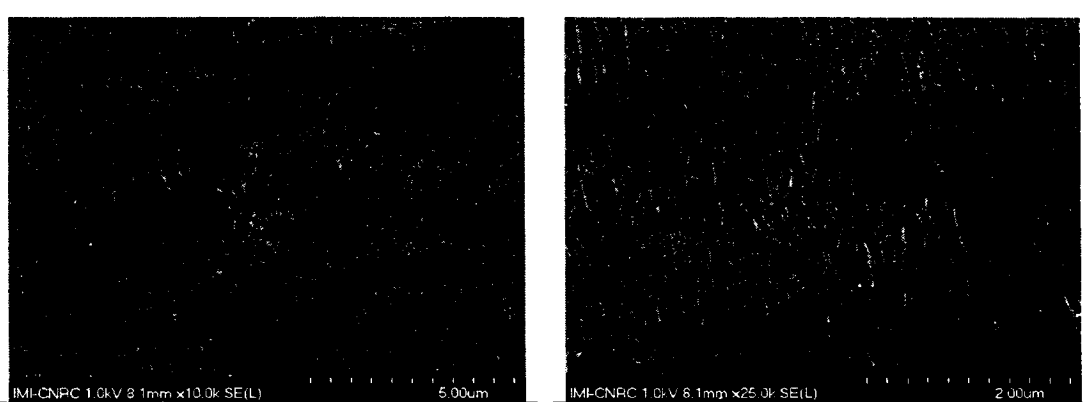

Cooling=50%	t=35μm	DDR=31	BUR=1.5	Die gap=1.1	Flow=23.4kg/h	Tdie=220°C

Fig.A-3- HD3

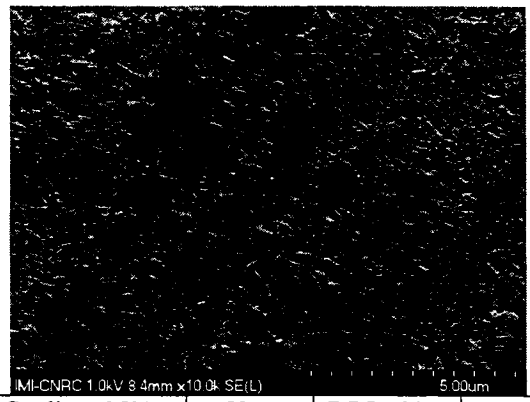

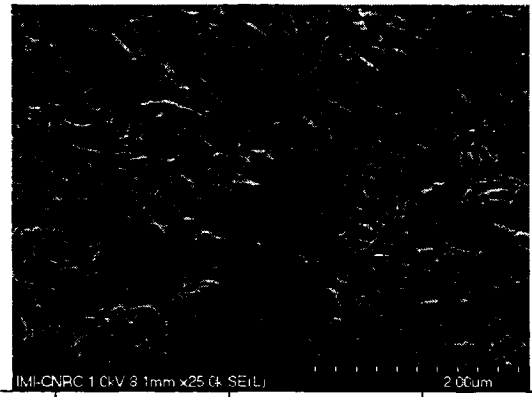

Cooling=35%	t=50μm	DDR=22	BUR=2	Die gap=1.1	Flow=14.2/h	Tdie=220°C

Fig.A-4- HD4

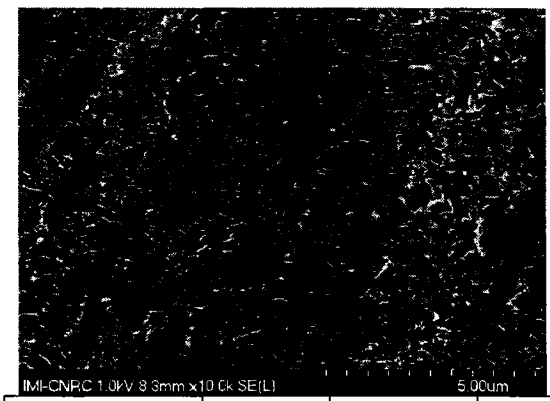

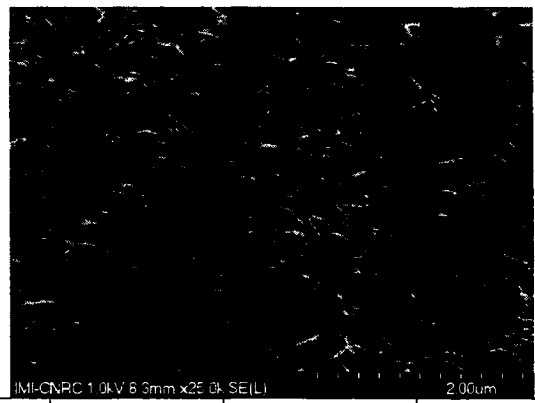

Cooling=27.6%	t=25μm	DDR=101	BUR=2.1	Die gap=2.5	Flow=16.6/h	Tdie=220°C

Fig.A-5- HD5

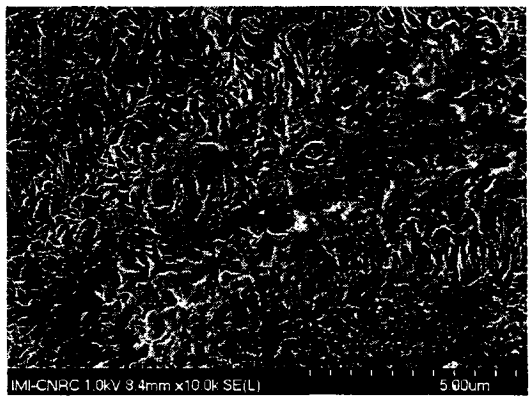

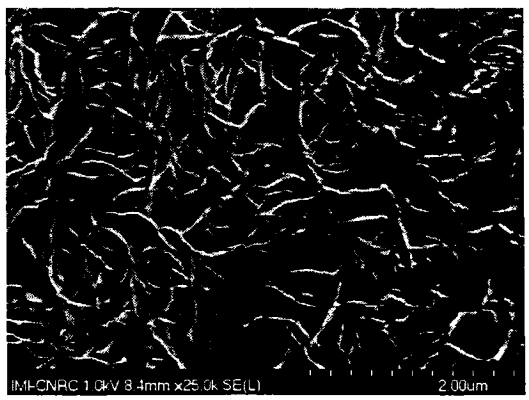

Cooling=26%	t=50μm	DDR=51.1	BUR=2.1	Die gap=2.5	Flow=16.6/h	Tdie=220°C

Fig.A-6- HD6

Discussion

The results for HDPE prove our idea about the cooling rate factor. HDPE is likely more sensitive to the crystallization process since its crystallization rate is slower than polypropylene. Low cooling conditions provide enough room for the entangled chains to be relaxed and only very long chains have the chance to survive. Reduction in the amount of elongated fibrils will disturb the network required for row nucleated lamellar structure. In very high cooling conditions the threads are appeared in large number and dispersed where are difficult to detect. For HD1, the lower cooling condition results in the fewer threads and the impingement of lamellae are clearly seen.

Appendix B

Calculation of strain rate and freezing line for the cast film extrusion

In this section we discuss the cast film extrusion in more detail. As we mentioned in order to obtain an appropriative row-nucleated morphology for all the resins, the process was changed to cast film. The advantage of cast film extrusion is the possibility of using a higher cooling rate and also the achievement of a pure uniaxial deformation. Figure B-1 shows the schematic of the process. The air knifes have been installed on the die to blow the air on the film surface in order to quench it.

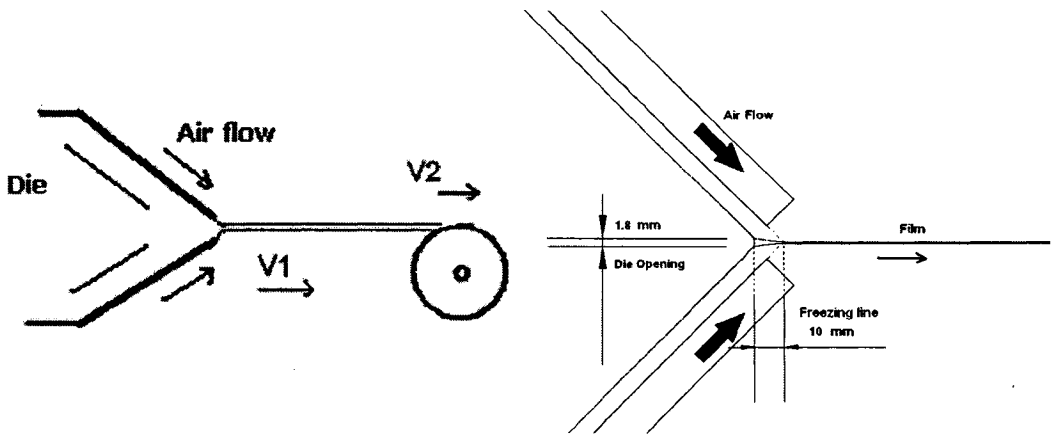

Fig. B-1. Schematic of the cast film extrusion

Heat Transfer Calculation

To show the evolution of the temperature for the film during the stretching at the die, the heat transfer equations will be developed. For solving the energy equation the following assumptions have been made to simplify the problem:

1-The film is uniform and the thickness is constant along the x axis (Fig B-2), in other words most deformation occurs before the air flows hit the melt.

2- The resistance to heat conduction along the thickness (in normal direction) is considered negligible. This is because the film is very thin.

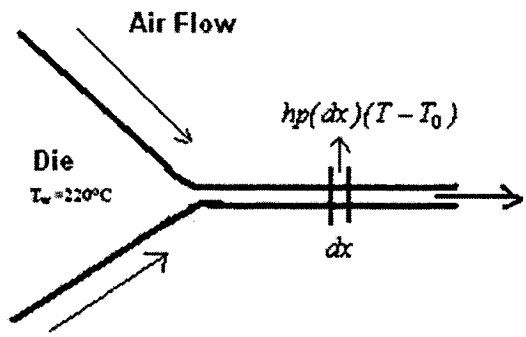

Fig B-2 The schematic of the cooling for the molten film

In this case the equation of conservation of energy can be written as (Bird R.B et al., 2001):

$$wC_p(dT) = h(p(\mathrm{dx}))(T - T_0) \qquad \text{(B-1)}$$

w is the flow rate (kg/s), C_P is the heat capacity of the film J/kg.°C, h is the heat convection coefficient. W/°C.m^2, p is the perimeter (m), T is the sample temperature and T_0 is the environment temperature.

Calculation of the heat transfer coefficient has been performed in the literatures for film blowing process (Sidiropoulos et al. 2005). For our case we consider a value of h=220 W/°C.m^2. The width of the film is considered as 20cm (0.2m).

The other parameters are listed as:

$C_p = 2300\text{J/kg.}^{\circ}\text{C}$

$p = 2(0.2) = 0.4\text{m}$

$T_o = 200^{\circ}\text{C}$

Replacing the values in the equation B-1 yields:

$$26.14w.\frac{dT}{dx} = (T - 20) \qquad \text{(B-2)}$$

With the modification: $\frac{dT}{T-20} = (3.8\times10^{-2}/w).dx$, with integration and applying the boundary condition: (x=0, T = 220°C), the temperature will be:

$$T(x) = e^{(-(3.8\times10^{-2}/w)x+5.3)} + 20 \qquad \text{(B-3)}$$

In the Fig.B-3, the temperature is plotted as the function of x for three flow rates: 0.5 kg/h, 1kg/h and 1.5 kg/h.

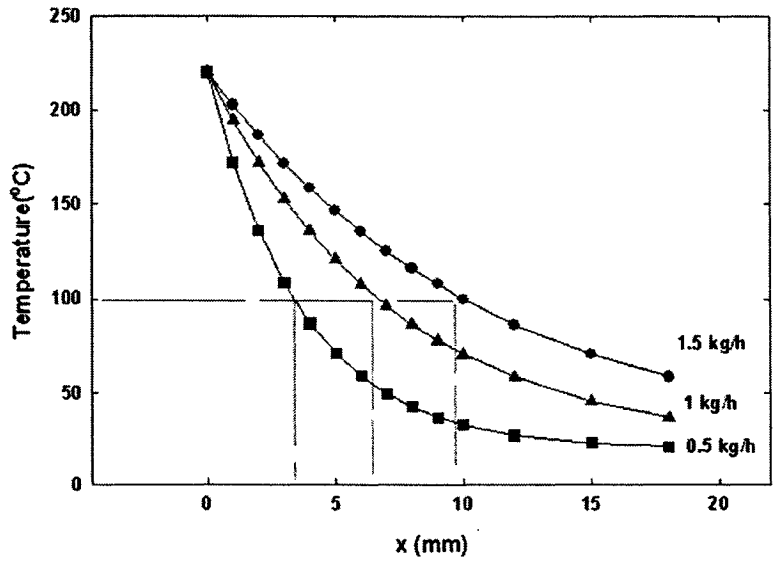

Fig.B-3 Temperature of the film as a function of x

It is clear that the temperature drops very fast. Any increase or decrease in the flow rate significantly affects the temperature. It should be noted that the crystallization of PP releases heat but this value is very small in comparison to the other heat terms.

Strain rate calculation for cast film extrusion

The air flow hits the film within 1cm from die lip. If we assume that the film is solidified when the temperature goes below 100°C, it could be said that melt stretching happens in the distance of 1 to 2 cm from the die lips (depending on the mass flow). It is also assumed that the temperature for such a short distance remains constant (the same as die temperature 220°C).

The flow rate is taken 1 kg/h and the calculations are based on the final thickness of 30 μm and maximum frost length of 1.5cm (Fig.5.3).

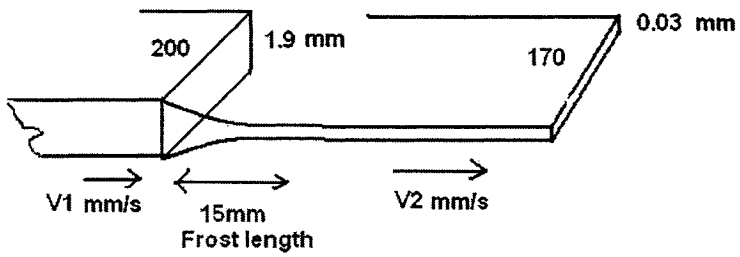

Fig. B-4.The schematic of the die and dimensions of the samples after stretching.

Then the continuity equation will be :

$$V_1 A_1 \rho_1 = V_2 A_2 \rho_2 = 1\text{kg/h} = 2.77\times10^{-4}\ \text{kg/s} \qquad \text{(B-4)}$$

Calculation of V_1: $2.77\times10^{-4}\ \text{kg/s} = V_1 A_1 \rho_1$

w_1=0.2m, t_1 = 0.0019 m, (ρ_1 at 230 °C = 733 kg/m^3 and at 220 °C =7 39 kg/m^3)

For a final film thickness of 30 μm and frost length=0.015m

$$V_1 = \frac{2.77\times10^{-4}}{0.2\times739\times0.0019} = 9.89\times10^{-4}\text{m/s} \quad \text{and} \quad V_2 = \frac{2.77\times10^{-4}}{0.17\times950\times30\times10^{-6}} = 0.057\text{m/s}$$

The speed of the melt at the die (before the frost line):

$$V_{2(melt)} = \frac{2.77\times10^{-4}}{0.17\times739\times30\times10^{-6}} = 0.074\text{m/s}$$

The process can be simulated with a system where in the melt is stretched (initially from a stationary position) by the speed of (V_2-V_1) that is about 0.073 m/s.

And an average estimation for the strain rate could be calculated:

$$\text{As: } \dot{\varepsilon}_0 = \frac{V_3}{x_3} = \frac{0.073}{0.015} = 4.86s^{-1} \qquad \text{(B-5)}$$

Appendix C

DSC Comparisons of lamellar and spherulitic morphology

The DSC tests with the rate of 20°C/min were performed for one of the precursor samples, PP12, prepared with the initial draw ratio of 65. The results have been shown in Fig. C-1.

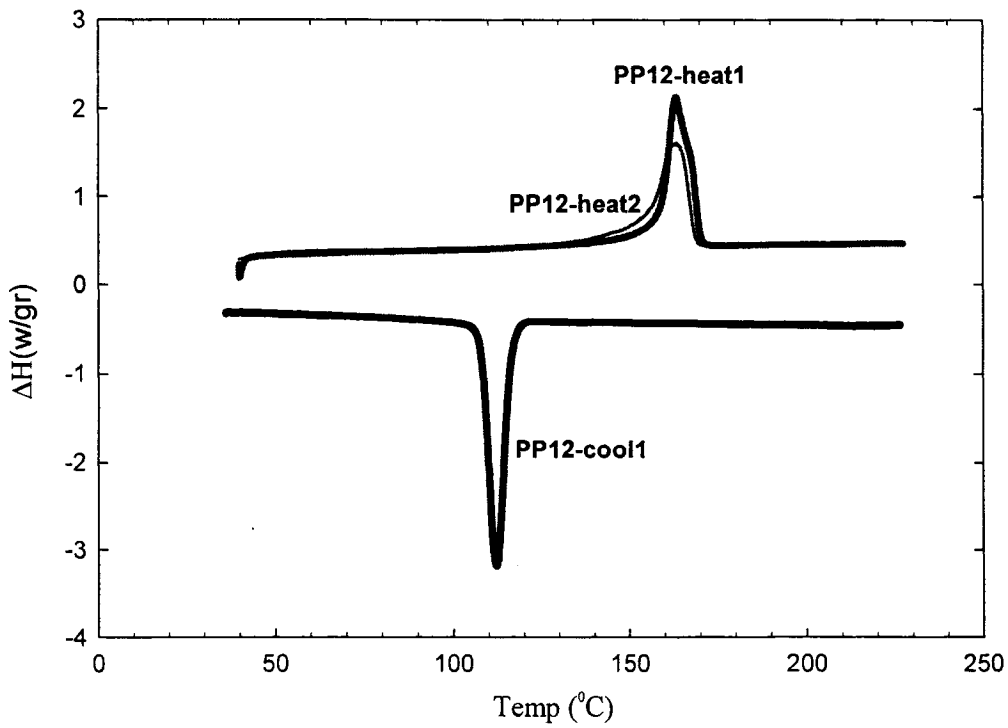

Fig. C-1 DSC of PP12 (DR=65) with heating and cooling rate of 20°C/min with a rest time of 10 min after first heating to assure complete melting.

The film, which represents a typical oriented lamellar structure, shows a sharp peak with a little shoulder shifted to the right. The slight shift of the main peak is a sign of the formation of thicker lamellae. Second, heat represents an isotropic spherulitic structure, which shows a broader peak.

Appendix D

Orientation Characterization

In this section we present our detailed orientation results for the PP films produced by casting extrusion. The name of the resin and draw ratio and attributed crystal plans are specified below the each figure.

The pole Figures for PP05:

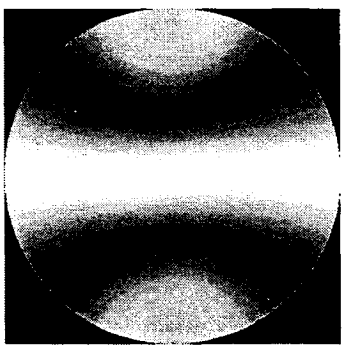

PP05-48-110

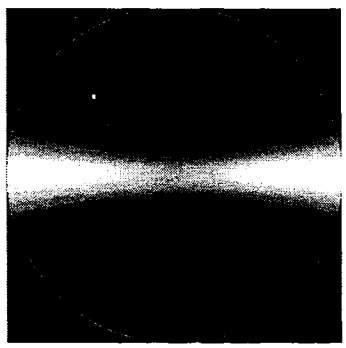

PP05-48-040

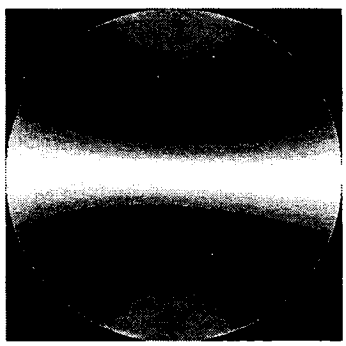

PP05-65-110

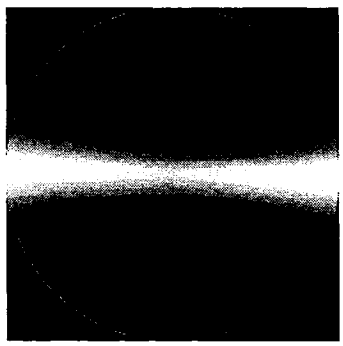

PP05-65-040

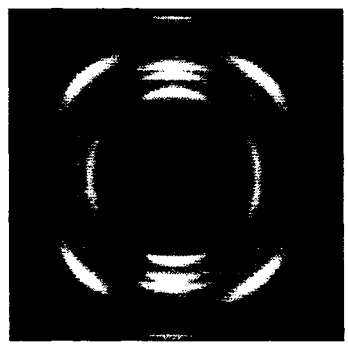

WAXD-PP05-65

For PP05, with rising draw ratio, 110 intensity reduces in MD and while it increases in TD and ND. For 040 Intensity is always in TD direction.

The pole Figures for PP12:

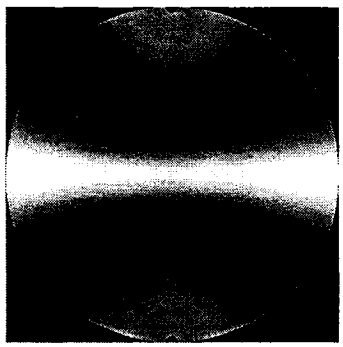

PP12-48-110

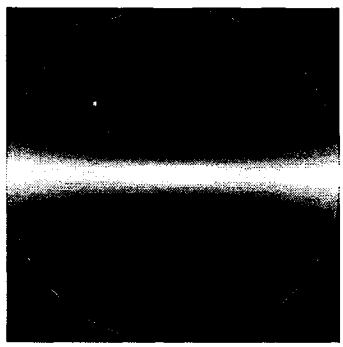

PP12-48-040

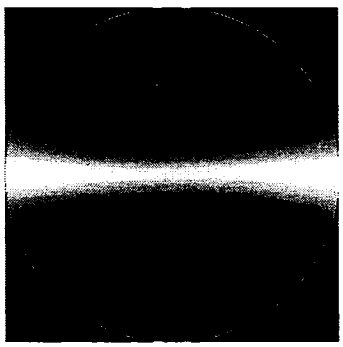

PP12-65-110

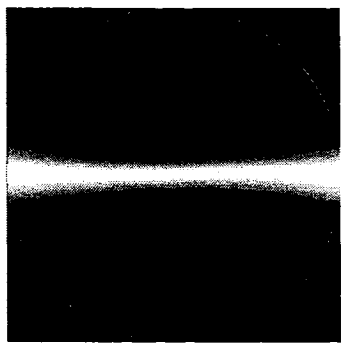

PP12-65-040

For PP12 with rising draw ratio, the intensity of 110 goes more to TD rather than ND direction. For 040 the intensity for low draw ratio is concentrated in ND. Increasing draw ratio dilutes the concentration for 040 from ND to TD.

The pole Figures for PP20:

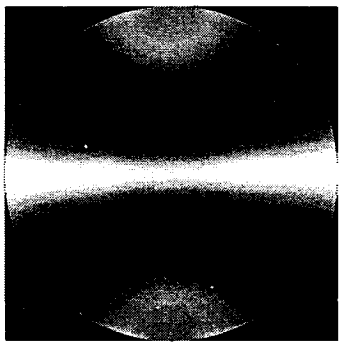

PP20-48-110

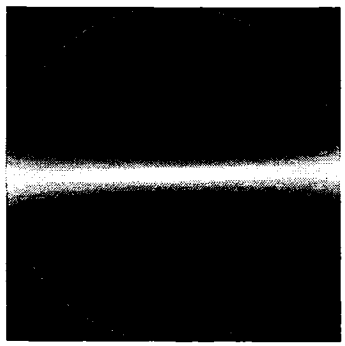

PP20-48-040

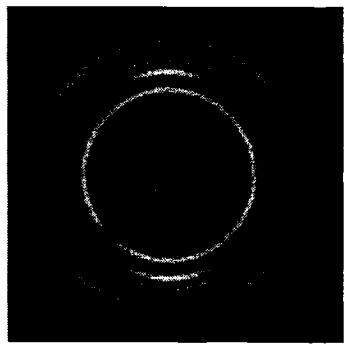

WAXD-PP20-48

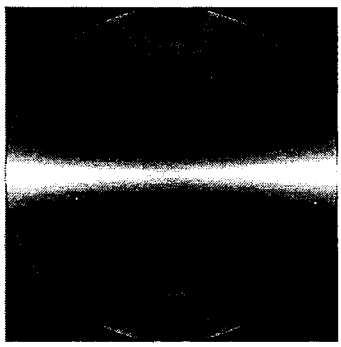

PP20-65-110

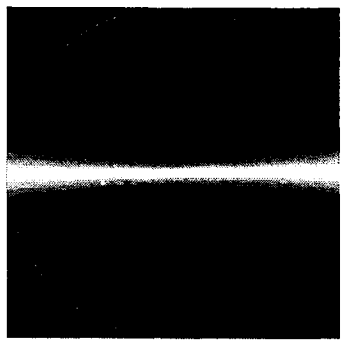

PP20-65- 040

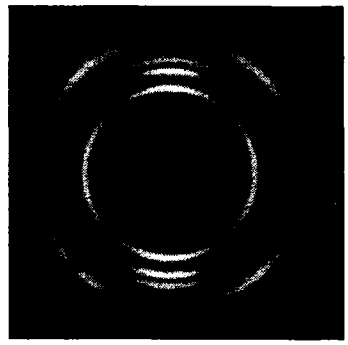

WAXD-PP20-65

For PP20 the situation is very similar to PP12.

The pole Figures for PP28

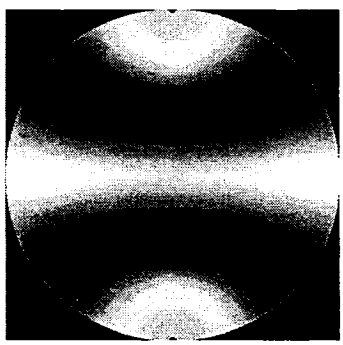

PP28-48-110

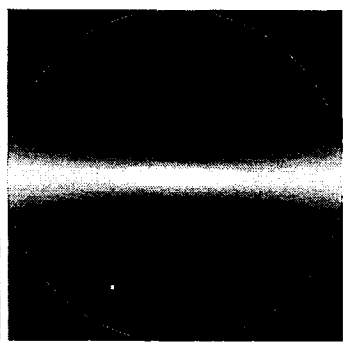

PP28-48-040

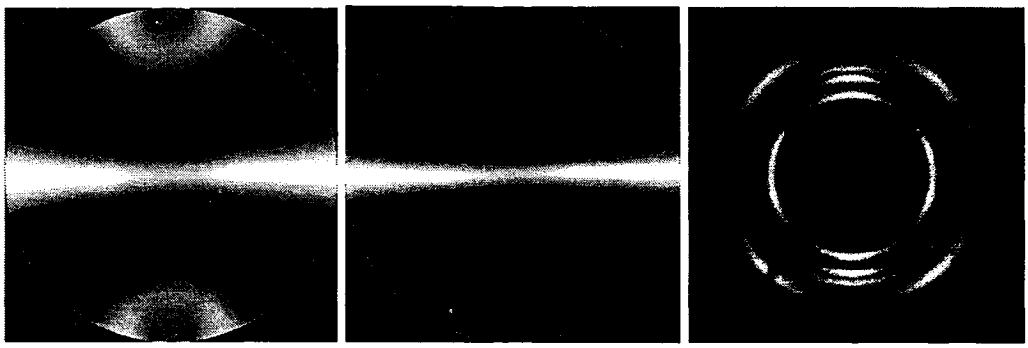

PP28-65-110 PP28-65-040 WAXD-PP28-65

In PP28 for both 110 and 040 planes the intensity is concentrated more in TD direction with increasing draw ratio.

Crystal Orientation in three dimensions from WAXD

Analysis of the pole figures would results in the orientation of a, b and c-axis towards MD, TD and ND directions. Table D-1 shows the results for two draw ratios. Increasing draw ratios will drive c-axis toward MD direction while a and b go to the plan of TD-ND. The results for the orientation of c-axis along MD follow almost the molecular weight trend, except for PP05-65 which the behavior is affected by the lower cooling conditions.

Table D-1. Orientation of samples obtained from WAXD analysis.

PP05-48	F'a	Fb	Fc	PP05-65	F'a	Fb	Fc
MD	-0.061	-0.447	0.508	MD	-0.201	-0.446	0.647
TD	0.015	0.239	-0.254	TD	0.087	0.241	-0.328
ND	0.046	0.208	-0.254	ND	0.114	0.205	-0.319
PP12-48	F'a	Fb	Fc	PP12-65	F'a	Fb	Fc
MD	-0.145	-0.464	0.534	MD	-0.215	-0.475	0.690
TD	0.107	0.199	-1.062	TD	0.136	0.239	-0.375
ND	0.039	0.265	-0.971	ND	0.079	0.235	-0.314
PP20-48	F'a	Fb	Fc	PP20-65	F'a	Fb	Fc
MD	-0.108	-0.471	0.579	MD	-0.197	-0.474	0.671
TD	0.077	0.199	-0.276	TD	0.121	0.235	-0.356
ND	0.031	0.271	-0.302	ND	0.076	0.240	-0.316
PP28-48	F'a	Fb	Fc	PP28-65	F'a	Fb	Fc
MD	0.001	-0.455	0.454	MD	-0.089	-0.476	0.565
TD	0.032	0.189	-0.221	TD	0.087	0.286	-0.373
ND	-0.033	0.267	-0.234	ND	0.002	0.190	-0.192

Appendix E

Effect of annealing on the morphology of the precursor films

In this section the effect of annealing on the morphology of polyethylene films are discussed. Fig. E-1 shows the effect of annealing on the morphology of one of the HDPE sample (which was already presented in appendix A).

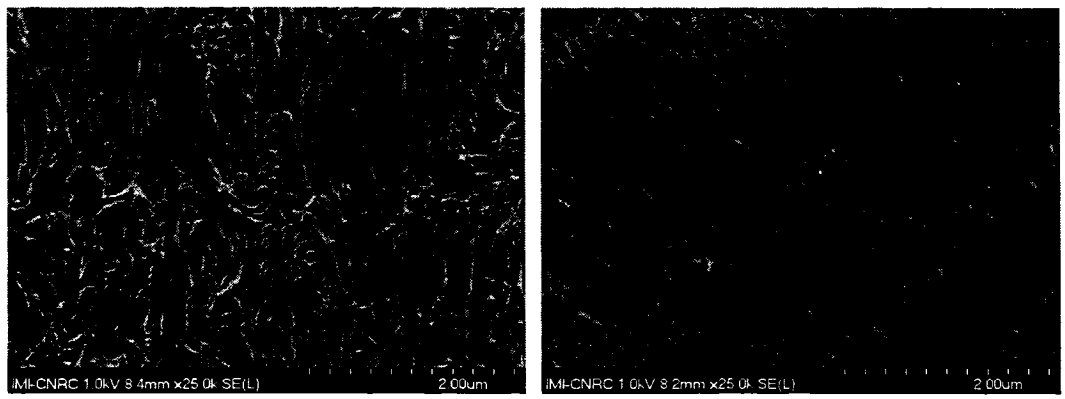

Before Annealing | After Annealing

Cooling=41%	t=35μm	DDR=31	BUR=1.5	Die gap=1.1	Flow=12.4kg/h	Tdie=220°C

Fig. E-1 The HD2 sample annealed at 120°C for 30 min

It is clear that annealing improves the uniformity of lamellar structure and removes the crystalline defects considerably while the lamellae thickness doesn't change so much.

Effect of annealing on WAXD patterns

Fig. E-2 shows the effect of annealing on WAXD patterns for PP28 (Draw ratio of 65). Improvement in orientation is clearly observed as the arcs are concentrated in center.

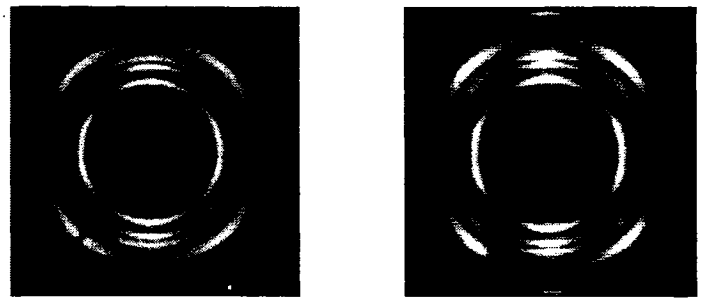

(a) PP28-65 **(b) PP28-65-An**

Fig.E-2 The WAXD patterns for PP28 (annealed and non-annealed) film

Effect of annealing on the tensile in TD direction

The TD tensile response was evaluated before and after annealing. In chapter 6, it was observed that annealing improves the tensile response in machine direction. As it is shown in Fig.E-3 it seems that annealing has negligible effect in the transverse direction. Tensile in transverse direction laterally concentrates the stress on elongated fibrils that cause the separation to take place very easily.

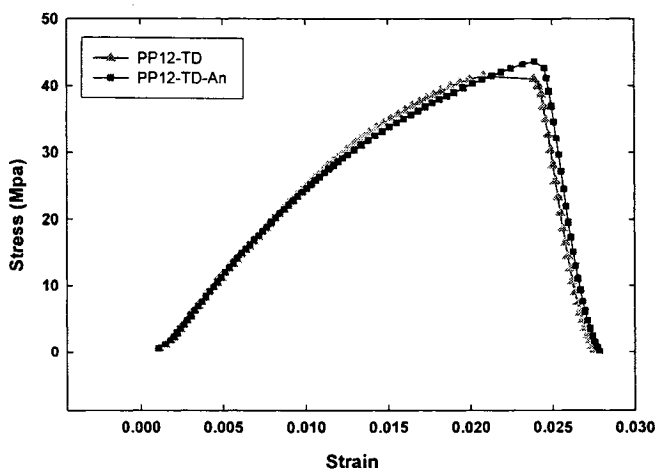

Fig. E-3. Tensile response in TD direction for annealed and non-annealed samples of PP12 with initial draw ratio of 56.5

Appendix F

Assessing the larger draw ratios for constant thickness

The idea to produce the samples with larger draw ratios while keeping the thickness constant was examined in this section. We changed the die gap from 1.9 mm to 3 mm. The draw ratio was then changed from 48 to 66 to obtain the film with approximately the same thickness of 34 μm. The graph F-1 shows the differences between two samples (the same thickness with different draw ratios). It seems that a very high draw ratio has a small effect on the tensile response. It should be noted due to the larger die gap we had to increase the extrudate flow rate, which might affect of the efficiency of the cooling and in turn mechanical properties.

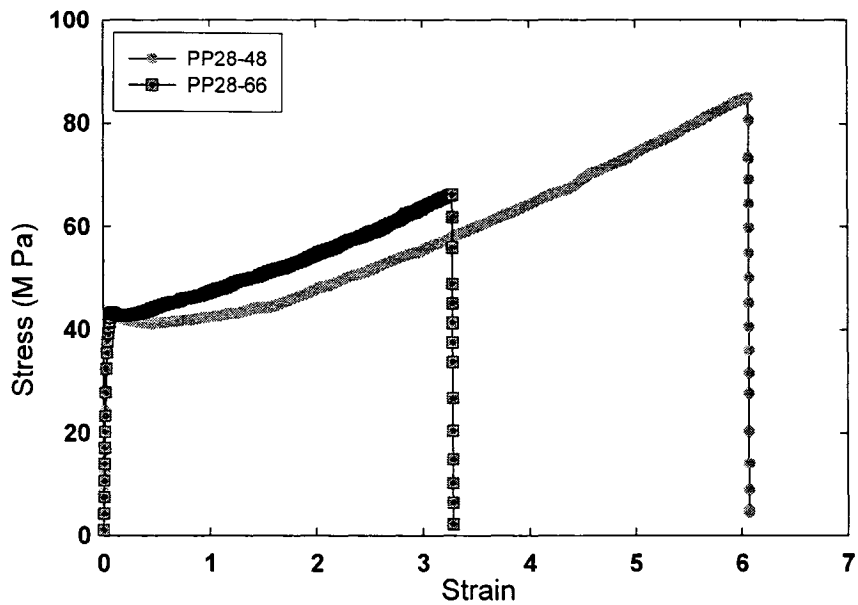

Fig.F-1 Tensile response for two samples for different draw ratios but having the same thickness of 34 μm

We also measured the water vapor permeability for the two samples. For sample with DR=48 a value of 10 900 (g/m^2.day) was obtained while for the sample with DR=66 that increased to 14 700 (g/m^2.day). As we mentioned in the chapter 7, the larger draw ratio can create more elongated chains leading to a higher orientation function for the precursor film. However, the efficiency of cooling could also affect the formation of a proper lamellar structure for the precursor films. In the other hand, the effect of thickness is also important in the process of pores interconnection. To study this effect more precisely we suggest that a bigger fan be installed to assure more efficient cooling.

Appendix G

WAXD pattern for a Membrane

The WAXD pattern for membrane shows a larger orientation with more intensity concentration of arcs in the middle. The new appearance of two spots in low degree (very close to center) almost at 2° angle is shown in Fig.G-1. The spots appeared right after stretching that reflects the pores formed during the process. From this pattern, two issues could be concluded: first, it shows that the pores have an order in formation, which means they are almost uniformly repeated; second they have an orientation, which means that the repetition order is in a specific direction (MD).

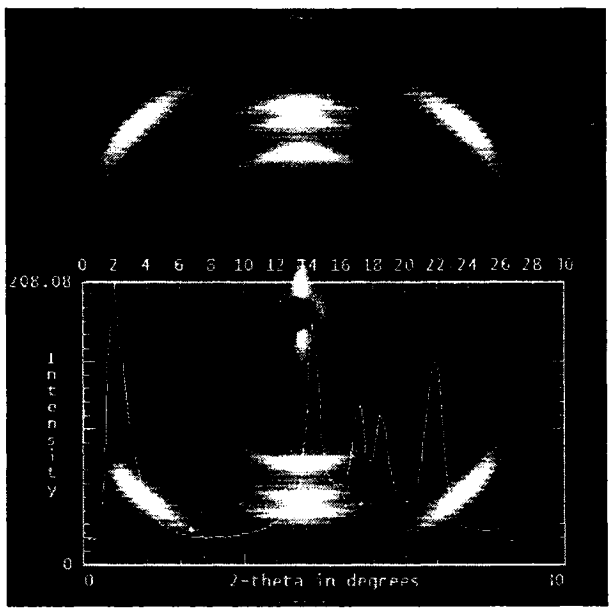

Fig.G-1 WAXD pattern for a microporous membrane obtained from PP20-DR=48